Small fatigue crack growth in high strength aluminium alloys

Thesis

oro.open.ac.uk

SMALL FATIGUE CRACK GROWTH

IN HIGH STRENGTH ALUMINIUM ALLOYS

DX 171964

A THESIS SUBMITTED TO

THE MATERIALS DISCIPLINE

OF THE OPEN UNIVERSITY

FOR THE DEGREE OF

DOCTOR OF PHILOSOPHY

Date of submission: 25 September 1992
Date of award: 20 November 1992

by

YAN HUI ZHANG

(BSc, MSc)

September, 1992

ProQuest Number: C348985

ProQuest C348985

HIGHER DEGREES OFFICE

LIBRARY AUTHORISATION FORM

STUDENT: _YAN HUI ZHANG_ SERIAL NO: _M7063441_

DEGREE: _PhD._

TITLE OF THESIS: _Small Fatigue Crack Growth in_
High Strength Aluminium Alloy

I confirm that I am willing that my thesis be made available to readers and maybe photocopied, subject to the discretion of the Librarian.

SIGNED:___ DATE: _2/12/92_.

Y. H. Zhang

The Open University

SMALL FATIGUE CRACK GROWTH

IN HIGH STRENGTH ALUMINIUM ALLOYS

ABSTRACT

This work presents an investigation of small fatigue crack growth behaviour in high strength aluminium alloys. Variation in slip distribution in Al-Zn-Mg-Cu alloys caused by the addition of different volume fractions of dispersoids, was not found to noticeably affect small fatigue crack growth rates. Small fatigue cracks grew more rapidly than long fatigue cracks under the same nominal ΔK and exhibited the familiar growth pattern of deceleration and acceleration.

The selected area electron channelling pattern (SAECP) method was used to measure the plastic zone size (PZS) and shape of small fatigue cracks. A novel experiment enabling PZS measurements on growing small fatigue cracks was developed to investigate the development of plastic zone size and shape with crack growth and the relation between PZS and small crack growth rates. It was revealed that small crack growth was accompanied by relatively large plastic zone sizes, with the ratio of plastic zone size to half crack length ranging from 0.8 to 0.2 and that small crack growth rates were proportional to their plastic zone sizes.

It was observed that small fatigue cracks began to decelerate when their relatively large plastic zones, not their crack tips, were blocked by grain boundaries. Both plastic zone size and shape were found to be dependent on crack length and growth morphology. Naturally initiated fatigue cracks were predominantly crystallographic in nature and were accompanied by a relatively long, slender plastic zone shape. However, during subsequent growth over 1-2 grain diameters this shape evolved, firstly to a semicircular shape, and finally to the lobed configuration typically found associated with long cracks.

The plastic deformation associated with small cracks was characterized by the introduction of a variable friction stress into the BCS dislocation model and the calculated PZS was used to correlate small crack growth. Crack deceleration was described by blocked PZS and the recovery of the growth was expressed by the necessity of a stress concentration within the plastic zone to overcome the grain boundary barrier to operate a dislocation source in the next grain. The prediction was compared with the experimental results and showed good agreement.

ACKNOWLEDGEMENTS

PREFACE

This thesis is submitted for the degree of Doctor of Philosophy of the Open University. It is an account of research performed in the Materials Discipline, Technology Faculty between September 1989 and August 1992 under the supervision of Dr. Lyndon Edwards. The work reported is original and has been performed without collaboration. None of this work has been submitted for a degree or other qualifications at this or any other university. Where the work of other authors has been included in the text, this has been acknowledged and its source given in the references at the end of the thesis. Some parts of the work have been published in the following papers:

Y. H. Zhang and L. Edwards, "The effect of grain boundaries on the development of plastic deformation ahead of small fatigue cracks", Script Metallurgica et Materialia (1992), 26, No.12, p1901-1906.

Y. H. Zhang and L. Edwards, "The development of plastic zone sizes ahead of small fatigue cracks and their consequences for crack growth rates", Proc. 3th International Conference on Aluminium Alloys, Trondheim, Norway, June 1992, 1, p563-568.

L. Edwards and Y. H. Zhang, "A plasticity based model of small fatigue crack growth", Proc. 13th RISØ International Symposium on Modelling of Plastic Deformation and Its Engineering Application, Roskilde, Denmark, September 1992, p259-264.

Y. H. Zhang and L. Edwards, "Measurement of plastic zones associated with small fatigue cracks by selected area electron channelling patterns", Materials Characterization, 29, No.3 (in press, accepted May 1992).

TABLE OF CONTENTS

LIST OF FIGURES

B.

LIST OF SYMBOLS

a	crack depth
a_0	intrinsic crack length expressed in equation 2.15
Δa	increment of crack extension
da/dN	fatigue crack propagation rate
b	the sum of half crack length c and plastic zone size r_p
c	half crack length
C, C'	material constants
C_1, C_2, C_3	constants
CTOD	crack tip opening displacement
CTSD	crack tip sliding displacement
D	grain size
E	Young's modulus
f_{ij}	dimensionless function of polar angle measured from crack plane
i	numbering of each subsequent grain boundary from crack initiation site
J	scalar amplitude of crack tip stress and strain field under non-linear elastic conditions
ΔJ	cyclic component of J
K_{cl}	closure stress intensity factor
K_I	stress intensity factor in mode I loading
K_{max}, K_{min}	maximum and minimum stress intensities during fatigue cycle
K_{th}	threshold stress intensity factor
ΔK	nominal stress intensity factor range ($K_{max} - K_{min}$)
ΔK_{eff}	effective stress intensity factor range ($K_{max} - K_{cl}$)
ΔK_{co}	The convergence value of ΔK at which the growth rates of small cracks begin to merge with those of long cracks
λ, z_0	the distance between a crack tip and the next grain boundary
m, m'	exponent in power law equations
m^*	crystallographic orientation factor
n	the ratio of c/b
N	number of cycles
N_i	number of cycles necessary to initiate macrocrack
N_p	number of cycles necessary to propagate macrocrack till failure
R	stress ratio (K_{min}/K_{max})
r	the distance from the crack tip
r_0	the distance between a dislocation source and a grain boundary

r_p, Δr_p	monotonic and cyclic plastic zone sizes
S	strain energy density
$S(\zeta_o)$	stress concentration ahead of the blocked plastic zone or the stress necessary to operate a dislocation source
W	remaining specimen ligament size
α	constant in the plastic zone size calculation
σ	applied stress
σ_c	the critical stress to operate a dislocation source in the next grain
σ_{cl}, σ_{max}	closure and maximum stresses
σ_f	friction stress opposing the movement of dislocations in the plastic zone
σ_{ef}	equivalent friction stress
σ_o, σ_o^*	intrinsic and equivalent intrinsic friction stress
σ_y	yield stress
τ	shear stress
γ, $\Delta \gamma$	plastic strain and plastic strain range
ν	Poisson's ratio
ζ_o	defined as $(b+r_o)/b$
ϕ	a scaling parameter correlating the predicted plastic zone size with that experimentally measured
Γ	integration path for J integral

CHAPTER ONE

INTRODUCTION

Fatigue fractures account for the vast majority of in-service failures in most engineering structures and components. They have received extensive industrial attention and academic research activity for many years. Conventional approaches to fatigue design involve the use of stress- or strain-life curves (S-N curves). Although based on total life, this approach essentially represents design against crack initiation, since near the fatigue limit, especially in smooth surfaces, the major portion of the fatigue life is spent in the formation of an engineering sized crack. However, for safety-critical structures such an approach can sometimes be dangerously non-conservative as the fatigue life of many components, especially those used in service in the as-processed condition (i.e. without any surface machining or polishing after the forming process), is controlled by crack growth from initial defects. Therefore, for such cases, the so-called defect-tolerant approach has been adopted. In this approach, the fatigue life is assessed in terms of the time, or number of cycles, to propagate the largest crack or crack-like defect (assuming the crack initiation time is zero) to failure which is usually controlled by the fracture toughness of the material. The application of this method to fatigue life prediction requires the determination of an expression for crack growth which is obtained from the relevant fatigue crack propagation data characterized, in general, in terms of the linear elastic stress intensity factor range, ΔK.

Conventionally, the crack growth behaviour for a particular material for a given application is determined from laboratory tests where testpieces containing cracks of 25 mm or so are used. However, many cracks and defects encountered in service are far smaller than this. When the fatigue behaviour of such small cracks, whose depth and length dimensions are generally less than 1-2 mm, has been studied, after pioneering work of Pearson (1975), it has been realized that, under the same nominal

1

driving force (such as ΔK), the growth rates of small cracks are frequently different from the corresponding growth rates of cracks obtained from laboratory testpieces (i.e. long cracks). In the large majority of cases, small cracks are observed to propagate faster than long cracks at the same stress intensity factor range, ΔK, and they are also found to grow at crack sizes and applied stress intensity levels which are below the long crack threshold value. Furthermore, their growth often exhibits patterns of deceleration and acceleration. The anomalous behaviour of small fatigue cracks has been attributed to a number of factors such as the interaction of small cracks with microstructure (causing growth rate acceleration and deceleration, and even crack arrest at microstructural features such as grain boundaries and inclusions), large scale plasticity, and crack closure (or lack of crack closure in small cracks).

So the use of long crack growth data in life calculations of components with small cracks or defects can lead to potentially dangerous over-predictions of fatigue life. As the lengths of small cracks and their plastic zone sizes are comparable with the microstructural unit (e.g., grain size), the characteristics of the local deformation ahead of small crack tips should be investigated and an alternative, local parameter developed to characterize small fatigue crack growth.

The main objectives of this work are to investigate the behaviour of small fatigue cracks, the influence of microstructural factors on their growth, and to find a suitable parameter to characterize small crack growth. As plastic deformation ahead of small cracks has been reported to be important for their anomalous growth behaviour, attention is paid to the measurement and analysis of these plastic zones and their relation to small crack growth. For this purpose, an experiment involving periodic plastic zone size measurements and fatigue crack growth tests has been developed. Based on experimental results and elastic-plastic fracture mechanics analysis, it was hoped to find an alternative and suitable correlating parameter for characterizing small fatigue crack growth and to set up a model to describe small crack propagation. The

2

materials for this work are based on commercial high-strength Al-Zn-Mg-Cu alloys. They are of interest to the aerospace industry due to their high ratio of strength/weight.

The next chapter of the thesis presents a literature survey relevant to the research objectives. Since the fracture mechanics approach to correlate cyclic crack advance begins with characterizing the local stress and deformation fields at the crack tip, the concepts of linear-elastic fracture mechanics (LEFM) and elastic-plastic fracture mechanics (EPFM) characterization of stress, or strain, fields ahead of crack tips are first considered. Due to the importance of plastic deformation ahead of small cracks with regard to their anomalous growth behaviour, the calculation and measurement of plastic zone sizes and shapes are then reviewed. Mechanisms of fatigue crack initiation and the description of crack propagation are presented next, and the small fatigue crack problem, including the definition of small cracks and the features of small crack growth, is then introduced afterwards. In the final section of this chapter, current models describing small fatigue crack propagation are reviewed.

The materials used, fatigue testing methods and experimental techniques employed in this study are described in chapter three. Chapter four presents and discusses the experimental results of the fatigue tests of small cracks and the effect of microstructure on their propagation. The results of plastic zone size measurement on growing small fatigue cracks and their relation with crack growth rates are given and discussed in chapter five. Based on the results of both small fatigue crack growth and the measurement of plastic zone sizes ahead of crack tips a model of small fatigue crack growth is developed in chapter six. A comparison is made between experiments and the predicted growth rates. Finally, the results are summarized and suggestions for future research work are given in chapter seven.

CHAPTER TWO

FRACTURE, FATIGUE AND SMALL CRACKS

2.1 Fracture Mechanics

Engineering components and structures inevitably contain small cracks, or flaws
which serve as stress raisers. The residual strength of high strength materials in the
presence of cracks is low. The occurrence of low stress fracture in high strength
materials induced the development of Fracture Mechanics.

2.1.1 Linear Elastic Fracture Mechanics (LEFM)

The local stress and deformation fields at a crack tip are characterized principally
through asymptotic continuum mechanics analyses where the functional form of the
local singular field is determined to within a scalar amplitude factor whose magnitude
is calculated from a complete analysis of the applied loading and geometry. For the
linear elastic behaviour of a nominally stationary crack subjected to tensile (mode I)
loading, the local crack tip stresses σ_{ij} can be characterized in terms of the K_I singular
field,

$$\sigma_{ij} = \frac{K_I}{\sqrt{2\pi r}} f_{ij}(\theta) + \cdots\cdots \qquad (2.1)$$

where K_I is the mode I stress intensity factor, r the distance ahead of the crack tip, θ
the polar angle measured from the crack plane, and f_{ij} a dimensionless function of θ.
Similar expressions exist for cracks subjected to pure shear (mode II) and anti-plane
strain (mode III). Close to the crack tip the higher order terms are negligible.
Provided this asymptotic field can be considered to be able to dominate the vicinity of

4

the crack tip over a region which is large compared to the scale of microstructural

deformation and fracture events involved, the scalar amplitude factor K_I can be

considered as a single, configuration independent parameter which uniquely and

autonomously characterizes the local stress field ahead of a linear elastic crack and can

be used as a correlator of crack extension.

For mode I type loading, the stress intensity factor K_I can be expressed as

$$K_I = Y\sigma\sqrt{\pi a} \qquad (2.2)$$

where σ is the nominal stress and Y is a dimensionless geometrical correction factor.

For a sharp crack in an infinite body, Y=1. The values of K for a wide variety of

crack and specimen configurations of engineering interest have been determined and

catalogued (Paris and Sih, 1965; Rooke and Cartwright, 1976; Broek, 1974). The

stress intensity factor K can be used in design as a measure of the stress field around a

crack. There is a critical value of K associated with fracture called K_c. It is a function

of specimen thickness as shown in Figure 2.1. Because of the desirability of a

criterion for fracture that is independent of geometry, published values of K_c are

nominally taken from the plateau of Figure 2.1 (i.e. under plane strain conditions).

Furthermore, it is important to specify the mode of loading (see Figure 2.2). Thus K_{Ic}

is defined as the plane strain fracture toughness under mode I loading. K_{IIc} and K_{IIIc}

are similarly defined for their respective modes of loading.

2.1.2   Crack Tip Plastic Zones

In equation 2.1, the elastic stress distribution in the vicinity of a crack tip shows that

as r tends to zero, stresses become infinite. However, in reality such stresses are

limited by local crack tip yielding, creating plastic zones around crack tips. The

mechanisms which govern fatigue crack growth are related to plastic strains generated

at the crack tip. For this reason, there has been a great deal of interest in the size and shape of crack tip plastic zones as one means of characterizing crack tip plastic deformation. Furthermore, from an engineering stand-point, these crack tip plastic zones can also be used as a prediction of stress state (plane stress vs plane strain) and as a judgement of the small scale yielding assumption if the size of the plastic zone is compared to the specimen or component thickness and the crack length. When small scale yielding condition is not satisfied, some fraction of the plastic zone size is often added to the true crack length to obtain an "effective" crack length for more accurate assessments of crack tip stress fields or tendencies for fracture (Irwin and Koskinen, 1963). And some researchers have even proposed direct use of estimated crack tip plastic zone sizes as correlating parameters for fatigue crack growth (Taira and Tanaka, 1972). It is desirable, therefore, to determine the sizes of crack tip plastic zones through both experimental measurements and numerical calculations.

The simplest estimate of plastic zone size is based on the elastic solution for the stresses at the tip of a sharp crack (Rice, 1967). By substituting the value of the yield strength, σ_y for σ_{ij} into equation 2.1 at $\theta=0^{\circ}$, the following expression for the plastic zone size r_p is obtained,

$$r_p = \frac{1}{2\pi} \left(\frac{K_I}{\sigma_y} \right)^2 \tag{2.3}$$

However, local yielding near the crack tip leads to a redistribution of the stresses as illustrated in Figure 2.3. Setting the areas of the two shaded regions equal to one another the following equation can be derived for a condition of plane stress, (Broek, 1974),

$$r_p = \frac{1}{\pi} \left(\frac{K_I}{\sigma_y} \right)^2 \tag{2.4}$$

6

Alternatively, both Dugdale (1960) and Bilby, Cottrell and Swinden (BCS) (1963)

derived a very similar expression for calculating plastic zone size under small scale

yielding conditions:

$$r_p = \frac{\pi}{8}\left(\frac{K_I}{\sigma_y}\right)^2 \qquad\qquad (2.5)$$

To accurately compute the elastic-plastic boundary around a crack tip, a yield condition

must be specified. The two most commonly used conditions are the Tresca, or

maximum shear stress, and the Von Mises, or maximum strain energy. When

applying these conditions to a two-dimensional problem, either plane strain or plane

stress must be specified. The extent of the plastic zone as a function of θ for a von

Mises yield criterion is given as (Broek, 1974)

$$\text{Plane stain:} \quad r_p(\theta) = \frac{K^2}{4\pi\sigma_y^2}\left(\frac{3}{2}\sin^2\theta + (1-2\nu)^2(1+\cos\theta)\right)$$

$$\qquad\qquad (2.6)$$

$$\text{Plane stress:} \quad r_p(\theta) = \frac{K^2}{4\pi\sigma_y^2}\left(1+\frac{3}{2}\sin^2\theta + \cos\theta\right)$$

where ν is Poisson's ratio. The boundary of the plastic zones as predicted by

equation 2.6 is shown in Figure 2.4 (a). On the basis of equation 2.6, the Von Mises

plastic zone is of the shape as shown in Figure 2.4 (a). The plane strain plastic zone is

appreciably smaller than the plane stress plastic zone. If the Tresca yield criterion is

used, the plastic zone shape is slightly different and slightly larger than the Von Mises

zone, see Figure 2.4 (b). More accurate analyses of plastic zones, by considering

yielding and stress redistribution within the zone, indicate that the farthest point of the

plastic boundary should be at an angle $\theta = 69^\circ$ (Tuba, 1966). This conclusion, as well

as the prediction of plastic zone shape, has been more or less confirmed by

measurement of plastic zones by Hahn and Rosenfield (1965). Similar analyses can

be made for mode II and III cracks.

7

The stress states at the surface and in the interior of a plate are different. At the surface, plane stress is dominant. As the depth penetration increases, the stress state changes over to plane strain. Consequently, the plastic zone gradually decreases from the plane stress size at the surface to the plane strain size in the interior of the plate, as illustrated schematically in Figure 2.5.

For LEFM to be applicable to the particular loading conditions, the extent of local plasticity must be small compared to the extent of the K_I-field, which is itself small compared to the overall dimensions of the body (including the crack length). The plastic zone can be considered as merely a small perturbation in the linear elastic field, and the K_I-field can be assumed to dominate the region around the crack tip. This situation, known as small scale yielding, occurs only when the size of the plastic zone is at most one-fifteenth of the in-plane dimensions of the crack length and depth of remaining ligament (Suresh and Ritchie, 1984).

In addition to theoretical estimates of plastic zones at crack tips, numerous measurement techniques have been used, including etching (Hahn and Rosenfield, 1965), X-ray microbeam (Tanaka, 1975), microhardness testing (Bathias and Pelloux, 1973), transmission electron microscopy (Wilkins and Smith, 1970), Moiré Interferometry (Nicoletto, 1989), stereoimaging (Davidson, 1979), and electron channelling patterns (Davidson and Lankford, 1980). Since the first discovery of the phenomenon of electron channelling in 1967 by Coates (1967), it has found application first in crystal orientation determination and then in the study of material deformation (Stickler, Hughes and Booker, 1971). The use of electron channelling patterns to map out crack tip plastic zone boundaries is comparatively a new technique. There are three principal advantages associated with this technique. Firstly, the plastic zone measurement can be made on a bulk specimen. Secondly, plastic zones can be measured accurately down to ≈ 5 μm in diameter. Thirdly, this method is very

sensitive to plastic deformation and a minimum equivalent tensile plastic strain of 0.3% can be detected with this method, (Davidson, 1984). The last two advantages are especially useful in the measurement of plastic zones of small cracks which possess small plastic zone sizes.

For fatigue cracks, in addition to the plastic zone mentioned above (called the monotonic plastic zone) there is a reversed or cyclic plastic zone, the smaller region of material within the monotonic zone where material is plastically deformed in compression upon unloading to minimum load. An estimate of the size of this zone was made by Rice (1967). He employed a superposition argument to demonstrate that, under reversed loading, the yield stress should be replaced by two times its value and the loading parameter replaced by load reversal. For zero-maximum loading, the size of the reversed plastic zone can be estimated as

$$\Delta r_p = \frac{1}{\pi}\left(\frac{\Delta K_I}{2\sigma_y}\right)^2 = \frac{1}{4\pi}\left(\frac{K_{max}}{\sigma_y}\right)^2 = \frac{1}{4} r_p \qquad (2.7)$$

Based on this model, the ratio of the reversed to monotonic plastic zone sizes for zero-maximum loading is predicted to be 0.25.

It needs to be pointed out that, although plastic deformation occurs ahead of a crack, LEFM still works for these materials provided the stress and strain fields outside the plastic zone are only slightly perturbed by the presence of small amounts of yielding. Indeed deformation inside the plastic zone can occur whilst the elastic fields outside the zone differ only slightly from the values occuring in the absence of yielding. In this small scale yielding regime, the elastic field looks almost identical to the solution for a crack in a perfectly elastic material, the only difference being that the field appears to correspond to a crack slightly longer than the crack actually is (Irwin and Koskinen, 1963).

2.1.3 Elastic Plastic Fracture Mechanics (EPFM)

Because there are applications where the small scale yielding assumption is not valid, elastic-plastic fracture mechanics parameters, whose applicability is equally valid in the presence of either small scale or large scale yielding conditions, have been proposed. The best known are the crack tip opening displacement (CTOD) (Wells, 1963; Bilby, Cottrell and Swinden, 1963) and the J integral (Rice, 1968).

The CTOD concept is based on the fact that, when the net section is near to yielding, additional applied stress affects only the crack tip strains, not the crack tip stresses. Consequently, the crack tip blunts and there is a critical value of this separation displacement required for crack advance. In the case of small scale yielding condition where $\sigma/\sigma_y \ll 1$, the elastic solution for the crack tip opening displacement (CTOD) can be used. There is a relation between CTOD and stress intensity factor K for the case of LEFM,

$$CTOD = (1-\upsilon^2)\frac{K^2}{E\sigma_y} \qquad (2.8)$$

where E is Young's modulus and σ_y is yield strength. Once a critical CTOD is reached, fracture will take place. Since CTOD can be taken as a measure of the intensity of the elastic-plastic crack tip field and can be considered to be equal to the number of dislocations entering the plastic zone multiplied by the Burgers vector (Lardner, 1968; Eastabrook, 1984), it has been used to correlate rates of fatigue crack growth through cyclic CTOD, i.e. ΔCTOD (Eastabrook, 1984; Tanaka et al, 1986; Navarro and de los Rios, 1988). The main problem in verifying this approach is the experimental difficulty of measuring the separation of the crack faces at the crack tip, especially for small cracks.

The J integral (Rice, 1968), which is path-independent, was derived for non-linear elastic materials as an expression for the rate of change of potential energy per unit thickness with respect to an incremental extension of the crack and is defined by the following line integral around the crack tip.

$$J = \int_{\Gamma} w \, dy - T \frac{\partial u}{\partial x} \, ds \qquad (2.9)$$

where T is the traction vector, u is the displacement vector in the x direction, w is the strain energy density, y is perpendicular to the crack line and Γ is a path that goes from the bottom crack surface to the top in an anti-clockwise direction, see a schematic diagram in Figure 2.6. Physically, J is a measure of the potential energy change associated with the growth of a crack in a non-linear, elastic solid. Because J is path-independent, any convenient path may be chosen to integrate over as long as the crack tip is surrounded. As a result, J is easier to calculate than CTOD.

Although strictly J is defined for a non-linear, elastic materials, it can nevertheless be applied to elastic-plastic materials. The main reason for this is that the stress-strain behaviour of non-linear, elastic materials and elastic-plastic materials is the same if the stress is monotonically increased. If the stress is decreased, of course, the stress-strain curve for a non-linear elastic material would retrace its path while the stress-strain curve for an elastic-plastic material would decrease linearly to some permanent offset. This raises difficulties when J is applied to fatigue. For elastic-plastic materials, J loses its potential energy interpretation, but retains physical significance as a measure of the crack tip strain field.

2.2 Fatigue

2.2.1 Introduction

Fatigue is the progressive, localized permanent structural change that occurs in a material subjected to cyclically varying stresses. The maximum applied stress values are usually much less than the tensile strength of the material. Fatigue in metals usually involves the following consecutive stages:

(i) initial cyclic damage in the form of cyclic hardening or softening

(ii) nucleation of initial microscopic flaws (microcrack initiation)

(iii) coalescence of these microcracks to form an initial fatal flaw (microcrack growth)

(iv) subsequent macroscopic propagation of this flaw (macrocrack growth)

(v) final catastrophic failure or instability.

In engineering terms the first three stages, involving cyclic deformation and microcrack initiation and growth, are generally classified together as (macro-) crack initiation, implying the formation of an 'engineering sized' detectable crack. Thus the total fatigue life N can be defined as the sum of the cycles needed both to initiate a crack, N_i, and to propagate it till final failure, N_p, i.e.

$$N = N_i + N_p \qquad (2.10)$$

In fatigue design, there are basically two approaches: the conventional approach (design against crack initiation) and the defect tolerant approach (design against crack propagation). Conventional approaches to fatigue design involve the use of S-N curves (stress v. number of cycles) as well as suitable adjustment to take consideration of other factors, such as mean stress, stress concentrators, variable amplitude loading, multiaxial stresses, environmental effects and so on. Although based on total life, this

approach, which is in widespread use, particularly in the automotive industry, essentially represents design against crack initiation, since near the fatigue limit, especially in smooth specimens, most of the fatigue life is spent in the formation of an engineering sized crack. For safety-critical structures, especially those with welded components, the approach is different. There has been a growing awareness that the presence of defects in a material below a certain size must be assumed and taken into consideration at the design stage. Under such circumstances the lifetime of a structure is the number of cycles spent in crack propagation. Since the crack initiation stage will be short, the use of conventional approach to fatigue design may lead to dangerous overestimates of life. Such considerations have led to the adoption of the so-called defect tolerant approach in which the fatigue life is assessed in terms of the time, or number of cycles, necessary to propagate the largest undetected crack to failure. This approach, the only one used for certain applications in the nuclear and aerospace industries, relies on the integration of an expression for crack growth.

2.2.2 Fatigue Crack Initiation and Early Growth

Fatigue cracks often initiate at or near notches, sharp scratches, pores, second phase particles or embrittled grain boundaries, on or just below the surface of materials. These microstructural singularities act as stress raisers and hence facilitate crack initiation by increasing the local stress amplitude. Microcracks may be initially present as from welding, heat treatment, or mechanical forming. However, even when the surfaces of metals are highly polished, the metal is flaw free and no stress concentrators are present, a fatigue crack may still form due to a sufficiently high alternating plastic strain amplitude. If the alternating stress amplitude is high enough, plastic deformation, i.e., dislocation motion will take place. When a dislocation emerges at the surface, a slip step of one Burgers vector is created which may increase in size under continued cycling in a local region leading to severe roughening of surface. When the process is stopped and polished surfaces are examined, many slip

13

bands can be observed. While most of these are removable easily by electropolishing, some required extensive electropolishing for removal and when the specimen is retested, slip bands form again in these places. These are called "persistent slip bands" (PSBs), the term which was first introduced by Thompson et al (1956). The role of slip bands in fatigue crack initiation has been known since the pioneering work of Ewing and Humphrey (1903) who used metallographic observation to study fatigue crack initiation and propagation. Nucleation of microcracks by slip bands is attributed to the creation of surface roughness by to-and fro slip along prominent slip bands. Forsyth and Stubbington (1957) observed intrusion-extrusion pairs (ridges and grooves) associated with PSBs in an Al-Cu alloy, and they stated that sometimes cracks developed at the intrusions. Cottrell and Hull (1957) suggested a simple model for forming an intrusion-extrusion pair, which is shown in Figure 2.7. In this model sequential duplex slip is proposed to occur. In the first half cycle, first one, and then the other, slip system is imagined to operate, giving two slip steps of the same sign. During the second half cycle, the first slip system is imagined to operate again and then the second slip system giving rise to an intrusion and extrusion pair, as shown in Figure 2.7. The literature on slip band crack initiation has been reviewed by Forsyth (1969), Frost et al (1974), Fine and Ritchie (1979) and Fine and Kwon (1986).

Forsyth (1961, 1963) proposed that the mechanism of crack growth occurs by two physically different processes, designated stage I and stage II. Stage I cracking results from dislocation motion along a slip plane, as mentioned above, and is determined by the magnitude of the resolved shear stress on the slip plane. Thus, cracks form preferentially on those planes which are closely packed and which are oriented in maximum shear stress directions. In polycrystalline metals, stage I cracks generally extend for only a few grain diameters before crack propagation changes to stage II. Stage II cracks grow on planes which are normal to the maximum principal tensile stress operating on the component.

14

Although the above slip initiated mechanism indicates that the nucleation and early growth of cracks should occur as stage I, it has been observed that, when a fatigue crack nucleates at an inclusion in high strength alloys, it grows in a stage II fashion even within a single grain. Fatigue cracks in 7075-T6 Al-alloy studied by Lankford (1982, 1983) are examples of this kind of crack.

2.2.3 Fatigue Crack Propagation

Considerable research has gone into fatigue crack propagation. Reliable crack propagation relations will permit the implementation of a defect-tolerant design philosophy which recognizes the inevitability of cracks in engineering structures and aims to predict the fatigue life of a structure, or a component, at a certain applied load. Fracture mechanics analysis of subcritical crack propagation is based on the concept that a parameter such as the stress intensity factor, K, derived from an elastic stress analysis of a stationary crack, describes the remote loading and geometry effects on the crack tip stress field. In the elastic case the stress intensity factor is a sufficient parameter to describe the whole stress field at the tip of a crack. When the size of the plastic zone at the tip is small compared to the crack length, the stress intensity factor may still give a good indication of the stress environment of the crack tip. If two different cracks have the same stress environment, i.e. the same stress intensity factor, they behave in the same manner and exhibit equal growth rates. Most expressions for describing fatigue crack growth are generally based on the original Paris-Erdogan power law relationship (1963):

$$da/dN = C \, \Delta K^m \quad\quad\quad\quad (2.11)$$

where C and m are experimentally determined scaling constants, da/dN is the crack growth increment per cycle, and ΔK is the alternating stress intensity factor range

given by the difference between maximum and minimum stress intensities in the fatigue cycle ($\Delta K = K_{max} - K_{min}$). Fatigue crack growth data are usually presented in the form of $\log(da/dN)$ vs $\log(\Delta K)$ plots, typically showing the sigmoidal curve, as seen from Figure 2.8. In its simplest form, the semi-empirical equation 2.11 provides a reasonable description of growth rate in the so-called intermediate range of growth rates, typically between 10^{-6} and 10^{-3} mm/cycle. In fact, due to its success in many practical applications, equation 2.11 is now incorporated in design codes. However, it underestimates propagation rates at higher values of ΔK, as final instability is approached, but overestimates propagation rates at lower values of ΔK approaching the so-called long crack fatigue threshold stress intensity factor range ΔK_{th}.

Due to the permanent tensile plastic deformation left in the wake of a propagating fatigue crack, as well as other factors, premature contact between the crack faces can occur even during the tensile portion of the fatigue cycle. Thus the effective stress intensity factor range ΔK_{eff} at the crack tip will be less than the applied ΔK so that:

$$\Delta K_{eff} = K_{max} - K_{cl} \qquad (2.12)$$

where K_{cl}, larger than K_{min}, is the stress intensity factor at which the two fracture surfaces first come into contact during the unloading portion of the stress cycle. The mechanisms that cause crack closure have been reviewed by Suresh and Ritchie (1984) as constraint of surrounding elastic material on the residual stretch in material elements previously plastically strained at the tip (plasticity induced closure), the presence of corrosion debris within the crack (oxide induced closure), and contact at discrete points between faceted rough fracture surfaces where significant inelastic mode II crack tip displacements are present (roughness induced closure). These mechanisms of crack closure are illustrated schematically in Figure 2.9. It has been

16

proposed by Elber (1971) that the fatigue crack propagation rate is governed by the

effective stress intensity factor range ΔK_{eff} as

$$da/dN = C (\Delta K_{eff})^m \hspace{3cm} (2.13)$$

ΔJ and $\Delta CTOD$ have also been proposed to correlate fatigue crack growth rates in

those cases where ΔK fails to predict crack growth rates primarily due to the presence

of large scale yielding. Similar power law equations as equation 2.11 have been

suggested using ΔJ and $\Delta CTOD$ as correlating parameters for fatigue crack

propagation.

2.3 Small Fatigue Cracks

The observations of Pearson (1975) and Kitagawa and Takahashi (1976) have drawn

attention to the fact that the fatigue crack growth behaviour of small cracks differs in a

non-conservative manner from expectations based upon long crack behaviour. The so

called small crack problem is that small cracks behave differently from long cracks

mainly in the following three aspects: (i), in the large majority of cases, small crack

growth rates exceed those of long cracks at the same nominal stress intensity range

ΔK; (ii), at low growth rates, small cracks are observed to grow at stress intensities

below the long crack threshold ΔK_{th}; (iii), some small cracks exhibit decaying growth

rates until arrest, while others propagate quite rapidly to merge with long crack growth

data. The problem therefore has practical significance, because damage-tolerant

fatigue lifetime computations are usually based on long crack data. As overall life is

most influenced by low growth rate behaviour, the accelerated and sub-threshold

extension of small flaws can lead to potentially dangerous over-predictions of life.

2.3.1 Definition of Small Fatigue Cracks

There are three kinds of small cracks as categorized by Suresh and Ritchie (1984):

(i), Microstructurally small cracks: cracks which are of a length comparable to the scale of the microstructure (e.g. of the order of the grain size). Thus the traditional LEFM assumptions that the material is homogeneous and isotropic are invalid.

(ii), Mechanically small cracks: cracks which are of a length comparable to the scale of the local plasticity. This implies a breakdown of the small scale yielding assumption of LEFM.

(iii), Physically small cracks: cracks which are simply physically small (e.g. ≤ 0.5-1 mm).

Most investigations to date have focused on the first two factors, which represent, respectively, a continuum mechanics limitation and a LEFM limitation to current analyses. The fatigue cracks studied in this work are both microstructurally and mechanically small.

2.3.2 The Behaviour of Small Fatigue Cracks

The propagation behaviour of long fatigue cracks is uniquely determined by the range of the stress intensity factor ΔK. However, when the crack length is small, the growth rate is no longer predictable from conventional ΔK-based fracture mechanics methodology. Small cracks can grow up to several orders of magnitude faster than long cracks under nominally the same ΔK. Furthermore, small cracks are observed to grow at stress intensities below the long crack threshold and frequently exhibit deceleration, or retardation, during their growth. The growth curves for small and long cracks converge at a certain value of ΔK. All these features associated with small

18

crack growth have been schematically illustrated by Lankford and Davidson (1986), see Figure 2.10. In addition, the threshold condition for no growth for small and long cracks are different, with small cracks being associated with a constant stress $\Delta\sigma_{th}$ and long cracks being associated with a constant stress intensity ΔK_{th} (Kitagawa and Takahashi, 1976), see Figure 2.11. Ritchie and Lankford (1986) have stated that the so called small crack problem is in essence one created by fracture mechanics through a breakdown in the similitude concept at small crack sizes. The similitude concept implies that, for two cracks of different sizes subjected to the equal changes in the value of stress intensity factor range (under small scale yielding) in a given material-microstructure-environment system, crack tip plastic zones are equal in size and stress and strain distributions along the borders of these zones (ahead of the crack) are identical, and equal amounts of crack extension Δa are to be expected (Suresh and Ritchie, 1984). However, this concept of similitude can not be applied when

(i) crack sizes approach the local microstructural dimensions

(ii) crack sizes are comparable with the extent of local plasticity for non-stationary flaws

(iii) through thickness, out of plane stresses (which are independent of K) are different

(iv) crack extension mechanisms are different

(v) extensive fatigue crack closure is observed

(vi) external environments significantly influence crack growth,

Most of these concerns are specific to the small crack problem and thus contribute to differences in the growth rate behaviour of long and small cracks at nominally identical driving forces (ΔK).

2.3.3 Reasons for the Breakdown of LEFM in the Characterization of Small Crack Growth

There are a number of reasons which have been reported to be responsible for the anomalous behaviour of small cracks. Here only three well accepted main reasons are addressed.

2.3.3.1 Large Crack Tip Plastic Zone Size

The usual description of the stress field ahead of a crack as a function of K is based on the assumption of small scale yielding. So it is assumed that the plastic zone is small compared to all length dimensions (thickness, crack length, remaining ligament), and small with respect to the distance over which the first term of the elastic stress field solution is dominant. For long cracks, the above condition is fulfilled and therefore K can uniquely determine the deformation field around crack tips and therefore can be successfully used to predict crack growth rates. For small cracks, however, a large plastic zone compared to crack length usually occurs ahead of the crack tip. This has been attributed to the high ratio of applied stress/yielding stress which is quite commonly used in small fatigue crack growth experiments (Suresh and Ritchie, 1984; Lankford et al, 1984; Tanaka et al, 1986; Chan, 1986), neglecting high order terms in the description of K (Allen and Sinclair, 1982), a specimen surface effect due to less constraint occuring at the surface on plastic deformation (Leis et al, 1986; Nicholls and Martin, 1990) and a microstructural effect with a lower effective yield (or friction) stress from "soft" grain(s) when a crack length is short (Chan, 1986; Tanaka et al, 1986; Sun et al, 1991).

There have been many numerical calculations of plastic zone size and shape ahead of small fatigue cracks (Chiang and Miller, 1982; Zhang and Beevers, 1992; Blom et al, 1986; Ritchie et al, 1987). All estimates indicate large plastic zone size compared to

20

crack length. Experimental measurement of these plastic zones has been carried out using electron channelling patterns (Lankford et al, 1984; Nicholls and Martin, 1990) and the stereoimaging technique (Morris et al, 1985). It has been reported by Lankford et al (1984) that the ratio of plastic zone size to crack depth approached unity when the crack length was comparable with microstructural dimensions. But so far, only limited data of plastic zone size measurement on small fatigue cracks is available and all measurements were carried out at relatively long crack lengths (over 100 μm).

2.3.3.2 Continuum and Isotropic Medium Limitations

Another condition for the successful use of K is the continuum medium assumption. In case of cracks with long fronts this requirement is satisfied on the average. However, if the crack front is short (on the order of several grains), this condition will generally be violated. This will result in sensitivity of small crack growth to crystallographic orientation. Crystallographic orientation undoubtedly has an important role both in determining the deceleration and acceleration growth pattern of small cracks and fast small crack grow rates. It has been widely reported that the deceleration, or arrest, of small crack growth is associated with the blocking effect of grain boundaries (e.g. Tanaka et al, 1981; Morris et al, 1981; Lankford, 1982; Akiniwa et al, 1988). When a small crack tip approaches a grain boundary, its growth rate will decelerate, or even arrest, if the orientation in the neighbouring grain is not favourable for the propagation of the crack. If it is favourable, however, the crack can readily pass through the boundary and less deceleration, or negligible deceleration, can be observed. Here, the so-called "blockage" of grain boundary on the growth of small cracks, as claimed by Lankford (1985), has little to do with the character of grain boundary per se, but the relative misorientation between neighbouring grains. He observed the role of barriers of grain boundaries to small crack growth in his work on Al 7075-T6 (1982).

Based on the theoretical analyses by Bilby et al (1977) and Cotterell and Rice (1980), Suresh (1983) has given an alternative interpretation for the interaction between crack tips and grain boundaries which results in the progressive deceleration of small cracks below the threshold stress intensity value for long cracks. He calculated the extent of reduction in the effective driving force as a result of crack deflection of various degrees at grain boundaries. For example, for a typical small crack emanating from the surface at an angle of $\theta_0 \approx 45^\circ$ and deflected at the grain boundary by $\theta_1 \approx 90^\circ$ (Figure 2.12), he showed that the resulting reduction in the effective driving force at the crack tip was about 78%. He postulated that if the deflection is large, the effective stress intensity range may be reduced to a value smaller than the true threshold for small crack growth (e.g. to the fatigue endurance limit) so that complete crack arrest will result. If the effective stress intensity ranges after deflection are above such threshold values, however, there would be no crack arrest and only a temporary deceleration in growth rate.

It is also found that microstructurally small cracks whose plastic zone is less than the grain size often prefer to propagate along crystallographic planes (stage I growth), which, in turn, contributes to the fast growth rates of small cracks compared to long cracks at the same ΔK (Brown and Hicks, 1983; Blom et al, 1986; Ritchie and Lankford, 1986; Tokaji and Ogawa, 1990; Plumtree and O'Connor, 1991). Small cracks grow crystallographically because their small size enables them to follow the slip planes which have the least resistance to cyclic slip (Suresh, 1983). As this path has less resistance, small cracks grow very quickly. By metallographic observation of crack path topography, Blom et al (1986) found that small fatigue cracks initially grow in stage I with fast growth rates compared to long cracks at the same ΔK. As the crack length increases, their growth first changes to crystallographic stage II (zigzagging growth along segments of crystallographic planes), and finally to conventional stage II. The transition from stage I to stage II growth was believed to be related to a characteristic crack length for a given material. LEFM can only be used beyond this

22

characteristic crack length. According to their explanation, the so-called small crack problem is related with the characteristics of stage I growth of small fatigue cracks.

2.3.3.3 Crack Closure

Following the early work by Elber (1970), it is now well established that the "driving force" for fatigue crack propagation is reduced by the crack closure effect. Both experimental measurement (Breat et al, 1983; Morris and Buck, 1977) and theoretical calculation (Newman, 1982) indicate that there is a difference in crack closure response between small and long cracks. When a crack is small, its wake is not fully developed, hence its opening load is much lower than that for an equivalent long crack possessing a steady-state wake. The lower crack closure stress associated with small crack length appears to be an important factor for the increase of effective stress intensity factor in the near threshold behaviour of small cracks, especially for physically small cracks. However, for microstructurally small cracks, it is now apparent that closure does not provide the entire solution, since their growth rates are still faster than long cracks even at high stress ratios. On the other hand, it was reported by Lankford and Davidson (1986) that, according to their measurements, the ratio of opening to maximum cyclic load (P_{op}/P_{max}) is roughly constant at about 0.5 for microcracks of all sizes. It is about the same ratio obtained for long cracks growing at cyclic stress intensities above the transition region. Hence, they claimed, small and short cracks are equivalent in terms of the effect of crack closure so there must be other contributing factors for the fast growth rates of small cracks.

2.3.4 Microstructural Effects

A number of models have been put forward to explain the growth minima of small crack growth by considering grain boundary blocking of small crack propagation (Hobson, 1982; Lankford, 1982; Eastabrook, 1984; Tanaka et al, 1986; Navarro and

de los Rios, 1988). These models all predict that increasing grain size will lead to faster crack growth rates in the small crack regime, as indicated schematically by Lankford (1982) in Figure 2.13, in marked contrast to long crack propagation behaviour where materials with large grain sizes possess high threshold stress intensity factor ranges ΔK_{th}. The experimental evidence for such a grain size effect on small crack propagation rates is somewhat less consistent however. Support for the models comes from the work of Taira et al (1978), Brown et al (1984), Gerdes et al (1984) and Wagner et al (1986). In contrast to these results, Zurek et al (1983) observed slower small fatigue crack growth rates in larger grained material. This was attributed to the increased plasticity-induced closure for cracks growing perpendicular to the tensile axis (mode I cracks).

The distribution of precipitates can influence the crack growth rate by affecting the uniformity of slip distribution. Homogenizing slip has been found to have a deleterious effect on long crack propagation in Al-Zn-Mg-Cu alloys (Lindigkeit et al, 1981; Edwards, 1983). This is because inhomogeneous slip promotes slip reversibility in the slip bands and high closure stresses associated with the rough faceted fracture surfaces (Brown and King, 1986). For small cracks, only reversibility of slip is likely to be important as small cracks are often seen to have lower closure level. The limited experimental data in this area gives conflicting results. By investigating small crack growth rates in both under- and over-aged 7010 aluminium alloy, Bollinbroke and King (1986) found the under-aged condition, where the precipitates are easily sheared and slip is localized, shows better small crack propagation resistance than the over-aged condition, in common with the long crack results. On the other hand, it has been found that slip distribution, which is controlled both by altering precipitate size and distribution (Brown et al, 1984) and dispersoid content (Güngör and Edwards, 1989), does not significantly affect growth rates of small fatigue cracks.

24

2.4 Characterization and Modelling of Small Crack Growth

2.4.1 Characterization of Small Crack Growth

The advantage of correlating fatigue crack growth rates for long cracks using concepts of LEFM is that stress and crack length are replaced by a single unifying parameter, i.e. the cyclic stress intensity factor, ΔK. The growth rates of long cracks can be uniquely determined by a simple LEFM parameter, ΔK. However, because of the lack of similitude between small and long cracks as mentioned before, the LEFM parameter ΔK fails to correlate small fatigue crack growth. Therefore, a number of workers have tried to find an alternative, suitable characterizing parameter to correlate small fatigue crack growth. A number of tentative parameters have been proposed which can be divided into three types (Lankford et al, 1984).

In the first case, it is assumed that long crack results are basically "correct", and that small crack data should be "fixed" by sliding it over to the long crack curve through modification of the crack length term in ΔK (El Haddad, Smith and Topper, 1979; McEvily, Eifler and Macherauch, 1991), or by including into ΔK another term, ΔK_i, which accounts for the additional plasticity at the crack tip (Davidson, 1988; Davidson et al, 1991). El Haddad et al (1979) have introduced an effective stress intensity factor range, ΔK_{eff}, to correlate small crack growth. ΔK_{eff} is defined as,

$$\Delta K_{eff} = A \Delta \sigma \sqrt{\pi(a + a_0)} \qquad (2.14)$$

where A is a geometry-dependent constant and a_0 is a constant for a given material and metallurgical condition, expressed by the empirical relation

$$a_0 = \frac{1}{\pi} \left(\frac{\Delta K_{th}}{\Delta \sigma_e} \right)^2 \qquad (2.15)$$

where ΔK_{th} is the threshold cyclic stress intensity for long cracks, and $\Delta \sigma_e$ is the smooth-specimen fatigue limit. Physically, a_0 reflects the reduced flow resistance of surface grains due to their lack of constraint, but, in fact, it serves as a sort of plastic zone correction factor as Irwin (1960) proposed for the modification of K by taking plastic zone size into consideration. But when this correction was carried out to correlate the growth data of long and small cracks of 7075-T6 in inert environments, Lankford et al (1984) found it did not produce a good correlation between the two crack size regimes.

The second approach suggests that neither the small crack nor the long crack data correlate with ΔK, but that both are governed by ΔK_{eff} (Tanaka and Nakai, 1983; Ritchie and Yu, 1986; Davidson, 1988; Davidson et al, 1991). This term is related to various crack closure mechanisms. The effective stress intensity factor range, ΔK_{eff}, has been defined in equation 2.12. Since the wakes of small cracks are believed to be physically less extensive than those of long cracks, small cracks should be less affected by closure, will experience a lower crack opening load, and therefore have higher ΔK_{eff} which results in faster growth rates than that predicted according to the nominal stress intensity factor range, ΔK.

The third approach is to consider the possibility that small cracks are truly different from long cracks, at least in the context of the small scale yielding approximation. This has been suggested by Ritchie and Lankford (1986), who noted that the similitude required for the use of ΔK may be lacking. As it has been recognized that one of the main reasons for the breakdown in LEFM analyses for small cracks is the presence of excessive plasticity over distances comparable with the crack size in the vicinity of the crack tip, EPFM solutions have been proposed through the use of J-integral (Dowling, 1977; Hudak and Chan, 1986; Nicholls and Martin, 1990), crack tip opening displacement CTOD (Tanaka et al, 1986; Navarro and de los Rios, 1988;

Lankford, Davidson and Chan, 1984), plastic strain range $\Delta\gamma$ (Miller, 1985; Lankford and Davidson, 1984; Hobson, 1986), and strain energy density S (Vecchio and Hertzberg, 1985) for characterizing small crack growth. However, as mentioned in section 2.1.4, the validity of ΔJ approach is often questioned since cyclic loading for elastic-plastic material breaks a basic assumption in the definition of J that stress is proportional to the current plastic strain (Rice, 1968). Despite this, Dowling (1977) has proposed the following equation for calculating ΔJ,

$$\Delta J = 3.2 \, \Delta W_e a + 5.0 \, \Delta W_p a \qquad (2.16)$$

where W_e and W_p are respectively the elastic and plastic components of the remote strain energy density ranges. The scaling constants in the above equation, which incorporate correction factors for specimen geometry and flaw shape, were derived from equivalent linear elastic solutions. With this equation, he successfully correlated small crack growth rates with ΔJ for the data he used (1977). But it failed to rationalize the differences in crack growth rates between small and long cracks in Al-Mg-Si alloys (Güngör and Edwards, 1989).

Another alternative parameter of EPFM, CTOD, has also been used to correlate small fatigue crack growth (Eastabrook, 1984; de los Rios, Mohamed and Miller, 1985; Tanaka et al, 1986). Based on the continuously distributed dislocation model of cracks first proposed by Bilby, Cottrell and Swinden (BCS) (1963), the CTOD has been calculated in situations where slip bands are both blocked and unblocked by grain boundaries (Tanaka et al, 1986) and correlates small crack growth well, especially concerning the prediction of deceleration, and arrest, of small fatigue crack growth. By calculating CTOD for both long and small cracks at the same nominal ΔK, Lankford et al (1984) claimed that, due to the different driving force controlling CTOD, the CTOD for small cracks is much larger than that which pertains for long

cracks at an apparently equivalent ΔK. Through comparison they concluded that the use of CTOD can at least partly account for the more rapid growth of small cracks.

Although correlation of small crack growth in terms of an EPFM parameter seems necessary, even with the more appropriate characterization afforded by such fracture mechanics, it is still often apparent that small cracks propagate at somewhat faster rates than predicted (Haddad, Topper and Mukherjee, 1981; Suresh and Ritchie, 1984). It has been suggested by Ritchie and Lankford (1986) that crack closure effects must be taken into account when J is used as a characterizing parameter. They have also suggested that for mechanically small cracks, characterization in terms of EPFM (e.g., through ΔCTOD and ΔJ) may help resolve differences in growth rates behaviour between small and long cracks. For physically small cracks the consideration of differences in the magnitude of crack closure (e.g., through the use of ΔK_{eff}) appears to be the predominant correlating factor. And in the case of microstructurally small cracks all these factors may be important, plus other factors associated with local inhomogenities in the microstructure, non-uniform growth, retardation at grain boundaries, and so forth.

2.4.2 Modelling of Small Crack Growth

Accompanying the large number of experimental investigations into the behaviour of small fatigue crack growth, several small fatigue crack growth models have been suggested (Tanaka et al, 1986; Navarro and de los Rios, 1988; Chan and Lankford, 1983; Sun et al, 1991). The BCS model of continuously distributed dislocations of cracks has been used and developed for describing small crack growth. For an infinite isotropic elastic medium subject to a uniform applied stress σ, the dislocation density $f(x)$ is obtained by solving the integral equation for the equilibrium of dislocations (bounded solution),

28

$$f(x) = \frac{\sigma_f}{\pi^2 A}\left(\cosh^{-1}\left(\left|\frac{M}{(c-x)}+n\right| \right) - \cosh^{-1}\left(\left|\frac{M}{(c+x)}+n\right| \right) \right) \qquad (2.17)$$

where $M=(b^2-c^2)/c$; c is the half surface crack length; r_p is the slipband size; $b=r_p+c$; x is the distance from the crack tip; A is a constant, its value depending on whether screw or edge dislocations are being considered; n is the ratio of c/b; and σ_f is the friction stress opposing the movement of dislocations in the plastic zone. Figure 2.14 shows the dislocation distribution that represents both the crack and crack tip plastic zones in this model (Navarro and de los Rios, 1988).

From the condition of vanishing dislocation density at the tip of a slip band, that is, at $x=\pm b$, the plastic zone size r_p can be obtained as

$$n = c/b = \cos(\pi\sigma/2\sigma_f) \qquad (2.18)$$

$$r_p = b-c \qquad (2.19)$$

The crack tip opening displacement, CTOD, can be obtained by integrating $f(x)$ and setting $x=c$,

$$CTOD = \frac{2c\sigma_f}{\pi^2 A}\ln\left[\sec\left(\frac{\pi\sigma}{2\sigma_f}\right)\right] \qquad (2.20)$$

For reversed loading, ΔCTOD is determined by the following conversion:

$$\sigma \rightarrow \Delta\sigma, \quad \sigma_f \rightarrow 2\sigma_f, \quad (\ \tau \rightarrow \Delta\tau, \quad \tau_f \rightarrow 2\tau_f \quad \text{for shear loading}) \qquad (2.21)$$

Based on the BCS model, Taira et al (1979) and Tanaka et al (1986) have extended the dislocation distribution function to include the unbounded solution (a slipband blocked by a grain boundary) at the ends of plastic zones and hence modelled small crack

growth. They modelled the threshold condition and deceleration of small cracks by

considering the interaction of slip bands ahead of crack tips with grain boundaries.

They calculated the CTOD when a slip band is blocked by a grain boundary and the

plastic displacement at the crack tip, for both bounded and unbounded solutions, was

derived and expressed as a single expression (Taira et al 1978):

$$CTOD = \frac{\sigma(b^2-c^2)^{1/2}}{\pi A}\left(1-\frac{2\sigma_f}{\pi\sigma}\cos^{-1}(\frac{c}{b})\right)+\frac{2c\sigma_f}{\pi^2 A}\ln\left(\sec(\frac{\pi\sigma}{2\sigma_f})\right) \qquad (2.22)$$

After calculating the crack tip opening displacement range, $\Delta CTOD$, or crack tip

sliding displacement range, $\Delta CTSD$, for both equilibrium slipband and blocked

slipbands, they assumed that small crack growth rates have a relation with $\Delta CTOD$

given by:

$$da/dN = C(\Delta CTOD)^m \qquad (2.23)$$

where C and m are material constants. According to this model, the anomalous

growth behaviour of small cracks manifested by fast growth rates and deceleration, or

arrest, in the $da/dN/\Delta K$ relation have been ascribed. They analytically demonstrated

that when a slip band was blocked by a microstructural barrier, such as a grain

boundary, the CTOD of the crack tip will be decreased and therefore the crack will

decelerate. By applying Tanaka et al's model (1986) for anisotropic media which is

believed to be applicable for microstructurally small cracks, Okazaki (1991) recently

found that the stage I crack growth rate obtained experimentally showed a good

correspondence with the calculated $\Delta CTSD$ from the model.

Navarro and de los Rios (1988) and Sun et al (1991) have also developed the BCS

model to describe small crack growth. In their model, Navarro and de los Rios (1988)

have described small crack growth by analysing successive blocking of the plastic

30

zone by slip barriers (e.g. grain boundaries) and subsequent initiation of slip in the next grain. After analysing the stress concentration on the leading dislocation and the requirement to attain a critical stress to operate a dislocation source in the next grain, a Hall-Petch type equation was derived as:

$$\sigma_y = \frac{1}{2} m^* \sigma_0 + m^* \sigma_c \sqrt{\frac{r_0}{D}} \qquad (2.24)$$

where σ_0 is the intrinsic friction stress, D is the grain size, m^* is the orientation factor, r_0 is the distance between the grain boundary and a dislocation source in the next grain and σ_c is the critical stress to operate a dislocation source in the next grain. Based on this equation, Sun et al (1991) have proposed the concept of an equivalent friction stress σ_{ef} by taking account of consecutive microstructural grain boundary barriers, at distances of iD/2 from the crack origin and incorporated it in the calculation of crack tip opening displacement, CTOD. When plasticity spreads to iD/2, the above Hall-Petch type equation can be written as,

$$\sigma_y = \frac{1}{2} m^* \sigma_0^* + m^* \sigma_c \sqrt{\frac{r_0}{iD}} \qquad (2.25)$$

where σ_0^* is the equivalent intrinsic friction stress. Noting that σ_y is constant, rearranging terms gives the following equation

$$\sigma_{ef} = \frac{1}{2} m^* \sigma_0^* = \sigma_y - m^* \sigma_c \sqrt{\frac{r_0}{iD}} \qquad i=1,3,5,....... \qquad (2.26)$$

The equivalent friction stress was then used in the calculation of small crack CTODs and the oscillating pattern of high and slow crack growth rates was predicted. It should be noted that the above models (Navarro and de los Rios, 1988; Sun et al, 1991) all assume that once a slipband is initiated in the next grain, plastic deformation

31

will spread across the whole grain. This is contrary to some experimental results on plastic zone measurements on small fatigue cracks (Lankford et al, 1984).

2.5 Conclusions and Current Work

At first sight, it appears that the problem of small cracks is a field at the interface between linear elastic fracture mechanics dealing with macrocrack growth and classical engineering mechanics dealing with macrocrack initiation. Research on the small crack problem is not only of academic interest, but also of practical significance. Their importance derives from two factors: (1), many practical situations involve dominant cracks which spend a major proportion of their lives as "small" cracks. For example, in the fatigue tests of annealed carbon steels, about 70% of fatigue life of a plain specimen is occupied by the life in which a crack propagates from an initial size up to 1 mm (Nisitani et al, 1992); (2), the universal application of stress intensity factor K for long cracks has failed to correlate small crack growth and led to a non-conservative estimation of defect-tolerant fatigue lifetime. The excessive plastic deformation associated with mechanically small cracks, as well as microstructurally small cracks, seems to be of major influence for the breakdown in LEFM analyses for small cracks. The failure of the global LEFM parameter ΔK to characterize small crack growth, as well as the deformation feature ahead of small crack tips, indicates that a local EPFM parameter, which is based on global variables, such as the applied load, crack length, yield stress, grain size, and closure load, should be sought to correlate small crack growth. This local parameter should (i) take into account the characteristics of large plastic deformation ahead of small crack tips, (ii) reflect the difference between small and long crack growth when characterized with ΔK, (iii) predict the convergence of long and small crack growth rates at longer crack length, (iv), display the deceleration and acceleration growth pattern of small crack growth.

Hence, the present research project was designed to possess three main objectives:

32

1. Small fatigue crack growth tests

Compare the growth rates of small and long cracks at the same nominal ΔK to examine the suitability of using ΔK as a correlating parameter for small crack growth. Investigate the effects of several factors, including microstructure (such as slip distribution and grain size), stress amplitude and stress ratio, on small crack growth rates to examine small crack growth characteristics.

2. Plastic zone measurement

Examine the plastic deformation features ahead of small crack tips by measuring their plastic zone sizes and shapes by means of selected area electron channelling patterns. Develop an experiment involving periodic plastic zone measurement and fatigue crack growth testing to investigate the relation between plastic zone size and small crack growth rate, and the interaction of plastic zones with microstructural barriers and their consequent effect on small crack growth deceleration.

3. Modelling of small fatigue crack growth.

Derive a small crack growth model to explain the fast growth rates of small fatigue cracks compared with long cracks at the same ΔK and their deceleration and acceleration feature during growth.
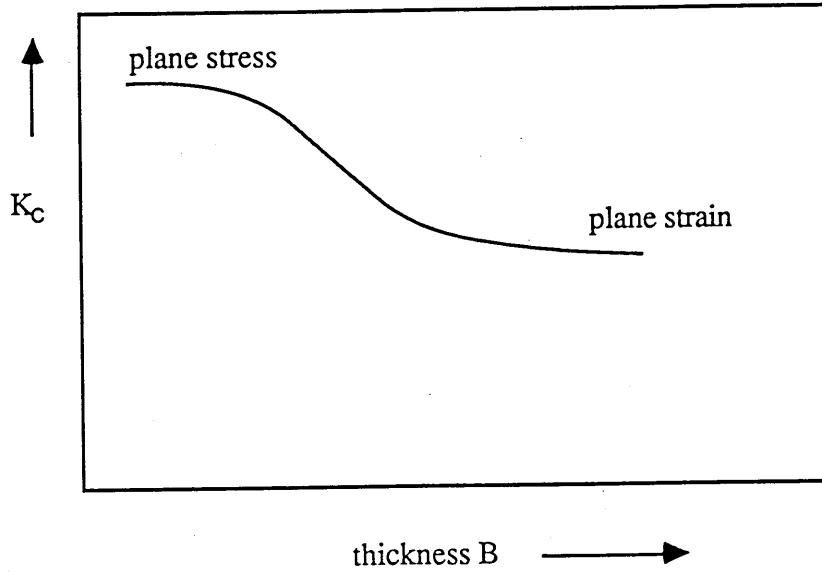
Figure 2.1   Toughness as a function of specimen thickness.

MODE   I   MODE   II   MODE   III
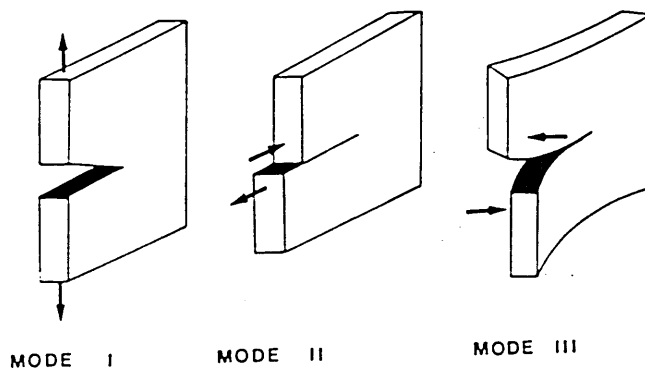
Figure 2.2   The modes of loading. Mode I opening mode. Mode II shearing
              mode. Mode III tearing mode (after Broek, 1988).
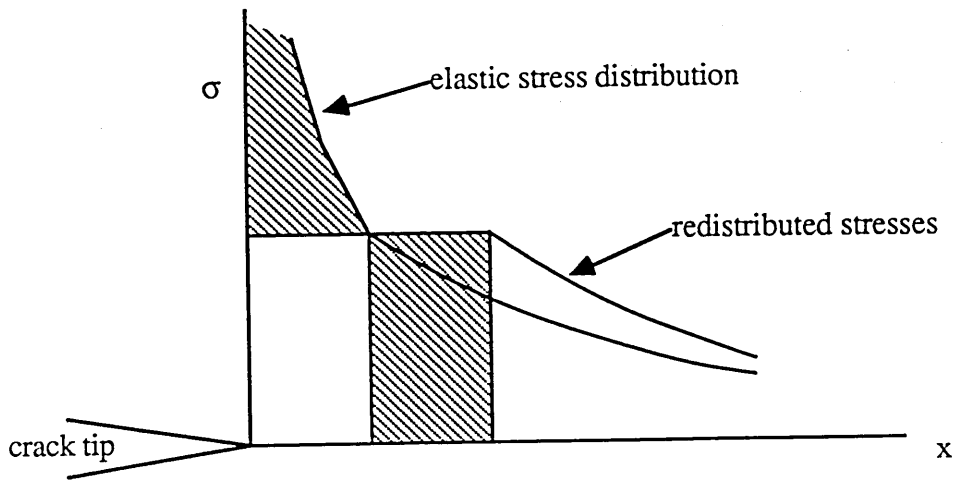
Figure 2.3   Redistribution of stress ahead of the crack tip.
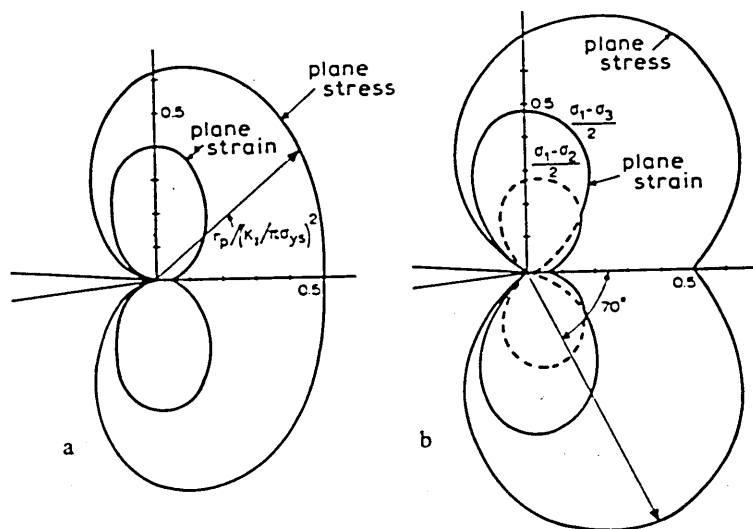
Figure 2.4   Plastic zone shapes according to Von Mises and Tresca yield criteria
a, Von Mises criterion; b, Tresca criterion (after Broek, 1974).
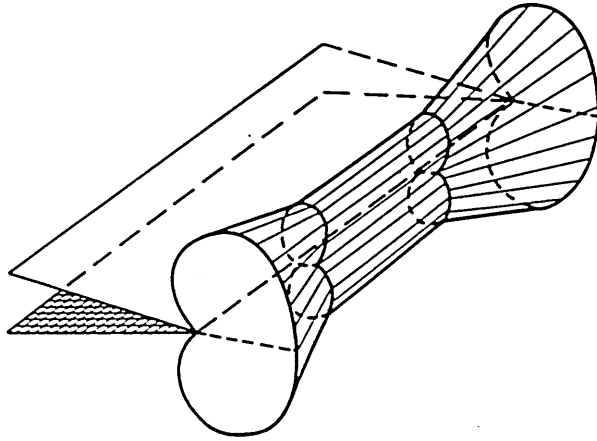
Figure 2.5   Three dimensional plastic zone (after Broek, 1974).
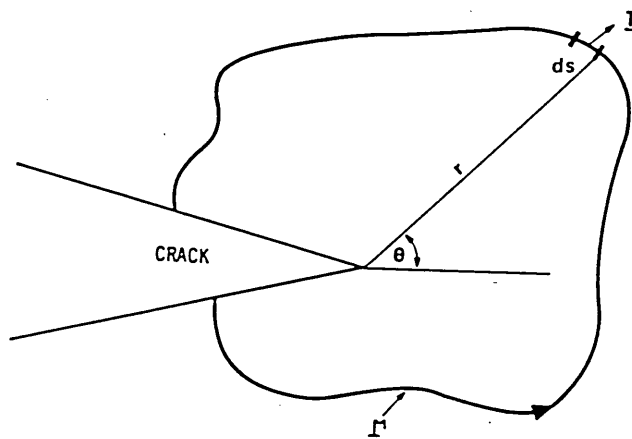
Figure 2.6   A possible path for the evaluation of J integral (after Chell, 1979).
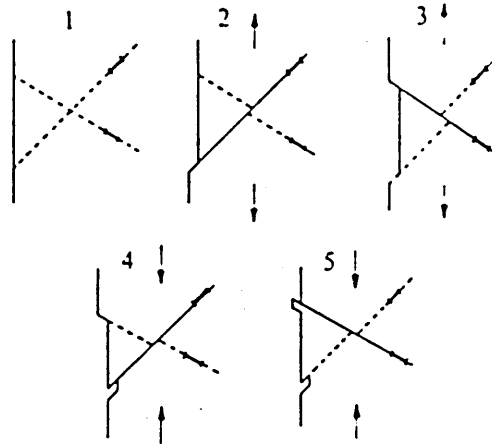
Figure 2.7   Cottrell and Hull model for formation of intrusions and extrusions (after Cottrell and Hull, 1957).
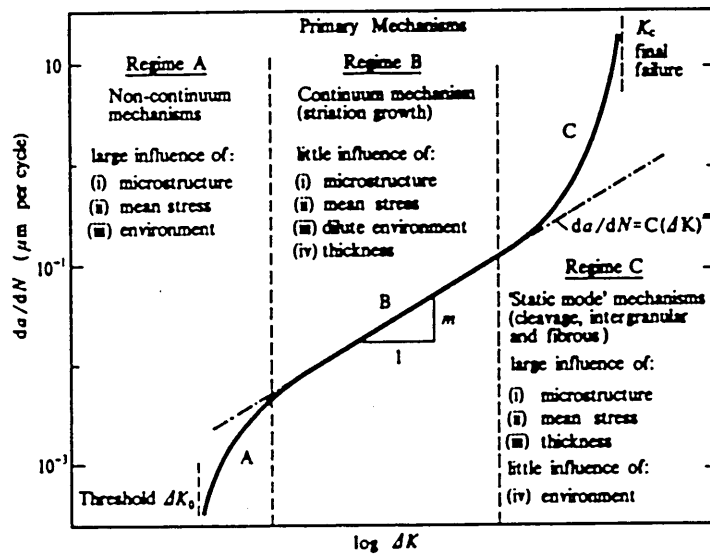
Figure 2.8   Sigmoidal curve of log(da/dN) vs log(ΔK) (after Beevers et al., 1975).

$\Delta K_{eff} = K_{max} - K_{min}$

(a)   (b)

$\Delta K_{eff} = K_{max} - K_{cl}$

(c)   (d)
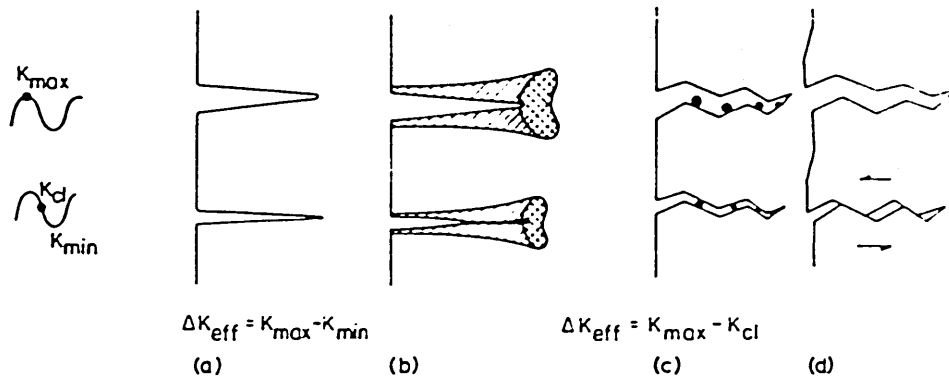
Figure 2.9   Schematic illustration of the mechanisms of fatigue crack closure (after Suresh and Ritchie, 1984)
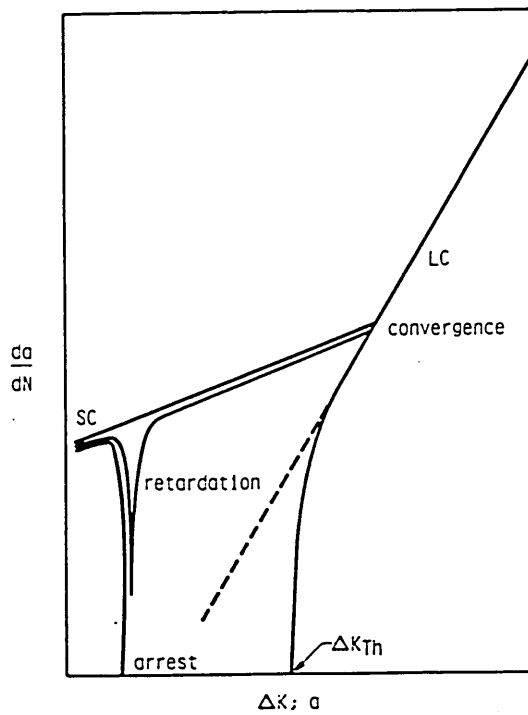
Figure 2.10   Schematic showing behaviour of small cracks (SC) versus long cracks (LC). Small cracks grow at rates above the extrapolation (dashed line) of the LC Paris regime and are subject to arrest and retardation (after Lankford and Davidson, 1986).
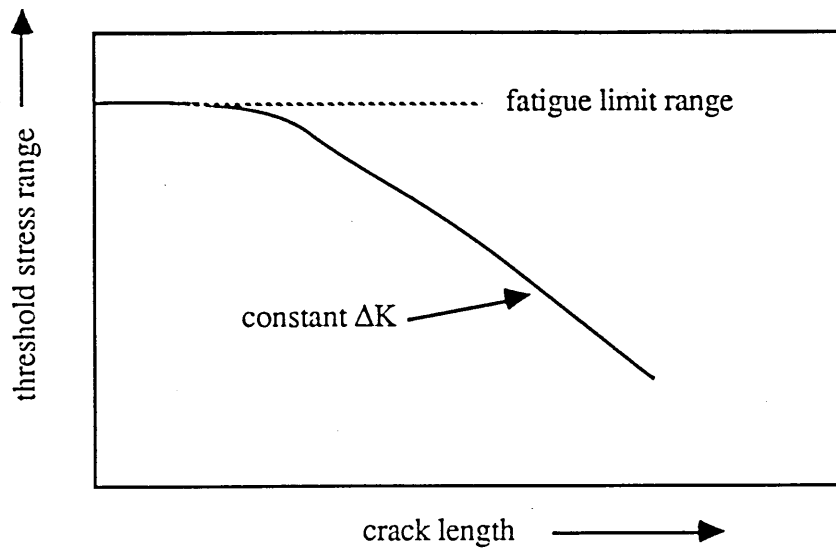
Figure 2.11   Schematic showing the variation of threshold stress range with crack length.
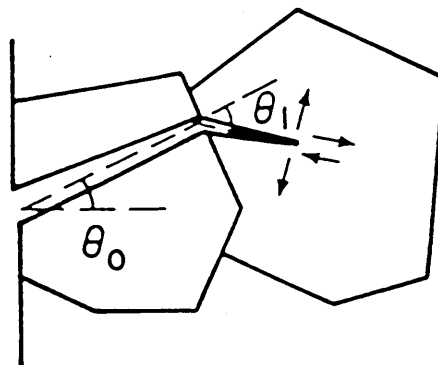
Figure 2.12   Schematic illustrating the deflection of a small crack at the first grain boundary (after Suresh, 1983).
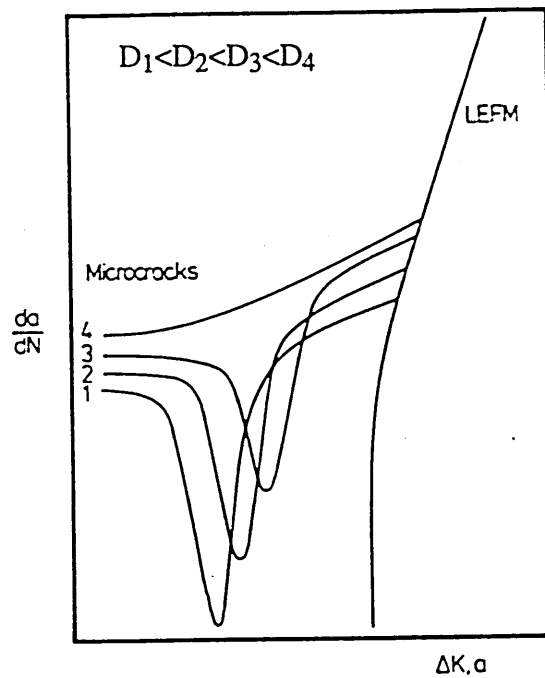
Figure 2.13   Schematic showing the dependence of crack growth rate of small cracks on grain size D (after Lankford, 1982).
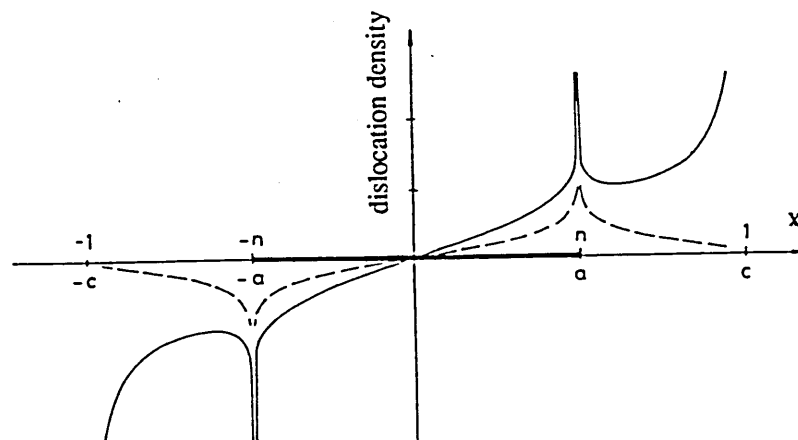
Figure 2.14   Distribution of dislocations representing the crack and crack tip plastic zones. Bounded solution (dashed line) and unbounded solution (solid line) (after Navarro and de los Rios, 1988).

CHAPTER THREE

MATERIALS AND EXPERIMENTAL PROCEDURES

3.1 Materials

The materials used in this work were four 7000 series aluminium alloys with different amount of dispersoid content. The chemical compositions of these alloys were the same as those used by Edwards (1983) who, after thermo-mechanical processing to produce comparable grain sizes in each alloy, investigated the effect of dispersoids, and hence slip distribution, on long fatigue crack propagation behaviour. The chemical compositions are given in Table 3.1.

Table 3.1. Chemical compositions of the four alloys (after Edwards, 1983).

Alloy	Zn	Mg	Cu	Cr	Fe	Si
A (ZT)	5.77	2.54	1.55	<0.01	<0.01	<0.01
B (ZL)	5.80	2.54	1.47	0.10	<0.01	<0.01
C (ZH)	5.84	2.60	1.53	0.19	<0.01	<0.01
D (ZC)	5.40	2.50	1.35	0.19	0.26	0.18

(N. B.: The code names in the brackets correspond to those used by Edwards, 1983)

3.1.1 Condition As Received

All four alloys were supplied by Alcan International Ltd with plates thickness of 20 mm. The plates had been DC cast, hot-rolled and homogenized.

3.1.2 Heat Treatment

After fatigue specimens were machined, they were separately solution treated at 460°C for one hour. They were then quenched in still water and aged to peak hardness at 125°C for 24 hours. Optical micrographs of the four alloys are shown in Figures 3.1 to 3.3. The grain sizes, in the longitudinal (L), transversing (T) and normal directions (N), were measured respectively by the mean linear intercept method and results, plus with mechanical properties of the four alloys, are given in Table 3.2. Alloy A has an equiaxed microstructure and a large grain size, while other three alloys exhibit pancake-like microstructures.

Table 3.2. Tensile properties and grain sizes of the four alloys.

Alloy	Longitudinal, (μm)	Transversing, (μm)	Normal, (μm)	Yield strength, (MPa)	U.T.S. (MPa)	ε_f (%)
A	192	185	134	495	539	18.0
B	155	80	23	522	570	16.5
C	142	68	22	527	588	16.2
D	120	50	17	516	572	15.4

3.2 Specimen Sizes and Orientation

Three kinds of specimen sizes were used. Standard and small four-point bending specimens were used for fatigue tests and tensile specimens for tensile property tests. The configuration and orientation of these specimens are given in Figure 3.4.

The dimensions of the standard unnotched four-point bending specimens are 7x12x60 mm. The advantage of this type of loading is that it provides a constant maximum bending moment between the short loading arms (Figure 3.4 (a)) so that a large area of

about 7x10=70 mm^2 on top surface of a specimen is subjected to a constant maximum tensile stress due to bending.

In order to carry out the periodic plastic zone size measurements and fatigue crack growth tests, which will be described later, small unnotched four-point bending specimens with dimensions of 5.5x3.1x26 mm were used, see the configuration in Figure 3.4(b). Since the standard specimens have an area subjected to the maximum stress which is 1.8 times the size of that in the small specimen tests, they have a higher probability for cracks to be generated and therefore shorter fatigue crack initiation lives compared to the small specimens. For example, the average number of cycles for the initiation of a crack of about 50 μm in alloy B at a stress amplitude of 210 MPa was 30,000 for the standard specimens, compared with 100,000 for the small specimen under the same testing conditions. Comparison of da/dN vs. ΔK for the two different specimen sizes were also made and good agreement was found between the two, see Figure 3.5. It indicates that the specimen sizes employed here did not affect small crack growth rates. As a result of these findings the initiation of fatigue cracks for the experiment of periodic PZS measurements was conducted with standard specimens. Another advantage of initiating small cracks with standard specimens is that the crack could be located in the centre of the small specimen, which is crucial for plastic zone size measurement as the specimen holder of the STEM used could only freely move ±1 mm in the x direction. Six of the standard specimens, once a small crack was detected, were removed from the testing machine and prepared into small specimens by electrical discharge machining. The subsequent crack growth tests, which were periodically interrupted for plastic zone size measurements, were carried out with small specimens.

All fatigue specimens were prepared with testing surfaces in the L-N plane and crack extension was measured in the normal direction, see Figure 3.4 (d). The stress due to bending was calculated using the equation:

$$\sigma = \frac{MY}{I}$$ (3.1)

where σ is the stress (MPa) at the distance Y (m) from the neutral axis, M bending moment (MPa m), I moment of inertia of specimen (m^2).

The axis of the tensile specimens, shown in Figure 3.4 (c), coincided with the L direction. The tensile tests were performed at a constant crosshead speed of 1mm/min. Load extension curves were plotted on a built-in recorder running at a speed of 50 mm/min.

3.3 Fatigue Tests

3.3.1 Specimen Preparation

After machining and heat treatment, all specimens for fatigue testing were ground and polished. Edges of all specimens were rounded-up by polishing to prevent crack initiation from the edges. Alloys C and D had large numbers of inclusions which could be removed by electropolishing. Therefore they were prepared by wet grinding on silicon carbide abrasive papers up to 1200 grade, followed by polishing with 3 μm and 1 μm diamond pastes on Texmet paper cloth. All abrading and polishing operations were along the length of the specimen to avoid introducing stress concentrations. Alloys A and B were prepared using electropolishing. This was carried out, after 1 μm diamond polishing, by using 64% ethanol, 18% perchloric acid and 18% glycerol solution. The voltage used was around 28 V at 10°C and constant agitation using a magnetic stirrer was applied. A stainless steel cathode was used. An adequate polish could be obtained in about 10 seconds. By comparison it was found that small crack growth rates were not affected by the different polishing methods.

37

3.3.2 Crack Shape Measurement

Crack geometry was determined using a crack sectioning technique. It involved progressive removal of material from the specimen top surface. Several specimens with different fatigue crack lengths were used for this purpose. At various intervals of specimen thickness the specimen was repolished mechanically, etched to reveal the cracks which were then measured. In this way a picture of the crack geometry could be built up by plotting crack length against depth of material removed, i.e. depth of the crack. This method allowed accurate measurement of crack shape and is especially useful when more than one cracks are present in a specimen. A specific example of the crack shape measurement using the crack sectioning technique is shown in Figure 3.6. The ratio of crack depth to half crack length, a/c, against crack length was plotted in Figure 3.7. It can be seen from these two figures that the ratio of a/c is approximately unity, which was also confirmed by fractography. This ratio was used in the subsequent calculation of stress intensity factor range ΔK.

3.3.3 Calculation of K

A number of solutions for calculating K of a semi-elliptical crack have been published. The Newman-Raju solution (1981) was selected in this work primarily because it has been found to be the most accurate (Mahmoud and Hosseini, 1986) and is often used by other workers for small fatigue cracks. According to the measurement of surface crack shape mentioned above, a semi-circular shape was assumed for small surface cracks of the four alloys and used in the calculation of stress intensity factor range, ΔK. Using the Newman and Raju linear elastic solution for semi-elliptical surface cracks under bending condition, the ΔK was computed as:

$$\Delta K = C \Delta \sigma \sqrt{a} \qquad\qquad (3.2)$$

38

where the parameter C is determined to be 1.18 for both the standard specimen and the small specimen, $\Delta\sigma$ is the applied cyclic stress range and a is the average crack depth calculated as

$$a = \frac{a_i + a_{i-1}}{2} \qquad\qquad (3.3)$$

The crack length used in the calculation of ΔK and crack growth increment was measured from the projection of the crack on a plane normal to the maximum bending stress.

3.3.4   Crack Growth Characterization

3.3.4.1   Crack Growth Recording and Calculation

A replication technique was used to monitor fatigue crack initiation and growth on the surfaces of specimens. To take the replicas, fatigue tests were periodically interrupted every 1,000 to 30,000 cycles depending upon the fatigue life of the specimen at the applied stress amplitude. A strip of cellulose acetate replicating tape, which was wetted with methyl acetate, was laid against the specimen surface with the crack being open at mean load to improve the accuracy to locate the crack tips. After about 7 minutes, the tape was carefully peeled off from the specimen with tweezers and stuck on another piece of acetate tape by double sided sticky tape to prevent curling. It was found (Güngör, 1990) that the acetate replicas continued to dry after removing from specimens and the shrinkage after 7 minutes replication time was only 3%. A correction was made to take this factor into account in the present crack length calculation. The resulting negative replica of the specimen surface were stored to form a permanent record of the crack growth for later examination using an optical microscope.

In order to improve the accuracy of examination of very small cracks ($\leq 20\ \mu m$), a double replica technique was used. The surface of the replica was sputtered with a thin layer of gold in a vacuum sputtering unit to make the replica conductive and resistant to the electron beam damage. It was followed by copper plating in an electrolytic solution of copper sulphate. After the thickness of the electroplated copper layer reached about 0.3 mm, the copper replica was separated from the plastic replica by dissolving the plastic in acetone. The resulting copper-backed positive gold replica was ready to be examined in SEM. Surface crack lengths, 2c, were measured on the replicas by taking the crack length as the projected length normal to the direction of maximum bending stresses, as mentioned above.

3.3.4.2 Fatigue Tests

All fatigue tests, including S-N curve determination and fatigue crack propagation, were conducted on an Instron servo-hydraulic testing machine with a 25 KN load cell at a frequency of 25 Hz and load ratio (R) of 0.1 in laboratory air. Tensile tests were also carried out on an Instron servo-hydraulic testing machine with a load cell of 200 KN. Crack growth rates (da/dN) were determined by differentiating the two adjacent data points on the crack depth (a) versus number of cycles (N). This can be expressed as

$$\frac{da}{dN} = \frac{a_i - a_{i-1}}{N_i - N_{i-1}} \tag{3.4}$$

3.4 Microscopy

3.4.1 Optical Metallography

To reveal the grain boundaries, a modified Keller's etchant was used to etch the specimens. The composition of this etchant was 2ml hydrofluoric acid, 3ml hydrochloric acid, 20 ml nitric acid and 175 ml water. Some polished specimen surfaces were anodised for microstructure observation. The anodizing solution used was 2% fluoroboric acid (HBF_4) in distilled water. The condition used was about 20 volts at room temperature using an aluminium cathode for about 20 seconds. All photographs were taken with a Reichert MeF3 microscope.

3.4.2 Periodic Plastic Zone Size Measurements By Means of Selected Area Electron Channelling Patterns

3.4.2.1 Introduction

In the scanning electron microscope, contrast can be obtained which is related to crystallographic nature of a specimen through the mechanism of electron channelling. This contrast originates from the periodic arrangement of atoms in a crystal and depends on the angular relationship between the beam and the lattice. When an impinging electron beam interacts with the planes of the crystal being illuminated, electron diffraction occurs, and as this beam is caused to sweep across the crystal, with the change of the incidence angle, diffraction conditions change. As a result, a contrast pattern, called an electron channelling pattern (ECP), results. The quality of ECP is strongly dependent on the perfection of the crystal. Any departure from lattice perfection results in a deterioration in the quality of the pattern. This has been used to delineate plastic zone size and shape ahead of fatigue crack tips (Davidson, 1984; Lankford, Davidson and Chan, 1984; Tekin and Martin, 1989). Channelling patterns

41

may be produced from a very small area in the form of selected area electron channelling patterns (SAECP). It can be achieved by rocking the electron beam about a spot on the specimen surface. This makes the technique very advantageous for the deformation studies of polycrystalline materials. SAECP have found a wide range of applications in deformation studies (Davidson, 1984), especially in measuring the plastic zone size around a crack and at a crack tip (Lankford et al, 1984; Davidson and Lankford, 1980).

3.4.2.2. Measurements of PZS

Six of the standard specimens from alloys A and B, once a small crack was detected, were removed from the testing machine for continuous measurement of their plastic zones ahead of the fatigue crack tips by means of SAECP method. To enable this, smaller specimens having dimensions of 5.5 mm in width, 3 to 3.2 mm in depth, 26 mm in length and containing the small fatigue cracks at their centre were cut from the standard specimens by electrical discharge machining. These were then re-electropolished in 20% perchloric acid + 80% methanol solution at -20°C. The solution was stirred with a magnetic stirrer during electropolishing. The applied voltage and polishing time were 15 V and about 8 seconds, respectively. The above procedure of electropolishing was found to give a very smooth polished surface and consequently intense and clear channelling patterns could be obtained in Scanning Transmission Electron Microscope (STEM).

Plastic zones were mapped by means of the SAECP method in a JEOL 2000-FX STEM using an EM-ASID-20 scanning attachment operating at 100 kV accelerating voltage. Since the plastic zone sizes of naturally initiated small cracks are very small, (less than 10 μm for very small cracks), it was crucial to know the spot size — that is the size of the area from which the information contained in the channelling pattern is taken.

This was determined by the following method. At the measuring condition, a channelling pattern was obtained in rocking mode as close to a grain boundary as possible without seeing any interaction from the boundary, i.e., keeping a single crystal orientation in the pattern. A photograph of this position was then taken in Secondary Electron Image (SEI) mode. This procedure was then repeated in the grain on the other side of the grain boundary. The distance between these two points in SEI mode was assumed to be the minimum spot size. For the present experiments this was determined to be 5 μm at a 5° rocking angle. As a further check, the spot size was estimated using the minimum particle method (Verhoeven and Baker, 1976), i.e., assuming the particle size which occupies the whole viewing screen in rocking mode to be the spot size. The two methods produced a comparable result.

In order to obtain the collimated beam condition and locate the exact position on a specimen surface which contributes to the channelling patterns in the rocking mode, the following procedure was carried out:

(1), Find a small particle of less than 5 μm in size and bring it to the centre of the scanning screen in SEI mode at high magnification.

(2), Switch to rocking mode with a rocking angle of 8°. The focusing process will increase the diameter of the particle image.

(3), During focusing, the image of the particle was moved to the centre of the screen. The collimated beam condition is obtained when the maximum image diameter of the particle is obtained.

(4). Switch back to SEI mode, the particle position corresponds to the area contributing to the ECPs in rocking mode.

Because of the small size of the cracks studied, it was difficult to directly locate them on the electropolished surface both in SEI and Back-scatter Electron Image (BEI)

modes. To aid this process, for each crack, two scratches, placed perpendicular to the crack propagation direction and about 150 μm from the centre of the crack, were made using a microhardness device with a 10 gram load. In this way, the small crack could be immediately found in rocking mode at 8° rocking angle. Then, the rocking angle was changed to 5° to achieve a small spot size suitable for the measurement of small crack plastic zones.

After each plastic zone measurement, the small fatigue cracks in these specimens were then further propagated under four point bending and periodically removed to the electron microscope for assessment of their crack tip plastic zones. The boundaries of the plastic zones were located by visually assessing the degradation of the electron channelling pattern in the deformed area by comparison with patterns from an adjacent undeformed area, normally in the same grain. The clearest indicator of degradation found was the disappearance of the fourth order line of {111} planes, which corresponds to about 0.3% equivalent tensile plastic strain (Lankford et al, 1984; Tekin and Martin, 1989). Basically, this method of plastic zone measurement is based on comparison of ECPs from areas near the crack tip to those remote from crack tip. So, the quality of the ECP from the latter case, called the background ECP here, effectively controls the sensitivity of the plastic strain measurement at the plastic zone boundaries, and consequently the accuracy of the plastic zone measurement. After sufficient electropolishing, the assessment of the quality of background ECP indicated that the maximum plastic strain was less than 0.3% equivalent tensile plastic strain (Davidson and Lankford, 1980). Taking into consideration of the eye judgement of human being, the error associated with the determination of plastic zone boundaries is around 0.5% equivalent tensile plastic strain. Multiple measurement of plastic zones associated with small cracks showed that if the PZS measurement is carried out (1), at the same condition of microscope operation (accelerating voltage, rocking angle, et al), and (2), the interval between two measurements is not long to reduce the oxidation of specimen, the ECP of PZS measurement method shows a very good reproducibility.

After locating the bounding points between deformed and undeformed area, the distance from the bounding point to the crack tip was measured directly from the screen by changing to SEI mode from rocking mode. It was found that using the digital voltmeter (DVM) attachment reading for measuring this distance would not give a satisfactory accuracy because of its mechanical drive and the smallness of PZSs measured. So they were measured in this experiment directly from the viewing screen by covering it with an acetate sheet. This procedure was repeated at no less than ten different locations ahead and around the crack tip so enabling its plastic zone to be mapped out by connecting the bounding points. Figure 3.8 shows a series of micrographs taken ahead of a crack tip. Note the change of quality in the channelling patterns on approaching the crack tip.

It was found during the experiment that tilting of specimen, to about $+20^{\circ}$, gave better contrast of ECPs, so facilitating more accurate measurement of PZS. The use of a LaB_6 filament increased the source brightness enabling use of a smaller spot size so making plastic zone size measurement more accurate. The use of brighter source and STEM with less lens aberration allowed a high resolution channelling pattern contrast to be achieved, as can be seen from Figure 3.8.

3.4.3 Fractography

The fracture surfaces of specimens and the positive copper replicas were examined by a JEOL JSM 820 scanning microscope with an accelerating voltage of 10-15 kV. Specimens for examination were cut about 5 mm below their fracture surface and mounted vertically into the specimen stubs. To ensure good mechanically stability and electrical contact with the stubs, mounted specimens were glued with a conductive glue.

L

N

(a)

300 μm

(b)

100 μm
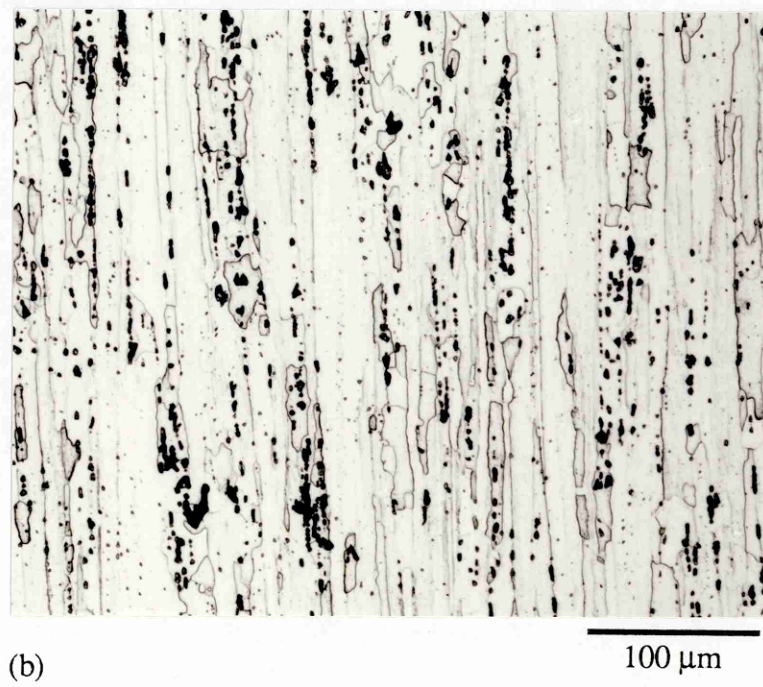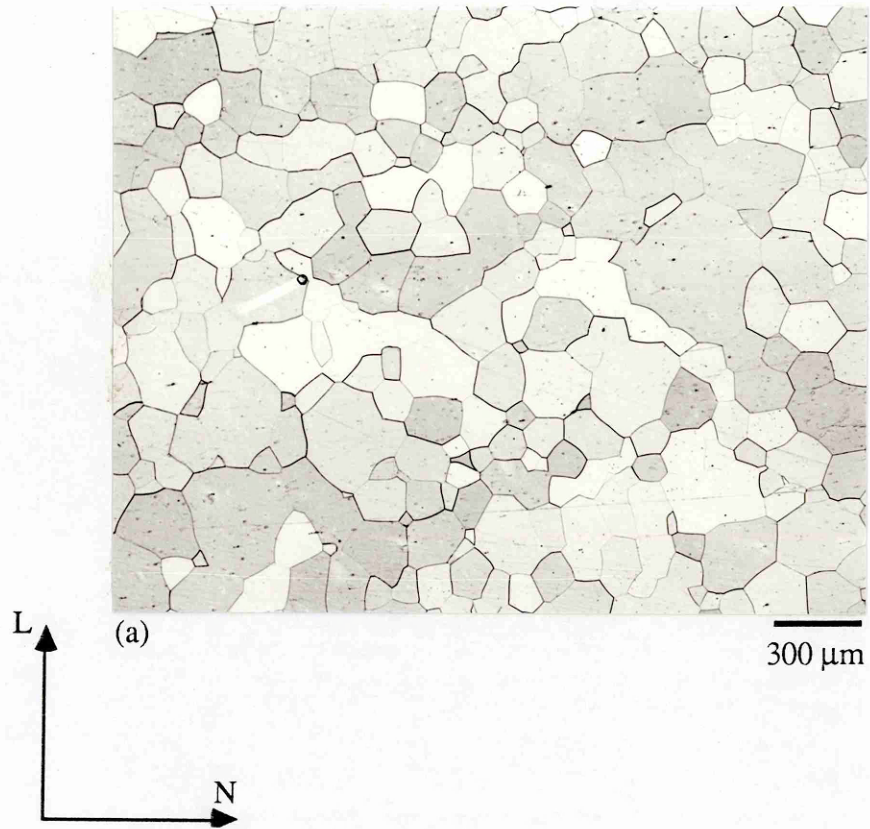
Figure 3.1   Optical microstructure of alloys A and D observed from the test
surfaces: (a), alloy A, (b), alloy D.

100 μm
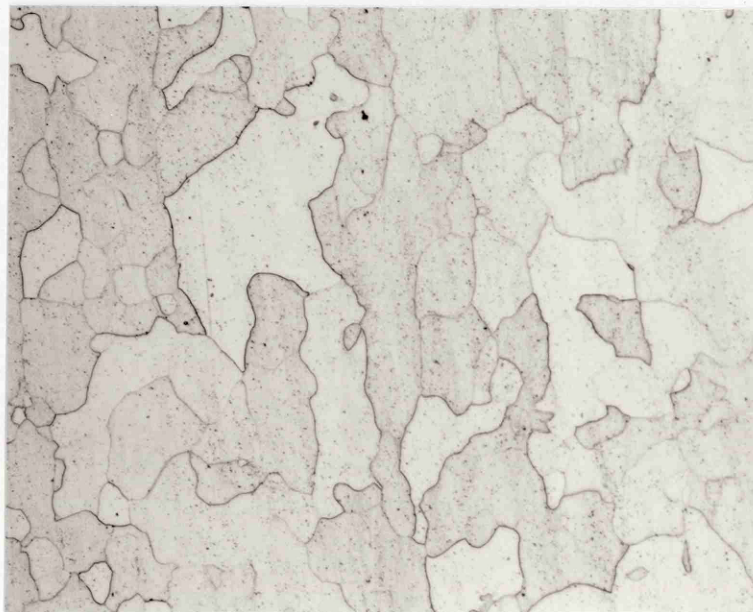
Figure 3.2   Optical microstructure of alloy B observed from: (a), L-N orientation,
(b), L-T orientation.

(a)

100 μm

(b)
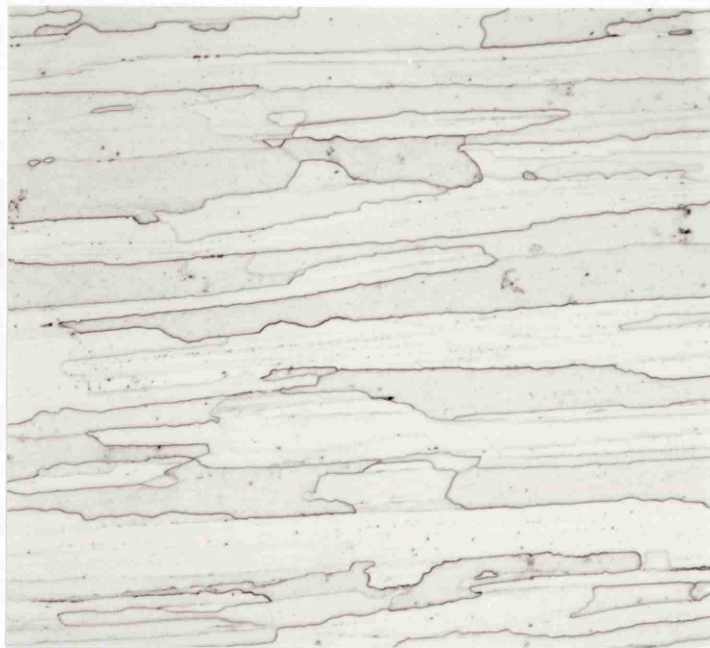
100 μm

Figure 3.3   Optical microstructure of alloy C observed from the testing surface:
(a), in normal light, (b), in polarized light, showing the grain structure.
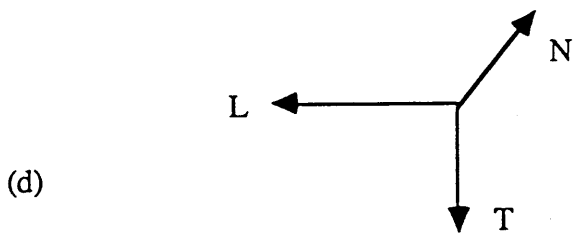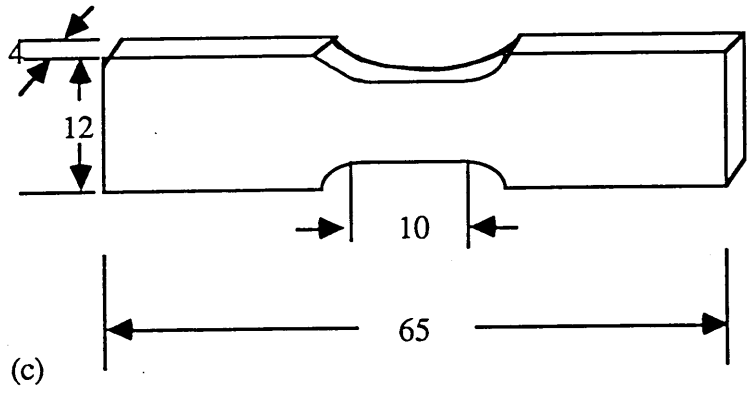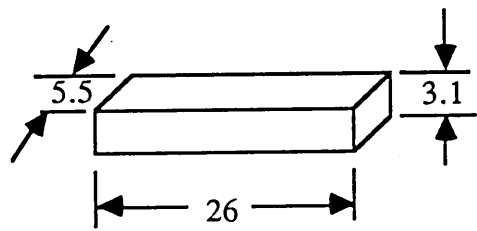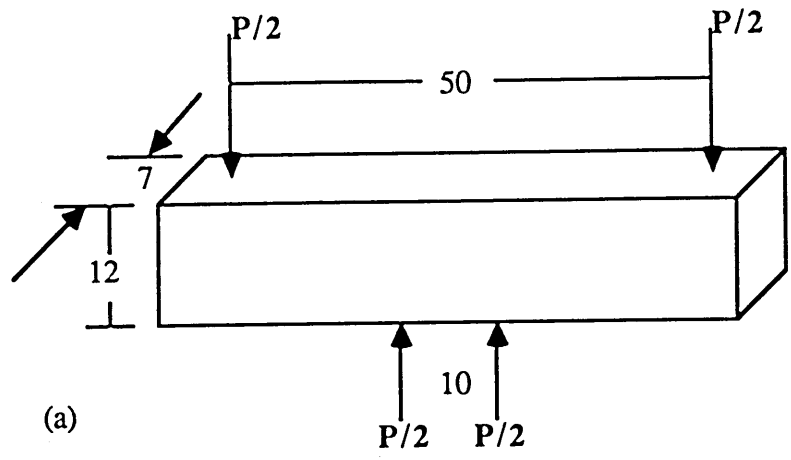
Figure 3.4   Configuration and orientation of test specimens: (a), standard
fatigue specimen. (b), small fatigue specimen. (c), tensile specimen.
(d), the orientation of test specimen.
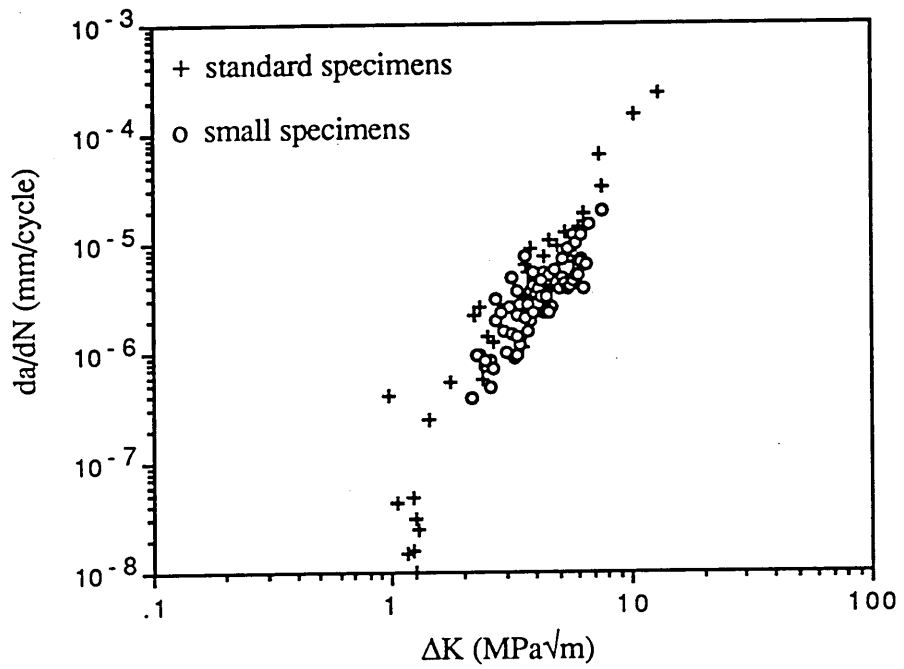
Figure 3.5   Comparison of small crack growth rates between the two different sizes of specimens.
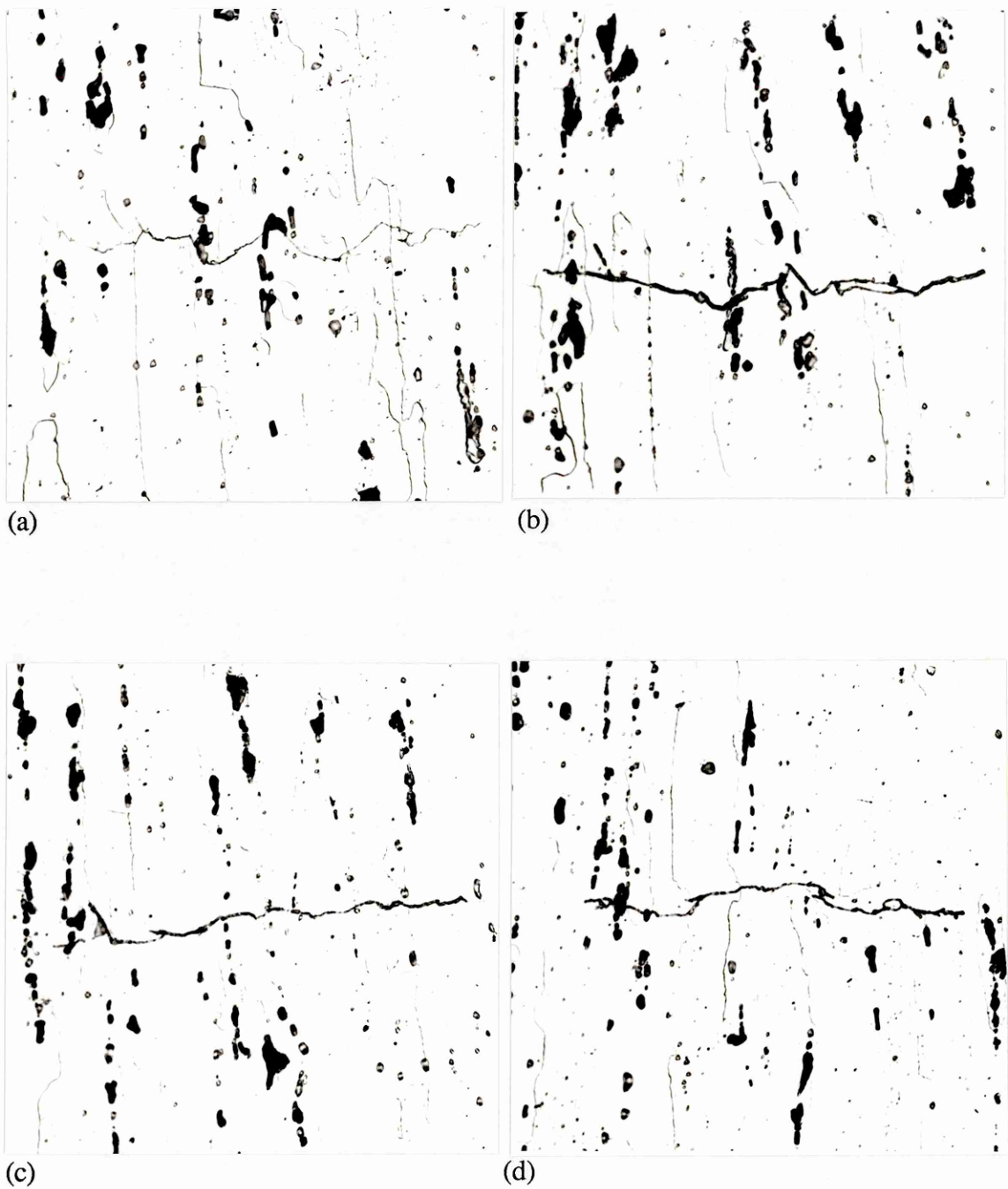
Figure 3.6   An example of crack shape measurement. (a), a=0 μm, 2c=150 μm;
              (b), a=10 μm, 2c=145 μm; (c), a=30 μm, 2c=136 μm; (d), a=50 μm,
              2c=120 μm;

(e)　　　　　　　　　　　　　　　(f)
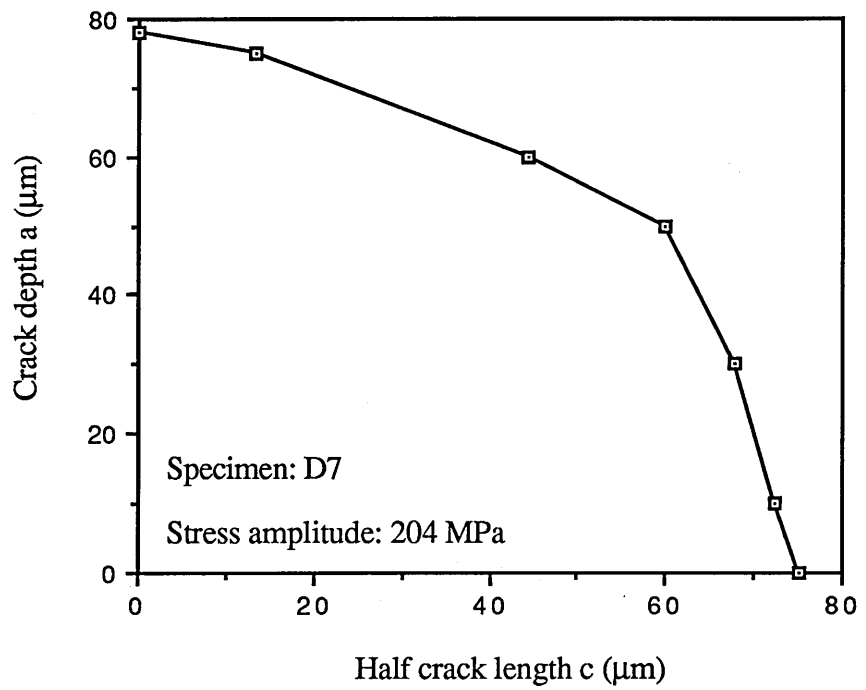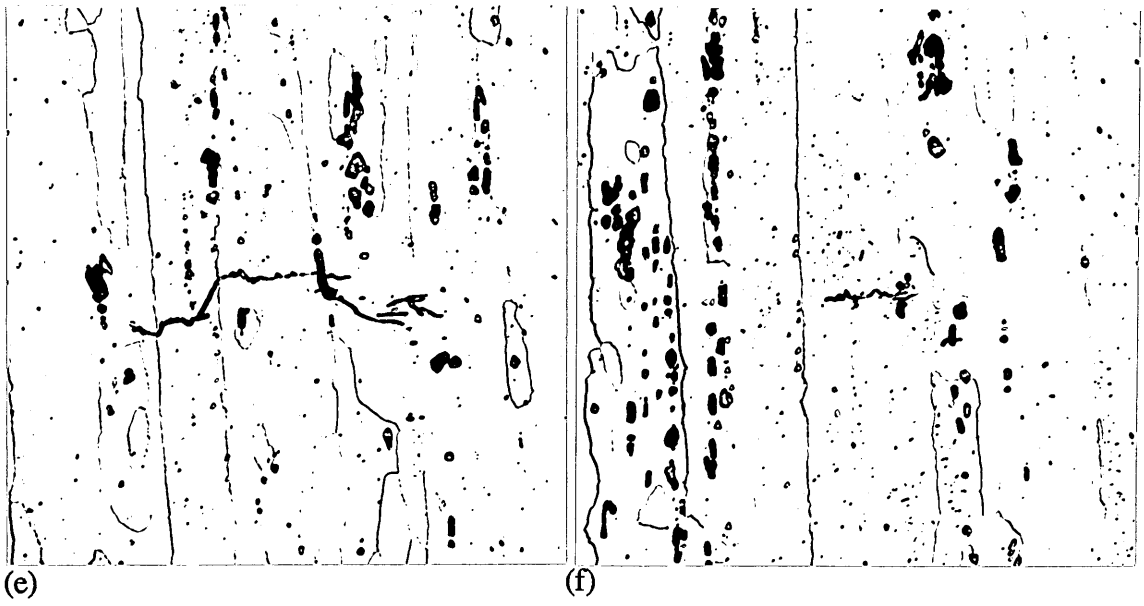
(g)

Figure 3.6 (cont.) An example of the crack shape measurement. (e), a=60 μm,

2c=89 μm; (f), a=75 μm, 2c=27 μm; (g), crack depth a plotted against

half crack length c showing the crack shape (σ_a=204 MPa).
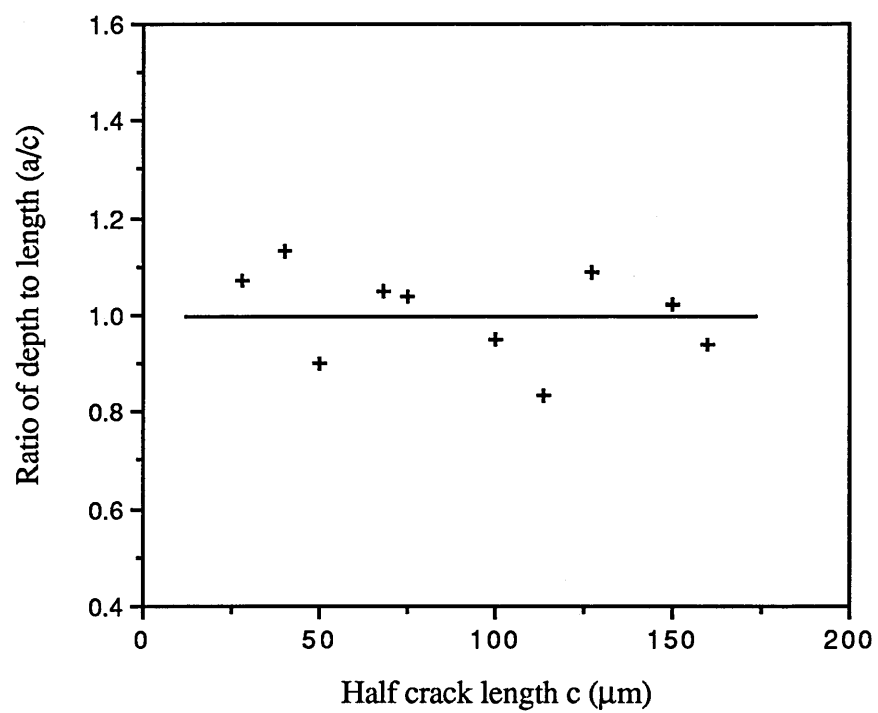
Figure 3.7   The ratio of a/c plotted against c, showing the measured result of the nearly semi-circular crack shape.
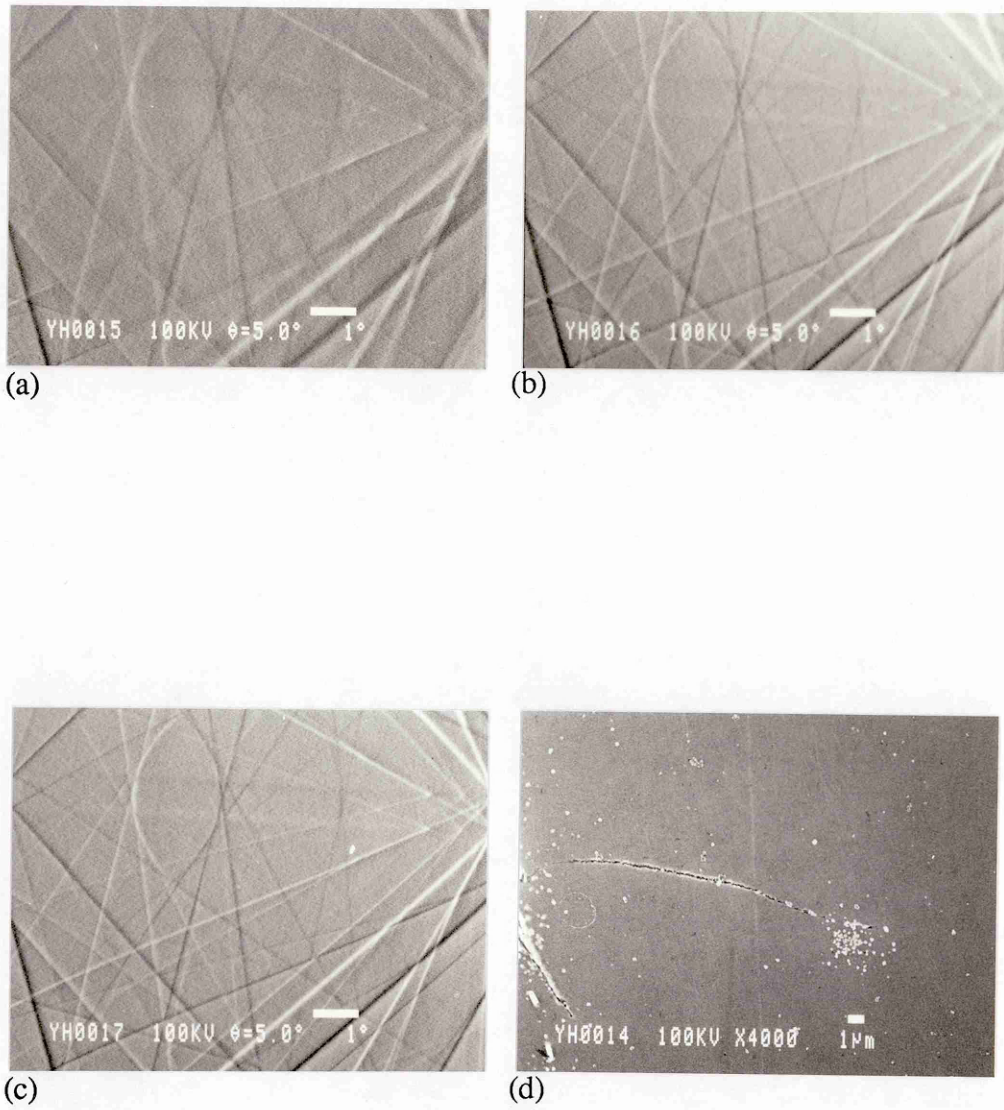
Figure 3.8   A series of channelling patterns taken ahead of a crack tip. Note the change of quality in the patterns while approaching the crack. (a), 8 μm from the crack tip. (b), 14 μm from the crack tip. (c), 20 μm from the crack tip. (d), the micrograph of the crack taken in SEI mode.

CHAPTER FOUR

EFFECT OF MICROSTRUCTURE ON SMALL
FATIGUE CRACK GROWTH

4.1 Introduction

Four 7000 series type alloys, whose chemical compositions and mechanical properties have been given in the previous chapter, were chosen for the study. Alloy A contains no transition element and thus contains no dispersoid and virtually no inclusions. It thus has a relatively large grain sizes. Alloys B and C contain increasing amount of chromium and thus have increasing volume fraction of dispersoids. Alloy D also contains iron and silicon and thus contains significant numbers of large inclusions. This chapter introduces the experimental results of small fatigue crack growth. The results will be discussed in terms of the anomalous behaviour of small crack growth. This chapter will lay the basis for the further investigation of small crack growth behaviour by the measurement of plastic zones ahead of small fatigue cracks and the subsequent modelling of small crack growth.

4.2 S-N Curves

The fatigue lives of the alloys against stress amplitude σ_a are plotted in Figure 4.1. There are basically two crack initiation mechanisms operating during the fatigue tests for the four alloys: involving either slipbands or inclusions. For alloy A which has a large grain size and almost no inclusions, slip deformation accumulates, and finally a crack will initiate from the slip band and quickly extend through the whole grain. Sometimes cracks were also found to initiate from grain boundaries. For alloy D which has a large volume fraction of inclusions, however, fatigue cracks were almost entirely initiated from these inclusions. Initiation from both slip bands and inclusions

was found in alloys B and C, but initiation at inclusions was more common in alloy C. In general, it can be seen that fatigue lives improve with dispersoid content (C>B>A), but that the addition of large number of inclusions to the microstructure leads to a decrease in fatigue lives, (alloy D).

4.3 Small Crack Growth

4.3.1 Crack Growth Rates

Small fatigue crack growth rates da/dN for the alloys are plotted against stress intensity factor range, ΔK, in Figure 4.2. It can be seen that at low ΔK range the data of small crack growth rates exhibits much scatter and shows no indication of a threshold stress intensity factor range. For comparison, long crack growth data from both Edwards (1983) for alloys with the same chemical compositions and from Lankford (1983) for a 7075-T6 aluminium alloy which is similar to alloy D in chemical composition and microstructure are also provided. As mentioned before, the four alloys in Edwards' investigation of the effect of the dispersoid content on long crack growth rates have experienced thermo-mechanical processing to produce comparable grain sizes and consequently comparable yield stress. Thus, they differ slightly from the alloys used here but are chosen to give a rough comparison with small crack growth rates via ΔK. It can be seen that the growth rates of small cracks, as widely reported, exceed those predicted by long crack data. Small cracks can even propagate at stress intensities well below the long crack growth threshold. It was also found that small crack growth often exhibited a pattern of deceleration and acceleration. However, at ΔK around 4.5 MPa$\sqrt{m}$, small crack growth rates begin to merge with those of long cracks.

The above experimental results, in particular, the fast growth rates and deceleration of small cracks, reveal that the growth small fatigue cracks can not be uniquely

47

determined using the stress intensity factor range ΔK, confirming the failure of LEFM to explain the small crack problem.

4.3.2 Effect of Stress Amplitude

Several stress amplitudes were applied in small crack growth tests to investigate the influence of mean stress on small crack growth rates. Experimental results revealed no evident effect of mean applied stress on small crack growth rates when correlated with ΔK. One example from alloy D is shown in Figure 4.3. It can be seen that although stress amplitude σ_a varies from 180 MPa ($\sigma_{max}/\sigma_y = 0.77$) to 210 MPa ($\sigma_{max}/\sigma_y = 0.91$), there is no significant influence on small crack growth rates.

4.3.3 Stress Ratio

As reviewed in chapter 2, the lower crack opening load of small fatigue cracks has been suggested to be an important factor for their fast growth rates and their ability to grow below ΔK_{th}. In order to investigate this effect, long crack growth rate data of alloys C and D tested at high stress ratio R=0.8 (Moffatt and Edwards, 1991) were compared to that of small cracks tested at R=0.1. It is expected that at R=0.8 the effect of crack closure of long cracks can be eliminated. The resultant crack growth rates were correlated with ΔK again and shown in Figure 4.4 by the circles. At R=0.8, the growth rates of long cracks are faster than those at R=0.1 at the same ΔK, presumably due to less crack closure. Through the comparison of the growth rates of small cracks at R=0.1 and long cracks at R=0.8, it can be seen that at low ΔK the growth rates of small cracks were still higher than those of long cracks. This implies that, although crack closure stress may contribute to the fast growth rates of small cracks, there must be other contributing factors for the fast small crack growth rates.

4.4   Microstructural Influence on Small Crack Growth

4.4.1   Effect of Dispersoid Content

Alloys B, C and D have similar grain sizes and strength, but possess different dispersoid contents and hence slip distribution. The comparison of growth rates of these three alloys against ΔK indicated that there is no significant difference in small crack propagation rates with dispersoid content, see Figure 4.5, showing that small crack growth is not sensitive to slip distribution. This is in agreement with the experimental finding of Güngör and Edwards (1989) and Nicholls and Martin (1990).

4.4.2   Effect of Grain Size

The effect of grain size on small crack growth can be investigated by comparing the growth rates of alloys A and B. Alloy A has a large, nearly equiaxed grain sizes of $\approx 150 \,\mu m$, while alloy B possesses a pancake-like microstructure with grain sizes of $23 \,\mu m$ and $80 \,\mu m$ in the normal and transverse directions, respectively. A comparison of their small crack growth rates is shown in Figure 4.6. It can be seen that the growth rates for the fine grained alloy B are, on average, below those for the coarse grained alloy A, although there is more scatter in the alloy A data. This is probably related to the role of grain boundaries as well as the different crack growth topography, as will be explained later.

4.5   Deceleration in da/dN Caused By Grain Boundary Interaction

One of the main features of the growth of small cracks is that they frequently exhibit deceleration, or retardation, which is believed to be associated with the blocking effect of grain boundaries. This phenomenon was often found in the present work, particularly when the ratio of applied stress/yield stress was low and the crack length

49

was less than about 5 grain diameters. Because of the L-N orientation of the testing specimens, small crack tips will reach grain boundaries on the surface before approaching grain boundaries in the depth direction, (assuming a semi-circular crack shape). This means that crack tip/grain boundary interactions observed on the surface are likely to be the first seen by the growing crack. Examples showing significant deceleration by grain boundary blocking are given in Figure 4.7 for an alloy C specimen and Figure 4.9 for an alloy D specimen. Turning first to Figure 4.7, on initial testing at σ_a=186 MPa, there was no crack detected even after 3,800,000 cycles. Subsequently the stress amplitude was increased to 196 MPa, and soon a large crack was found. By tracing back through the replicas, it was found that a small crack, 12 μm long, actually initiated from an inclusion after 120,000 cycles. The crack grew to about 17 μm after 960,000 cycles (Figure 4.7 a) and virtually had stopped growing at 3,800,000 cycles when the stress amplitude was increased. Figure 4.8 gives the corresponding growth rates of the crack before the stress amplitude was increased. By observing both the specimen surface after etching (Figure 4.7 b) and the fracture surface (Figure 4.7 c), the retarded crack tips were found in the vicinity of the grain boundaries, indicating the possibility that the crack growth was temporarily arrested by the first grain boundary.

A similar phenomena in alloy D is shown in Figure 4.9. Here, the growth minima was also found to correspond to the moment when the crack tips approached the first grain boundaries on the specimen surface. A small crack initiated from an inclusion after 20,000 cycles. Its growth rate first increased with crack length and then decelerated at a length of about 18 μm (Figure 4.9 a). It slowly grew to about 22 μm after 600,000 cycles (Figure 4.9 b) where the two tips of the crack was in the vicinity of the grain boundaries. After temporarily arresting, the crack recovered its growth rate quickly after passing the barriers of the first grain boundaries. Figure 4.10 gives the corresponding growth rate of the crack at each stage of its crack length. It is

interesting to note that the deceleration in crack growth rate actually began before the crack tips touched the grain boundaries.

The above two specific examples indicate that grain boundaries, especially from the first grain, are barriers for small crack growth and responsible for the deceleration, or even temporarily arrest, of small crack growth. It appears that the deceleration of small crack growth actually started before the crack tips reached grain boundaries. Both the etching of specimen surfaces and fractographic analyses revealed that the minima of small crack growth rates corresponded to the crack tip position where it nearly approaches the grain boundary.

Fracture surfaces of the above two specimens from alloys C and D, as well as similar evidence from alloys A and B (see Figures 4.11 and 4.12), revealed crystallographic facetting at early stages of small crack growth. The depth of this faceted regime ranged from about 70 to 150 μm, depending on the alloys and applied stresses. This suggests that the "blocking" effect of grain boundaries on small crack growth may depend on the relative crystallographic orientation between neighbouring grains. If a slip plane in the next grain is nearly parallel to that with the crack on it, the crack can easily propagate through the grain boundary into the next grain. One example of this in alloy A is given in Figure 4.13. The crack initiated from a slip band and still followed the original growth direction with no measurable deceleration on crossing the grain boundary. It can be seen that the shear deformation of the crack produced an offset at the grain boundary. More commonly, small cracks decelerated and exhibited growth path deflection on passing grain boundaries. This implies that the blocking effect of grain boundaries on small crack growth probably has little to do with the character of grain boundaries, but rather the relative misorientation between neighbouring grains. This argument is further supported by measurement of crystallographic orientation on both sides of a grain boundary in one case, as will be discussed in the next chapter.

4.6 Discussion

As widely reported, small fatigue cracks were found to exhibit fast growth rates compared to long cracks at the same stress intensity factor range, ΔK. The high crack growth rates observed in small cracks, when compared to long cracks at the same nominal ΔK and below the long crack threshold stress intensity factor range, and the discontinuous growth of small cracks have been attributed to several factors, including microstructural influences, large scale yielding, and crack closure. The following discussion will focus on these three main factors.

4.6.1 Effect of Crack Closure

Comparison of small crack growth data with those for long cracks tested at high stress ratio (R=0.8) showed that small cracks still exhibit faster growth rates than long cracks. This is in accordance with the conclusion (Wagner and Lütjering, 1987; Lankford and Davidson, 1986) that the lack of crack closure of small cracks can not wholly explain their comparatively fast growth rates. Therefore, there must be other factors which contribute to the failure of ΔK in correlating small fatigue crack growth.

4.6.2 Effect of Microstructure

Crystallographic orientation plays an important role in small crack growth. This is reflected mainly by the deceleration of small cracks when they approach grain boundaries. In the early growth of small cracks, the low restraint on cyclic slip promotes a predominantly crystallographic mode of failure, which was designated as stage I growth by Forsyth (1961). It has been suggested that the growth of small cracks along crystallographic planes is favoured (Brown 1986). As it may be assumed that a crack will always adopt the mechanism which gives the fastest growth rates, this means that initial small crack growth is often crystallographic and thus

52

following the initially fast, stage I growth of a small crack within a single grain, retardation, or even complete arrest will be observed at the first grain boundary encountered by the crack. This behaviour has been recognized by numerous workers and many explanations and models have been put forward. Most of these models are based on an assumption that for the blocked crack tip to pass a microstructural barrier, the stress concentration ahead of the blocked crack tip must be high enough to operate a dislocation source in the next grain (Tanaka et al, 1986; Navarro and de los Rios, 1988).

An alternative explanation has been suggested by Suresh (1983) who considered the effect of crack deflection on the propagation of small cracks. When a crack tip reaches a grain boundary, it tends to reorient itself in the adjacent grain to advance by the shear mechanism, and can be considerably deflected by the grain boundary. He claimed that the effective driving force for crack growth depends on the extent of the crack deflection at the grain boundary, which is a function of the relative orientation of the most favourable slip systems in the adjoining grains. All these models stress the importance of the misorientation between two neighbouring grains and relate it to the deceleration of small crack growth. However, as already mentioned the present work revealed that small crack deceleration actually started before crack tips reached grain boundaries. This suggests that, although crack deflections at grain boundaries will cause the decrease of effective driving force for small crack growth, the reason for the deceleration of small crack growth is probably, as assumed in the model of Tanaka et al (1986), related with the interaction of slip bands ahead of crack tips with grain boundaries. But this lacks experimental confirmation.

The lack of a relation between slip distribution and small crack growth has some support from the literature. By adding different amounts of dispersoid particles to an Al-Mg-Si alloy to produce varying slip distribution, Güngör and Edwards (1989) found that slip distribution has no effect on small fatigue crack growth in this series

aluminium alloys. It appears that small crack growth is not sensitive to slip distribution. However, the large scatter in small crack growth data in the low ΔK region associated with the deceleration and acceleration of small cracks makes it difficult to precisely determine the effect of dispersoid content on small crack growth.

Comparison of small crack growth rates of alloys A and B implies that grain size affects small crack growth rates. For coarse grained material, the crack can extend a comparatively long distance before it approaches a grain boundary. By that time, the local stress concentration ahead of the crack tip is comparatively high, so grain boundaries will cause less blocking effect on the propagation of the crack. A coarse grained microstructure also facilitates early crack growth in stage I, which contributes to the fast growth rates when compared to those from the fine-grained microstructure. Comparison of the growth rates of alloys A and B (Figure 4.6) confirms the schematic in Figure 2.13 from Lankford (1982), which shows the influence of grain size on small crack growth rate.

4.6.3 Effect of Large Plastic Deformation

The fast growth rates of small cracks compared with long cracks at the same stress intensity factor range, ΔK, can also be traced to the inability of K to describe the crack tip stress and deformation fields of small cracks when the extent of local plasticity is comparable with crack size. It has been suggested that it is inappropriate to use the parameter K to characterize small crack growth when the ratio of plastic zone size r_p to crack length 2c is larger than 0.1 (Smith 1977). It has been often reported that small crack growth is always accompanied with comparatively large plastic deformation ahead of crack tips both based on numerical calculations (Chiang and Miller, 1982; Zhang and Beevers, 1992; Blom et al, 1986; Ritchie et al, 1986) and experimental measurements (Lankford et al, 1984; Nicholls and Martin, 1989). This implies that the breakdown of K to correlate small crack growth could be related with the failure of

54

small scale yielding assumption for small crack problem. Since the importance of a comparatively large plastic zone size associated with small crack growth has been widely reported and few measurements of the PZS for small fatigue cracks have been attempted so that only limited data exist, it was decided to measure the PZS of small cracks.

It is worth noticing that the growth data of the small cracks studied began to merge with that of long cracks when $\Delta K \approx 4.5$ MPa$\sqrt{m}$ (Figure 4.2). The convergence of two sets of data of long and small crack growth has been observed by many researchers (Lankford, 1982; Suresh and Ritchie, 1984) and the value of the ΔK corresponding to the transition from the behaviour of small cracks to that of long cracks depends on many factors, including microstructure. It may be assumed that after converging with long crack growth data, small crack growth can be characterized by ΔK, indicating that stress intensity factor range, ΔK, can now be used to describe the stress and deformation fields ahead of the now "long" small cracks. Therefore, any successful explanation, or model, of small crack growth must be able to predict the convergence of the growth rates of small cracks with those of long cracks beyond a certain critical value of ΔK. By reviewing a number of experimental data on the growth of small fatigue cracks, Lankford (1985) concluded that the point of convergence of long and small crack growth rates corresponds to a plastic zone size approximately equal to a relevant microstructural dimension. But experimental data about plastic zone sizes of small fatigue cracks is limited (Lankford et al, 1984; Nicholls and Martin, 1990). It seems that the plastic zone size ahead of a small fatigue crack may be an important parameter. This is because: (1), fast growth rates of small cracks are nearly always believed to be related with the large plastic deformation ahead of crack tips, but few experiments on the measurement of these sizes have been carried out; (2), since CTOD seems to be a function of plastic zone size (Lankford et al, 1977) and has been used to correlate small crack growth (Tanaka et al, 1986), the plastic zone size associated with small cracks could also be used to correlate small crack growth; (3), it will decide

whether small scale yielding conditions, which is the principal assumption for the successful application of LEFM analysis, exist for small cracks; (4), it can justify the above assumption for the convergence of long and small crack growth data.

It is also of significance to obtain knowledge of the development of small crack plastic zone size and shape during fatigue tests. This can give much information on small crack growth. One particular interest is to examine the interaction of plastic zones with grain boundaries and its influence on small crack growth rates. In order to study the development of small crack plastic zones, a novel experiment of periodic plastic zone size measurement and small fatigue crack growth was developed and is described in the next chapter.
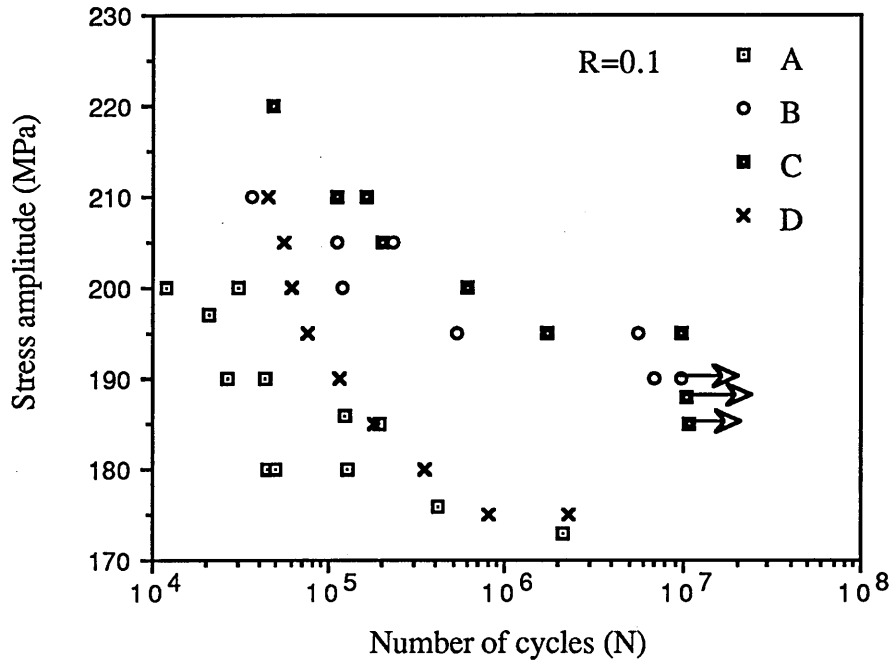
Figure 4.1   S-N data of the four alloys at R=0.1.
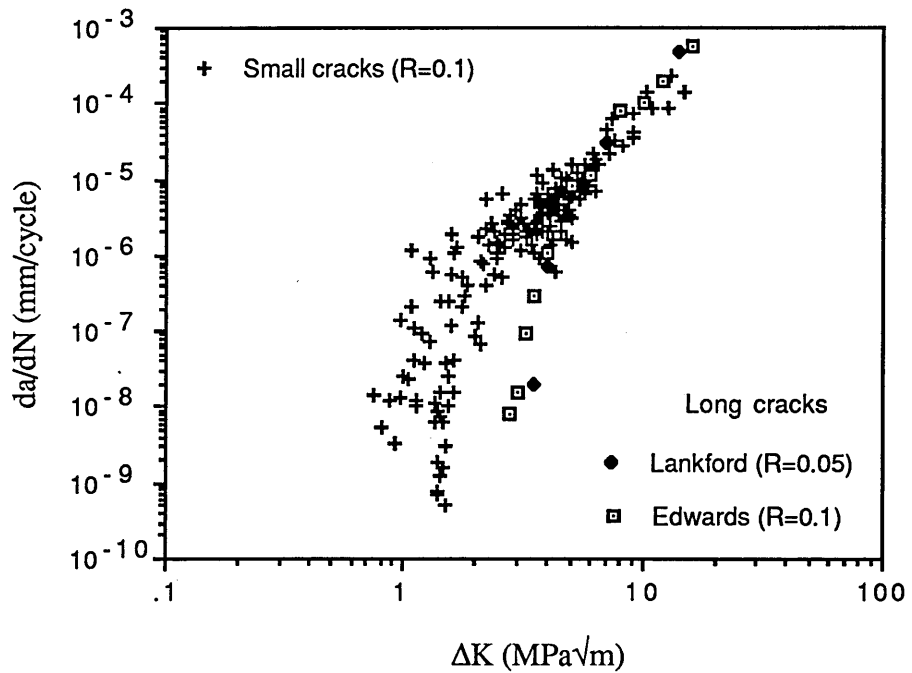
Figure 4.2   Comparison of long and small fatigue crack growth rates characterized
with stress intensity factor range, ΔK.
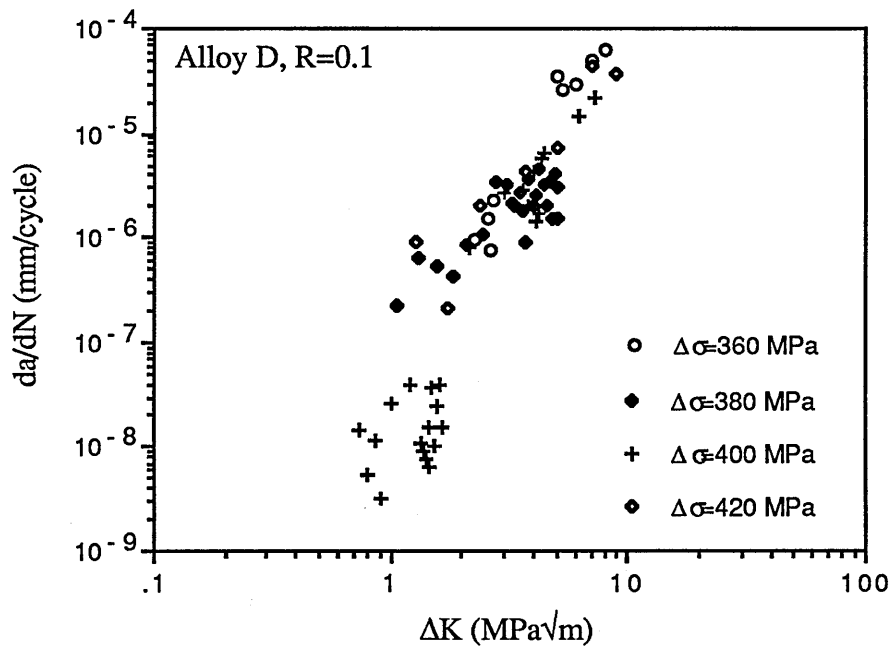
Figure 4.3   Comparison of small crack growth rates versus ΔK at different stress amplitudes.
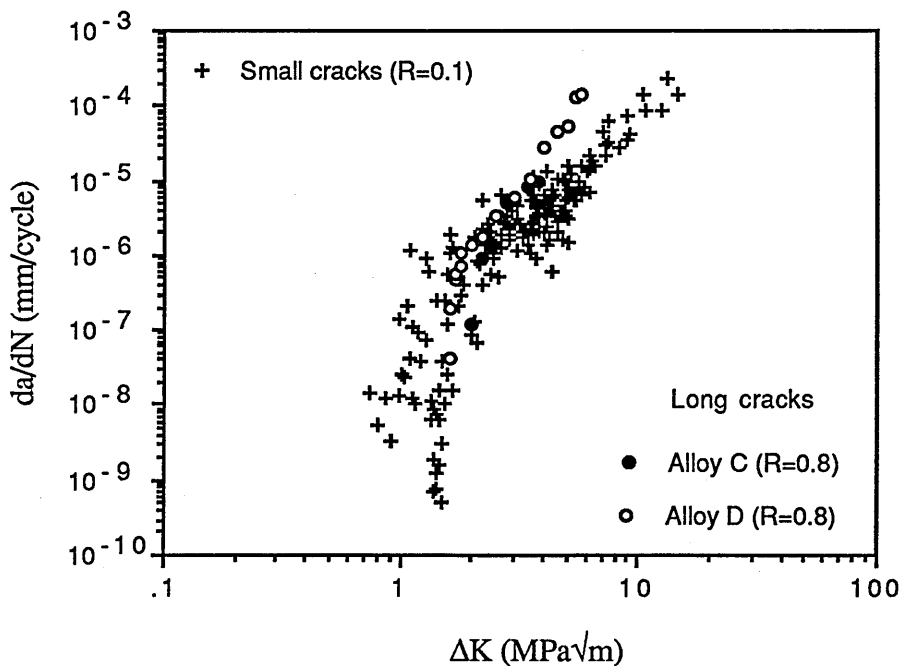
Figure 4.4   Comparison of long (R=0.8) and small (R=0.1) fatigue crack growth rates characterized with stress intensity factor range, ΔK.
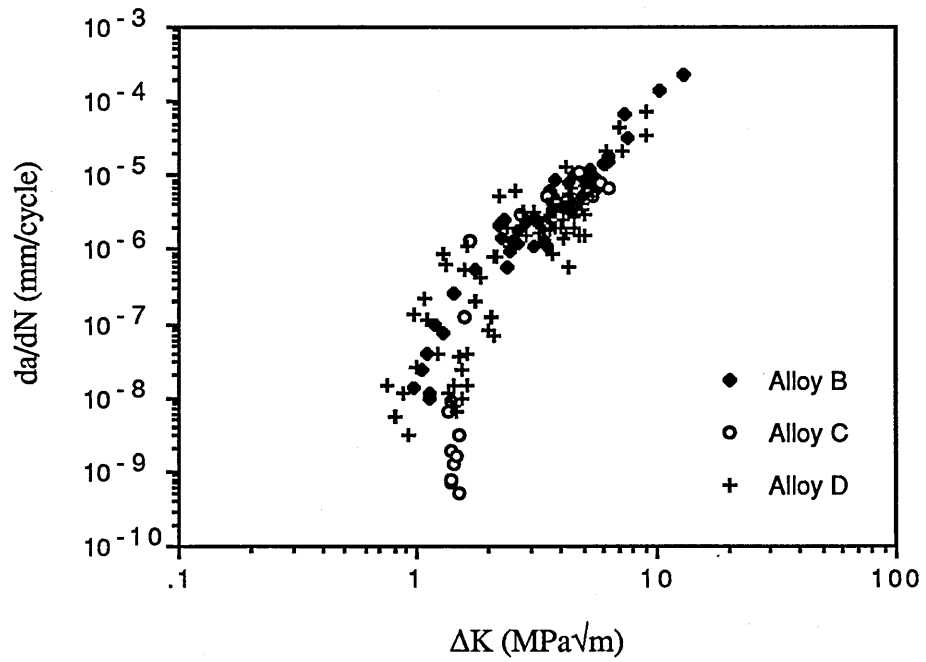
Figure 4.5   Comparison of small crack growth rates of the three alloys with different dispersoid content versus ΔK.
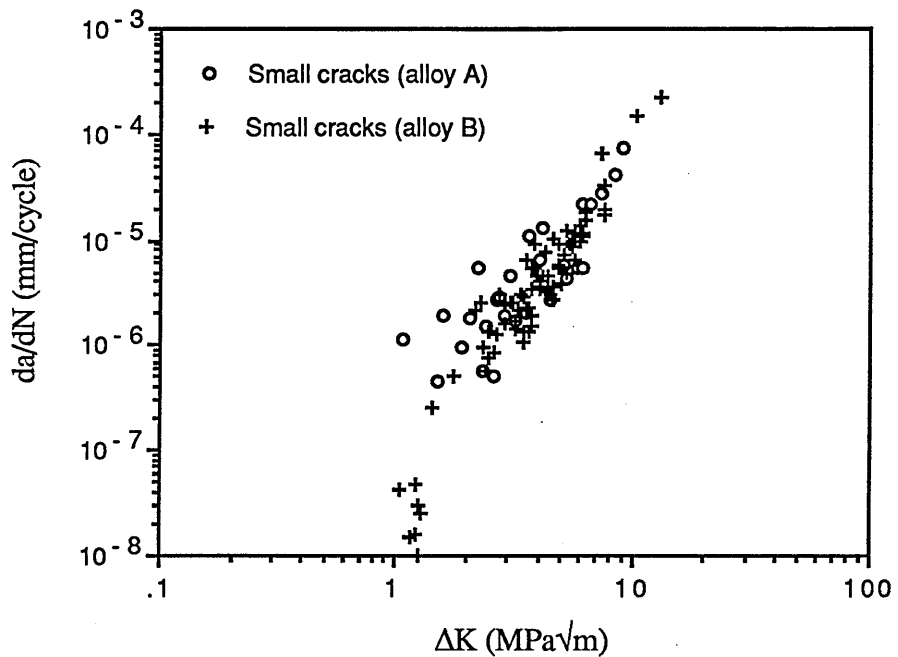
Figure 4.6   Comparison of small crack growth rates between alloys A and B.

10 μm
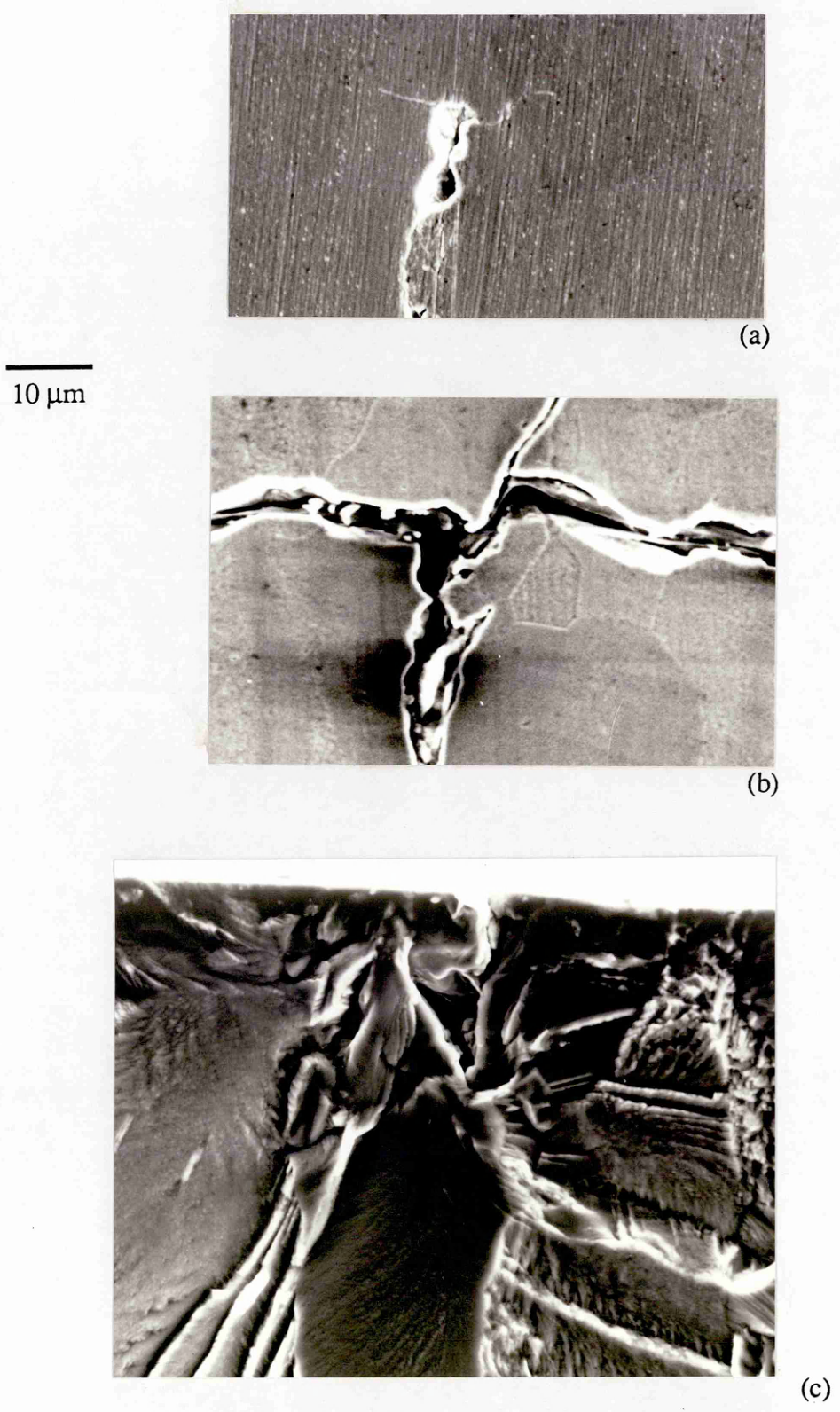
Figure 4.7   The deceleration of a small crack in alloy C due to grain boundary
blocking: (a), replica micrograph of the crack temporarily arrested after
960,000 cycles. (b), etched surface. Note the arrested crack tips
corresponded to the first grain boundaries. (c), fracture surface.
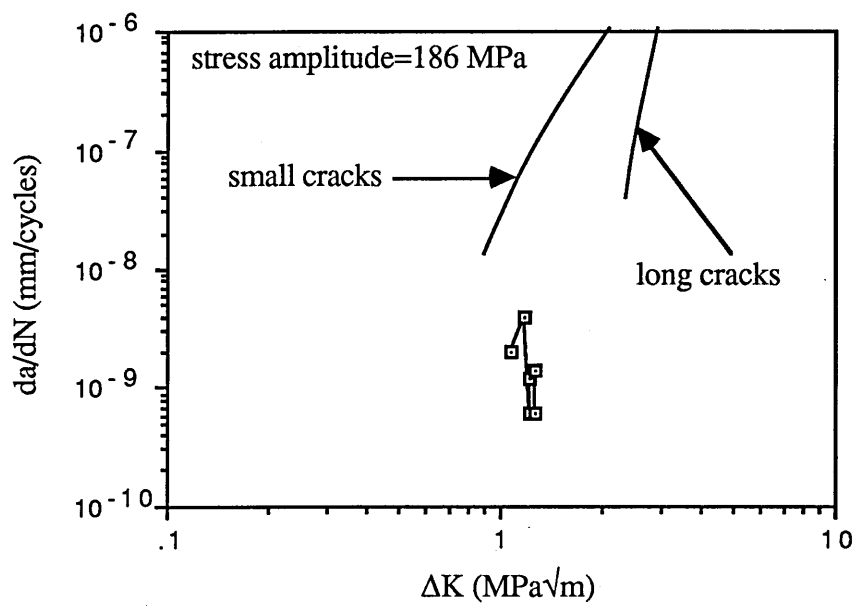
Figure 4.8   The decelerating and temporarily arrest of the crack seen in figure
4.7 before the stress amplitude was increased.

10 µm
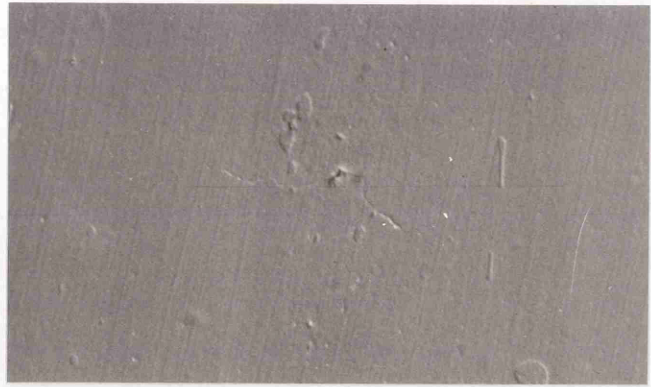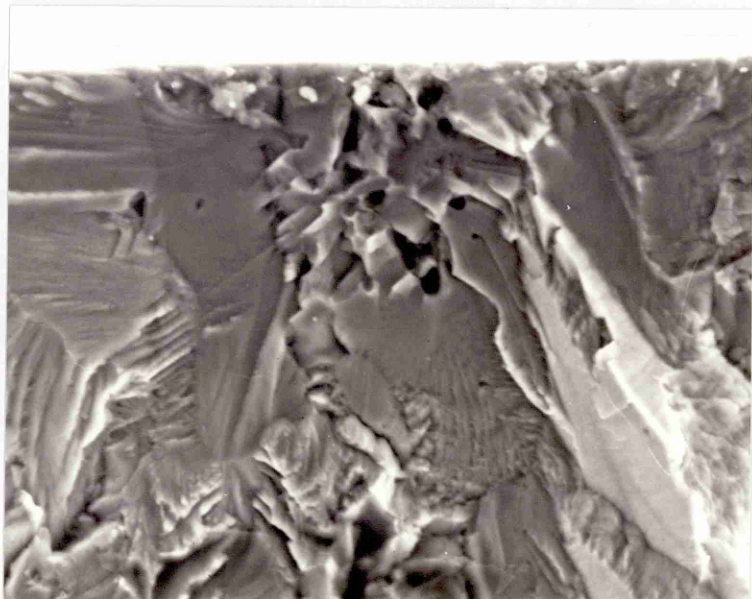
Figure 4.9   The deceleration of a small crack of alloy D due to grain boundary
             blocking: (a), replica micrograph of the crack at length of 18 µm when
             it began to decelerate. (b), replica micrograph of the crack at length of
             22 µm when it temporarily arrested. (c), the fracture surface.
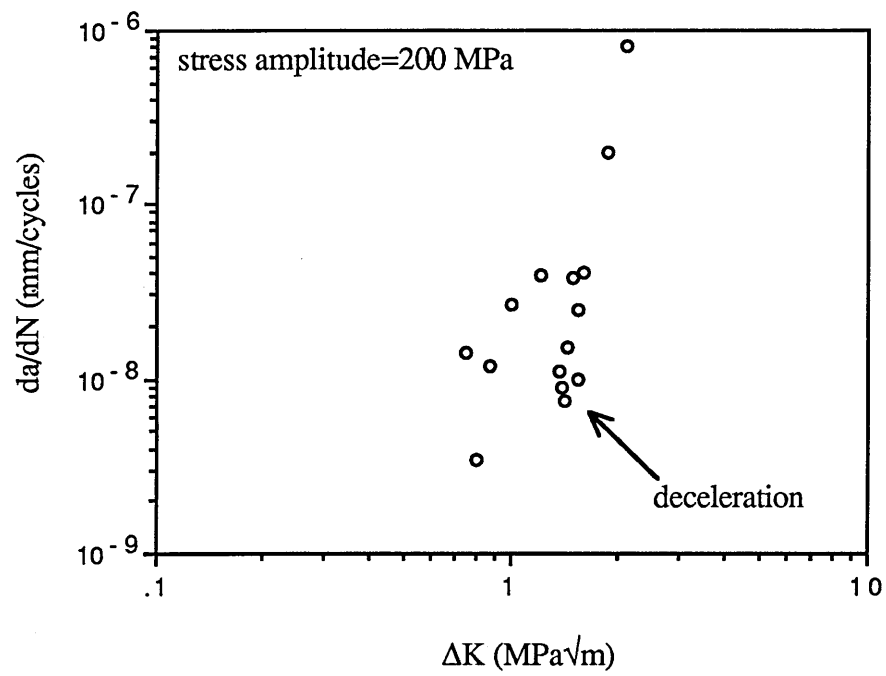
Figure 4.10   The decelerating small crack corresponding to figure 4.9.
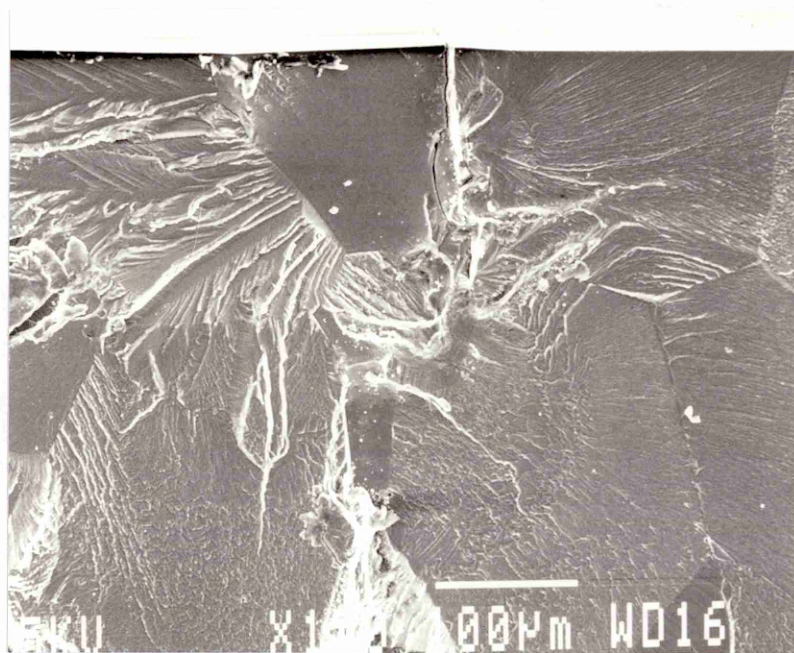
Figure 4.11   Fracture surface of alloy A, showing a facetted fracture feature associated with stage I growth.

Figure 4.12   Fracture surface of alloy B, showing a facetted fracture feature associated with stage I growth.
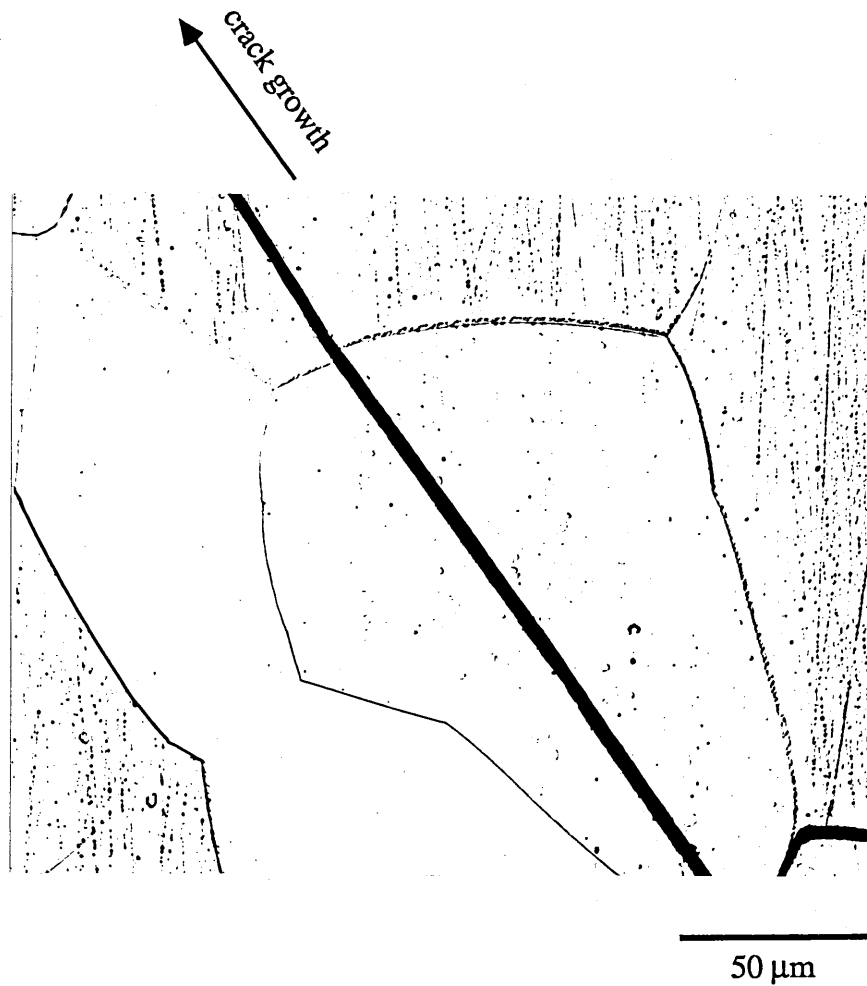
Figure 4.13   Grain boundary offset caused by the shear propagation of a small
crack along a crystallographic plane in alloy A.

CHAPTER FIVE

THE CHARACTERISTICS OF PLASTIC DEFORMATION
AHEAD OF SMALL FATIGUE CRACKS

5.1 Introduction

The fracture mechanics approach to correlate cyclic crack advance begins by

characterizing the local stress and deformation fields ahead of cracks. The usual

description of the stress field ahead of a crack as a function of K is based on the

assumptions of continuum mechanics and small scale yielding. Microstructurally

small crack growth, however, violates these two assumptions, since it is associated

with small dimensions, (comparable with grain size), and a relatively large plastic zone

size. A minimum limit of the ratio of plastic zone size to crack length has been given

by Smith (1977) as 1/10 for the successful application of the LEFM parameter K to

characterize crack growth. The importance of the comparatively large plastic zone

sizes associated with small cracks in explaining their fast growth rates compared to

long cracks at the same ΔK has been realized for some years (Suresh and Ritchie,

1984; McEvily et al, 1991; Suresh 1991). However, although many estimates of PZS

have been calculated (Chiang and Miller, 1982; Zhang and Beevers, 1992; Blom et al,

1986; Ritchie et al, 1987), few measurements of the PZS for small fatigue cracks have

been attempted and only limited data exist, (Lankford, Davidson and Chan, 1984;

Nicholls and Martin, 1991).

Bearing this in mind, to further understand and explain small crack growth behaviour,

the work was focused on the investigation of the characteristics of small crack tip

plastic deformation. For this purpose, SAECP was employed for the measurement of

plastic zone size and shape of small cracks and a novel experiment of periodic PZS

measurement and crack growth rate test was developed to investigate the

57

characteristics and development of small crack tip plastic zone sizes and shapes and their relation with small crack growth. Alloys A and B were chosen for this study. Alloy B is based essentially on 7075 but contains no iron or silicon so that whilst it contains similar precipitate and dispersoid distributions to commercial 7000 series alloys it contains a much smaller volume fraction of coarse constituent particles. The low number of such particles in both alloys A and B facilitated the measurement of plastic zone size around small crack tips as initial experiments on commercial purity materials had shown that coarse constituent particles deteriorate the electropolish in their locality and hence limit the total area of the specimen surface in which the small fatigue crack plastic zone can be accurately mapped. In addition, large numbers of particles often inevitably result in the beam spot covering the interfaces between particles and the matrix, causing degradation of the quality of ECP which, in turn, affects the accuracy of plastic zone measurement.

In the periodic PZS measurement, the specimens were about 3.1 mm thick. In order to keep the depth of remaining ligament W of these small specimens long enough in case it may affect the small scale yielding situation, the cracks for the plastic zone measurements using the small specimens were no more than 400 μm long to comply with the requirement of the maximum ratio: $r_p/W=1/15$ (Suresh and Ritchie, 1984). For a crack of 400 μm long, the estimated ratio of r_p/W is about 1/30 for both alloys at the stress amplitudes used which were 180 MPa for alloy A ($\sigma_{max}/\sigma_y=0.8$) and 200 MPa for alloy B ($\sigma_{max}/\sigma_y=0.85$).

For fatigue cracks, there are two plastic zones, i.e., the monotonic or maximum zone and the reversed or cyclic zone, as described in chapter 2. The plastic zones measured here belong to the former, i.e., monotonic plastic zones.

5.2 Plastic Zone Sizes Ahead of Small Fatigue Crack Tips

5.2.1 Unconstrained Plastic Zones: The Equilibrium Condition

When crack tips are sufficiently far from the next grain boundaries (i.e. the plastic zones are not blocked), the majority of each grain was found to be undeformed, in agreement with the finding by Lankford et al (1984). The PZS in this situation is defined here as the equilibrium condition. As mentioned in chapter 3, the SAECP technique uses degradation of channelling patterns as an indication of plastic deformation. The indicator of degradation used was usually the disappearance of the fourth order line of {111} planes, which corresponds to about 0.3% equivalent tensile plastic strain (Davidson, 1984; Tekin and Martin, 1989). The distance from the crack tip to the elastic plastic boundary is the plastic zone size. One example of PZS measurement is given in Figure 5.1 (hatched area is plastic zone and dashed line delineates plastic zone boundary).

Data describing plastic zone size measured ahead of small crack tips on the projection of the plane normal to the applied load in equilibrium condition is plotted against half crack length c for alloy A in Figure 5.2 and for alloy B in Figure 5.3. The measured plastic zone size data of alloy A shows significant scatter. This was caused by the differing crack initiation sites, which caused differing plastic zone shapes in this coarse grained material, as will be introduced later. It can be seen that plastic zone size constitutes a large fraction of crack length. It was found that the ratio r_p/c reached a maximum value of about 0.8 when the crack was small (about one or two grain sizes), and gradually decreased during crack growth to a value of about 0.2 as the crack became longer. These results suggest that the small scale yielding requirement necessary for the successful use of linear elastic fracture mechanics parameter K (Smith, 1977) is violated for small fatigue cracks.

There are three possible explanations for the large plastic zone sizes measured ahead of small fatigue crack tips:

1. The first is the high ratio of σ_{max}/σ_y used for small fatigue crack growth. Small crack growth tests are usually carried out at relatively high stress amplitudes approaching the yield strength of the alloy, from $\sigma_{max}/\sigma_y=0.6$ to 0.9. Although the applied maximum external stress σ_{max} is still below the bulk yield stress of the material, the stress ahead of a small crack tip is high enough to cause a large plastic zone. Rice (1967) has shown that, when the applied stress is high, a complete solution must be used, which will shift calculated values of r_p/c upward for σ_{max}/σ_y ≥ 0.5. Thus a high ratio of r_p/c is expected. In an analysis of the behaviour of small cracks, Allen and Sinclair (1982) plotted the stress distribution ahead of a crack as a function of crack length with both a single term and higher order terms in the description of the crack tip stress field (see equation 2.1) and showed that the neglect of the higher order terms for small cracks can cause substantial error. By using a Westergaard semi-inverse procedure for a straight crack of length 2c in an infinite plate subject to uniform tensile stress σ remote from and perpendicular to the crack, the stress distribution $\sigma(r)$ ahead of a crack can be described as

$$\sigma(r)=\frac{\sigma(1+r/c)}{\sqrt{2(r/c)+(r/c)^2}} \tag{5.1}$$

where r is the distance from the crack tip. Assuming that the very high near tip stresses are redistributed over a zone of length r_p carrying the same yielding stress σ_y, that is,

$$\sigma_y\,r_p=\int_0^{r_p}\frac{\sigma(1+r/c)dr}{\sqrt{2(r/c)+(r/c)^2}} \tag{5.2}$$

Integration gives the plastic zone size as

$$r_p = \frac{1}{2\pi} \frac{K^2}{(\sigma_y^2 - \sigma^2)} \qquad\qquad (5.3)$$

As the applied stress is increased, the above equation will predict large plastic zone size compared to that estimated from equation 2.3. The above prediction is compared to both the experimentally measured plastic zone size and the one-term prediction of equation 2.3, see Figure 5.4. It can be seen that the consideration of high order terms in the description of K does predict a comparatively large plastic zone size. It correlates with the experimental data of PZS well at low value of K but predicts much larger PZS at high value of K.

2. The surface measurement of PZS could also be another factor for the high ratio of r_p/c of small cracks. The plastic zone size data in Figures 5.2 and 5.3 represent surface measurements for half-penny surface cracks. At the free surface, plane stress conditions prevail and the flow resistance is reduced so that the plastic zone size will become comparatively large compared to that in the interior where plane strain conditions prevail, as seen from Figure 2.5. It is estimated (Broek 1974) that the plastic zone size under plane stress conditions is three times as large as under plane strain conditions. To investigate the latter explanation, two specimens of alloy B, tested at stress amplitude of σ_a=200 MPa with one crack length of about 100 μm and another crack length of about 300 μm were sectioned and the plastic zone sizes ahead of crack tips in the depth direction were measured. Figure 5.5 shows the 300 μm crack after sectioning and its measured plastic zone. The measured plastic zone sizes were 19 μm for the 100 μm crack and 26 μm for the 300 μm crack, which correspond to a ratio of r_p/c about 0.38 and 0.17, respectively. Comparison with crack plastic zones measured from the surface shows that the measured result of the ratio r_p/c of the 100 μm crack is just a little lower than the average value of the ratio measured from the specimen surface. For the 300 μm crack, however, the ratio of r_p/c is much lower

than the average value of about 0.3 measured from the specimen surfaces at the corresponding crack length. This suggests that, for small fatigue cracks, the plane stress condition will dominate ahead of crack tips up to a certain crack depth. Since the fast growth of small cracks happened usually within the first 250 μm, it seems that small crack growth is at first mainly under plane stress conditions and is accompanied with comparatively large plastic zone sizes ahead of crack tips both on the surface and in the depth direction. With increase in crack length, the deformation ahead of the crack tip in depth direction gradually changes to plane strain conditions, causing a relatively low value of the ratio r_p/c. In a review of the growth of small fatigue cracks, Leis et al (1986) stated that the transition in flow behaviour from that controlled by the free surface to that controlled by the bulk flow behaviour begins at a depth equal to about 5-10 grain diameters. Therefore, the large plastic zone sizes associated with small crack growth can be partly attributed to the characteristics of small crack growth near surfaces which is related with plane stress dominant conditions. Although only two specimens were sectioned for the plastic zone size measurement in depth direction, the limited data indicated that the transition crack length from plane stress to plane strain dominant condition is between 100 to 300 μm for alloy B for the stress amplitude used. Recalling Figure 4.2 for the convergence value of ΔK at about 4.5 MPa$\sqrt{m}$ of long and small crack growth rates, which corresponds to a crack length of about 170 μm at σ_a=185 MPa and about 220 μm at σ_a=210 MPa, it is anticipated that when the small crack length reaches the point where long and small crack growth data converge, it nearly corresponds to the transition from plane stress dominant surface to plane strain dominant bulk behaviour.

3. The blocking effect from grain boundaries associated with small crack growth may also affect the plastic zone size of small cracks. It was found that crack tips often changed their growth direction when they propagated through grain boundaries. The measured plastic zone size after a crack tip just passed a grain boundary was smaller than that expected from the developing trend in the previous grain. It is expected that a

crack within a single grain will have the largest ratio of r_p/c, because it corresponds to single crystal situation with favourable orientation for operation of the relevant crack extension mechanism. In this case the yield stress in the calculation of plastic zone size in Equation 2.3 represents the single crystal situation and should have a value less than that for polycrystals.

All these three factors causing comparatively large plastic zone size are specific for small fatigue cracks. For long cracks, however, the applied stress is low (usually less than $0.5\sigma_y$), the crack front is immersed in the interior of material and covers many grains so that an average value of friction stress corresponding to the yield stress of the material is expected. Therefore the plastic deformation ahead of long crack tips is comparatively small and the assumption of small scale yielding is usually valid, which results in the successful application of the LEFM parameter K for characterizing long crack propagation.

5.2.2 Blocked Plastic Zones

As mentioned in Chapter 3, periodic plastic zone measurement was carried out on a total of six specimens. As each specimen contains two crack tips a significant number of crack tip/grain boundary interactions were observed in varying degrees of detail. The propagation behaviour of all the small cracks studied was typical in that whilst the general tendency was for cracks to accelerate as they became longer, grain boundaries were often significant barriers to crack growth and both deceleration and temporary arrest were commonly observed. On occasion, both the crack and its preceding plastic zone were found to easily pass through a grain boundary into the next grain and it was observed that in these instances, there was almost no deceleration in the growth rate. But more usually, particularly when the ratio of applied stress/yield stress was low and the crack length was ≤5 grain diameters, the plastic zone would be blocked by a grain boundary, and a decrease in crack growth rate was observed before the crack tip

reached the grain boundary. With continued fatigue cycling, the crack tip moves gradually closer to the grain boundary, the plastic zone becomes more truncated and the growth rate further decreases. Finally, when plastic deformation has initiated in the next grain, the growth rate increases rapidly and typically the crack growth will have almost completely recovered before the crack tip encounters the next grain boundary. Although, the relative misorientation from grain to grain were not determined, the limited information obtained were consistent with the reasonable expectation that the blocking effect of a grain boundary depends on the misorientation between adjacent grains as crack retardation was usually accompanied by significant crack deflection as it crossed the grain boundary.

This point can be best illustrated by first considering an example where a grain boundary did not cause measurable crack tip deceleration. Figure 5.6 (a) is a SEM photo for such a crack and only a slight deviation in crack path can be seen as it crosses a grain boundary. Figure 5.6 (b) is a schematic of this figure illustrating the relative positions of the crack and grain boundary whilst Figures 5.6 (c) and (d) are channelling patterns taken from undeformed areas within grains B and A respectively. Calibration of the image rotation between the channelling and scanning imaging modes allowed tentative identification of the crack propagation plane in each grain to be made using the method employed by Nicholls and Martin (1991). By assuming the plane of crack propagation to be either {100}, {110} or {111}, they made observations to determine which of these possibilities was compatible with the trace of the crack plane on the specimen surface. Observations made here under constant tilting conditions are consistent with crack growth on a {111} plane in grain A and on a {200} plane in grain B. Although {200} plane is not the suitable slip plane in f.c.c. material, crystallographic crack propagation on both {100} planes (Garrett and Knott, 1975) and {111} planes (Davies and Stoloff, 1965) have been reported. There is just a 3° deviation as the crack crosses this boundary suggesting that the poor blocking effect of this boundary is due to the small angle between the crack growth planes.

In contrast, an example of the interaction of a small fatigue crack plastic zone with a grain boundary that causes crack deceleration and retardation is illustrated in Figure 5.7 (a) which schematically maps the crack tip and its attendant plastic zone as it propagates through the microstructure. Figure 5.7 (b) shows a micrograph of the same area taken at a crack length corresponding to schematic A in Figure 5.7 (a). The crack growth rate vs. the crack length is plotted in Figure 5.7 (c) from which the growth rate corresponding to each stage in Figure 5.7 (a) can be deduced.

Turning to the schematic illustrations in Figure 5.7 (a), A shows a fully developed plastic zone typical of the situation when all the plasticity ahead of the crack tip is enclosed within a single surface grain. Note that the plastic zone size is relatively large being about 20% of the crack length. We can use information from the mapping of this plastic zone to illustrate the technique used. Figure 5.7 (d) shows channelling patterns taken from either side of the plastic zone boundary directly ahead of the crack tip in A. Both general loss in definition and disappearance of fourth order lines can be seen in Figure 5.7 (d, i), which is taken from just within the plastic zone, when compared with Figure 5.7 (d, ii) which is a channelling pattern taken from a deformation free area of the same grain.

As the crack propagates across the grain, its plastic zone is blocked by the next grain boundary ahead and its growth rate decreases. Schematic B shows the situation when the growth rate is a minimum and it can be seen that at this point the plastic zone is severely truncated by the grain boundary. After further cycling plasticity is initiated in the next grain and a plastic zone quickly develops within it accompanied by a sharp increase in crack growth rate as may be seen from Figure 5.7 (c). Note that this acceleration has occurred before the crack tip has encountered the actual grain boundary. Finally, on entering this grain the crack quickly becomes crystallographic, presumably due to the suitable orientation of this grain for this mode of propagation.

As shown in schematic D, this was accompanied by a change in plastic zone shape which became very long and slender and soon encountered the next grain boundary where it was prevented from propagation into the adjacent grain. Thus the growth rate was again decreasing and the whole process repeated itself.

Another example of grain boundary blocking on the development of plastic zone size is shown in Figure 5.8. Heavy deformation, which can be seen from the blurring of channelling patterns taken at blocked crack tip, occurred within the truncated plastic zone. The pattern of one crystallographic plane has even been rotated to about 8° by the local heavy deformation, although the mechanism of this rotation is not clear. But just over the grain boundary and 10 μm ahead of the crack tip, the ECP taken there indicated almost no deformation. The maximum plastic zone size at the other tip without the influence of a grain boundary, however, was measured to be 35 μm. A comparison of the blurring extent of channelling patterns taken at the same distance from the two tips also revealed that the blocked plastic zone was much more heavily plastically deformed.

It was noticed that the strongest influence of grain boundaries on plastic zone development, and hence on small crack growth came from the first grain boundary. Figure 5.1 shows a small crack of around 25 μm in length growing at a ΔK of 1.7 MPa√m and its measured plastic zone sizes. It shows an optical micrograph of the crack, (Fig. 5.1, a), channelling patterns from significant points in the microstructure, (Fig. 5.1, c), and the same crack imaged in SEI mode in the STEM, (Fig. 5.1, b). The growth of the left hand crack tip has been retarded and finally temporarily arrested by a grain boundary for 42,000 cycles and as can be seen from the channelling pattern taken from point A, this is associated with an absence of plasticity on the far side of the grain boundary. In the mean time, the right hand crack tip has grown about 3 μm and it has a fully developed plastic zone typical of the situation when all the plasticity ahead of the crack tip is enclosed within a single surface grain.

It is clear from these observations that grain orientation plays an important role on both plastic zone development and subsequent crack growth. The development of plastic zone size ahead of a crack exhibits discrete characteristics and this discontinuity of measured plastic zone size with the crack growth was most often found to be related with grain boundary blocking. In this case, the growth rate of the crack always shows the same developing trend as the plastic zone size. Indeed, the above results are generally in agreement with Lankford, (1982), who related crack deceleration to grain boundary crack deflection and indicated the importance of crystallographic misorientation across grain boundaries to small crack growth retardation. It seems likely that it is the initiation of plasticity in the next grain that is the controlling factor and thus crack retardation or arrest will only cease when the stress concentration caused by the accumulated strain in the blocked plastic zone is of sufficient magnitude to overcome the barrier caused by the misorientation of grains and thus activates slip sources in the next grain. It is worth noting that even if such blocking mechanisms operate in the case of long cracks, their growth fronts will sample many grains so that macroscopic growth rates will not show fluctuation due to crystallographic orientation.

5.3 Plastic Zone Shapes

In the early stage of small crack growth corresponding to a crack length typically less than about 200 μm for the present applied stress amplitudes (σ_a=200 MPa for alloy B and σ_a=180 MPa for alloy A), the plastic zone shapes were found to be dependent upon both crack length and crack propagation path. When the cracks were small, that is no more than about one or two grain sizes in length, they were usually accompanied by a slender plastic zone with the maximum plastic zone dimension extending directly ahead of the crack tip, similar to that ahead of right hand crack tip shown in Figure 5.1. At this stage the cracks are predominantly crystallographic in nature and this suggests that the plastic zone is dominated by a single slip band which extends parallel

to the crack faces. As the crack length increased during the fatigue test, the plastic

zone shape gradually changed firstly to a more semi-circular shape, and finally, at a

length of about 200 μm to the distinct "rabbit ear" shape predicted by LEFM. A

schematic figure of the crack growth path from one specimen is illustrated in Figure

5.9, together with three different plastic zone shapes measured at different crack

growth stages. A semi-circular plastic zone shape was observed at point A and a

"rabbit ear" like shape at point B, see Figure 5.9 (c), and (d). This evidence suggests

that as the crack grows, it becomes no longer crystallographic and the crack tip plastic

zone then is associated with slip along a number of bands.

But sometimes, although crack lengths were comparatively long (2c>50 μm), they still

showed typically crystallographic growth, especially for alloy A. This was suggested

by a straight segment of crack growth path. When crack growth was typically

crystallographic, the measured plastic zone always showed a much slender shape,

(e.g. point C in Figure 5.9), and usually had a much longer length ahead of the crack

tip than that for a non-crystallographic crack at the same crack length, see Figure

5.9(e). A numerical indicator of plastic zone shape is produced by calculating the ratio

r_p^o/r_p^*, where, as can been seen from Figure 5.10, r_p^o is the largest plastic zone

dimension on the projection of the crack plane and r_p^* is the largest plastic zone

dimension on the projection of the plane perpendicular to the crack. Crack tips

growing in a typically crystallographic manner possessed plastic zones with r_p^o/r_p^*

ratios of between 5 and 10. However, even non-typically crystallographic cracks

exhibited changes in plastic zone shape with crack length as may be seen from Figure

5.11 which only contains data of alloy B from crack tips where the plastic zone was

not blocked by a grain boundary. So data from blocked crack tips with severely

truncated plastic zones and crack tips exhibiting typically crystallographic growth are

excluded from this figure. It can be seen that a tendency towards slender extended

plastic zones can be seen even for cracks at small lengths but a semi-circular shape,

$(r_p^o/r_p^* \approx 1.0)$, is achieved by the time they exceed about 40 μm, ($\approx$2 grain

diameters), in length. With increase in crack length, the ratio gradually changed to a value of about 0.5.

Lankford et al (1984) have measured similar dimensions of plastic zones at small fatigue cracks grown at ΔK values of about 3 to 5 MPa$\sqrt{m}$. Their results showed that the plastic zone shape was roughly semi-circular in shape which accords well with our results for the same ΔK range. However, their measurements were of cracks initiated at inclusions which were thought to grow in a stage II fashion even within one grain (1982). This was also sometimes observed in the present work. Figure 5.12 shows an example where plastic zones were measured for a crack initiated from an inclusion in alloy A which usually exhibits crystallographic growth in the early stage. A nearly semi-circular plastic zone was seen for crack lengths from 2c=120 μm to 2c=230 μm. It can be seen from Figure 5.12 (b) that macroscopic stage II growth is actually made up from alternating segments of short ($\approx$ 2 μm) crystallographic growth. This suggests that the plastic zone shape is controlled by the macroscopic crack behaviour and not the local crack tip growth mechanism.

It has been observed that crystallographic microcracks have large plastic zone size ahead of cracks and exhibit fast growth rates compared to those from non-crystallographic microcracks. A similar result has been noted by Brown and Hicks (1983) that crystallographic microcracks in IMI 685 Ti alloy grow much faster than equivalent long cracks, while small cracks constrained to grow in a non-crystallographic manner showed just slightly higher growth rates than long cracks.

The above results indicate that the plasticity associated with small fatigue crack growth has three stages. When the crack is small in length compared to the grain size, little constraint is provided from the surrounding grains and the crack sees an essentially single crystal environment. Consequently the crack has a large proportion of stage I growth, that is, crack growth along crystallographic planes mainly along a single slip

69

system causing a Mode II dominant deformation field ahead of the crack. This can be further supported by (i), the fracture surface observation in SEM revealing the planar fracture characteristics which was thought to be related with stage I growth of fatigue cracks (Tokaji and Ogawa 1990); (ii) the deceleration, or arrest of small crack growth which is believed to be associated to a large extent with the characteristics of crystallographic growth of small cracks. This mode II dominant stage I crack growth results in a slender plastic zone shape.

After passing about one or two grain boundaries, the crack growth changes from Stage I to Stage II and the deformation field ahead of the crack tip becomes a combination of Mode I and Mode II, causing a roughly semi-circular plastic zone shape. Finally, as the crack grows further so that yet more grains are encountered, the deformation within the plastic zone is constrained by the need to maintain compatibility among the randomly oriented grains and the crack tip finally acquires a mode I dominant deformation, inducing the typical plastic zone shape seen in long fatigue cracks loaded in mode I, (Broek 1974). For alloy B tested at σ_a=200 MPa, the transition crack length from stage I to stage II growth is about 170 μm from both specimen and fracture surface observations.

Finite Element calculation of PZS and shape of small fatigue cracks (Blom et al 1986) has suggested that small cracks have a relatively large PZS and a slender shape. For long cracks with deformation mainly in mode I, the width of PZ shape will increase, indicating agreement with the above explanation. By metallographic observation of crack path topography, Blom et al (1986) found that small fatigue cracks initially grow in stage I. As the crack length increases, its growth first changes to crystallographic stage II (zigzagging growth along segments of crystallographic planes), and finally to conventional stage II. The transition from stage I to stage II growth was believed to be related with a characteristic crack length for a material. It is suggested that LEFM can only be used beyond this characteristic crack length. The phenomenon of fast

70

growth of small cracks in stage I has been reported separately by other researchers (Tokaji and Ogawa, 1990; Plumtree and O'connor, 1991).

It is therefore thought that the discrepancy of long and small fatigue cracks can be partly related with their different growth characteristics, one in stage II, another mainly in stage I, although the mechanism of the latter is still not clear. The fast growth rates of small cracks are partly attributed to the influence of stage I crack growth.

5.4 Relationship Between PZS and Crack Growth Rate

Through the periodic plastic zone size and crack growth measurement of small fatigue cracks, it was found that plastic zone sizes are proportional to small fatigue crack growth rates, whether the zone was blocked by a grain boundary or not, see Figure 5.13 for alloy A and Figure 5.14 for alloy B. It is suggested that the following relation exists between crack growth rate and plastic zone size measured ahead of small fatigue cracks:

$$\frac{da}{dN} = C\, r_p{}^m \qquad\qquad (5.4)$$

where C and m are material constants. The efficacy of this equation using plastic zone size as a correlating parameter for crack growth can be firstly judged by comparing the present experimental data of small cracks with that from long crack data using the following equation to calculate long crack plastic zone size:

$$r_p = \alpha \left(\frac{K_{max}}{\sigma_y}\right)^2 \qquad\qquad (5.5)$$

where α is a constant depending on the state of stress and the angular orientation relative to the crack tip. Lankford et al (1977) have determined this parameter to be

0.6 for long cracks of 7075-T6 Al alloy by measurement on the specimen surfaces using the SAECP method. Assuming $\alpha=0.2$ for the PZS in the interior of the material which is taken to be 1/3 of that from surface, and using this value to calculate r_p for long cracks of the similar alloy (alloy B) from Edwards (1983), the measured small and calculated long crack data are compared in Figure 5.14. Comparison with Figure 4.2 shows that the difference between long and small cracks has been reduced. Even better agreement between long and small crack growth rates when characterized with plastic zone size r_p can be anticipated if the two following factors are noticed. The PZS data of small cracks are from surface measurements where plane stress is dominant. With increasing crack length, the actual stress state ahead of small crack tips in depth direction will gradually change to a plane strain dominant condition. This will result in a comparatively smaller PZS which will shift the small crack growth data left towards long crack data. Secondly, at low ΔK, the growth rate of long cracks will be reduced because of the effect of crack closure. The elimination of the influence of crack closure stress will shift the long crack growth data up towards small cracks. The latter factor does however highlight the weakness of the assumption of equation 5.4: the effect of crack closure of long cracks was not taken into consideration. Therefore, for an accurate description of long crack growth with plastic zone size r_p, the influence of crack closure should be considered.

These results reinforce the conclusion that it is inappropriate to use stress intensity factor range, ΔK, to characterize small fatigue crack growth and an alternative correlating parameter should be used which must take into account the comparatively large deformation ahead of small cracks into consideration. It seems that the use of plastic zone size ahead of crack as a correlating parameter may fulfil such conditions.

As mentioned earlier, the plastic zone shape associated with small fatigue cracks evolved during crack growth. The different plastic zone shapes reflect the differing number of slip systems and growth mechanisms dominant at different stages of small

72

crack growth. Of course, the plastic zone shape will affect propagation rate. Although much work is needed for the quantitative investigation on how the plastic zone shapes affect the efficacy of equation 5.4, the general trend is for the growth rates of small cracks to be proportional to the plastic zone size ahead of their crack tips. When crack growth took a crystallographic path, its related long and slender plastic zone ahead of crack tip always corresponded to a fast growth rate compared to the non-crystallographic crack growth. The fast growth rates associated with crystallographic cracks have been reported by many researchers (Brown and Hicks, 1983; Ritchie and Lankford, 1986; Tokaji and Ogawa, 1990; Lynch, 1979).

5.5 The Convergence Condition for Long and Small Crack Growth

It has been often reported that small cracks grow faster than long cracks at low ΔK, and gradually the two sets of data converge at certain values of ΔK, defined as ΔK_{co} here, depending on the material. For example, for Al-7075 the converging value ΔK_{co} has been reported to be about 5 MPa$\sqrt{m}$ (Lankford, 1983). Two criteria for the converging condition of long and small crack growth rates when characterized with ΔK have been reported. After compiling small crack sizes for a number of materials at which the da/dN versus ΔK curves of long cracks and fast growing small cracks converge, Taylor and Knott (1981) have found that the best converging condition can be described by the form: 2c=10D, that is, the anomalous growth behaviour of small cracks will disappear when the length of the crack extends to about 10 times the microstructural unit. It was explained that once a small crack had propagated long enough to cover many grains, the surrounding constraint would force the crack to behave like a long crack. By comparing the plastic zone size, mainly by calculation, at ΔK_{co} with microstructural dimensions for a number of materials collected, Lankford (1985) concluded that the convergence of long and small crack growth rates corresponds to plastic zone size being approximately equal to the relevant microstructural dimension. This well explains why small cracks in some fine-grained

73

microstructures do not exhibit fast growth rates compared with long cracks. And it was indeed observed in the present study that the growth behaviour associated with small cracks occured when the PZS of small cracks was within one grain, or near one grain size. The efficacy of these two conditions is judged below according to the present experimental data.

Table 5.1 Some relevant parameters at ΔK_{co} for the four alloys.

	2c (μm)	D (μm)	r_p (μm)	2c≈10D	r_p≈D
Alloy A	224	134-185	~40	no	no
Alloy B	180	23-80	~30	yes	yes
Alloy C	180	22-68		yes	
Alloy D	180	17-50		yes	

Table 5.1 compares the relevant parameters taken at ΔK_{co}=4.5 MPa√m with grain sizes for the four alloys studied. The data taken from alloy A is at σ_a=180 MPa, and for alloys B, C and D, at σ_a=200 MPa. It can be seen from the table that the converging condition can be described well for alloys B, C and D which have an almost similar grain size using the criterion proposed by Taylor and Knott (1981) and for alloy B, of which the plastic zone has been measured, using the criterion proposed by Lankford (1985). But none of these two criteria is suitable to describe the converging condition for alloy A which has a comparatively large grain size. At ΔK=4.5 MPa√m with a stress amplitude σ_a=180 MPa, the crack length of the alloy is about 224 μm, only about 2 times of the grain size; the measured plastic zone size being about 40 μm, much smaller than the grain size, especially for cracks initiated from inclusions growing in stage II. A new criterion for predicting the converging condition for long and small crack growth rates seems to be needed.

It is assumed, when using ΔK_{co}, that the stress fields ahead of small cracks can be characterized by LEFM, that is, a similitude exists between long and small cracks for a given material. Therefore the plastic zone sizes of both long and small cracks will show the same dependence on K on the basis of LEFM. Recalling Figure 5.14 where both long and small crack growth rates of alloy B have been correlated with plastic zone sizes and they began to merge at a certain value of PZS, r_p. It was about 30 μm for alloy B. Then, an immediate reaction is: does the convergence condition for long and small crack growth rates possess the form r_p (small cracks) = r_p (long cracks) at ΔK_{co}? To consider this, the relation between PZS and ΔK for alloy B was plotted, see Figure 5.15. The PZS calculated for long cracks, as mentioned in the previous section, was compared with that of small cracks measured using SACP. It can be seen that at all ΔK, the PZSs of small cracks measured from specimen surfaces were larger than those of long cracks, and the difference between them gradually reduced with increase of ΔK. But the actual PZSs ahead of small crack tips in the depth direction were smaller than that measured from the specimen surfaces. The limited data on PZSs measured in depth indicated that the actual PZSs merged with that of long cracks at about ΔK=4-5 MPa$\sqrt{m}$, which is very close to ΔK_{co} for alloy B. This result implies that the fast growth rates of small cracks will merge with that of long cracks once their PZS can be predicted by LEFM parameter ΔK as is the case for long cracks.

The above proposed converging condition for long and small crack growth rates is in agreement with the experimental finding that small crack growth rates were proportional to the plastic zone size ahead of their crack tips. It can also explain the following phenomenon associated with small crack growth. Small cracks initiated from inclusions usually grew in stage II and had small PZS and slow growth rates compared to cracks with the same length initiated from slip bands. The growth rates of these cracks merged with long cracks at lower ΔK values. The crack growth rate calculation and PZS measurement on the alloy A specimen where a crack initiated from

75

an inclusion, which has been introduced before, strongly implies that the convergence of long and small crack growth rates at a lower ΔK value than ΔK_{co} is due to the validity of LEFM to predict the PZS for this kind of crack at lower ΔK. From the above analysis, it appears that the fast growth rates of small cracks compared to long cracks when characterized with ΔK is associated with less crack closure stress and the less constraint on the plastic deformation ahead of small fatigue crack tips. For physically small cracks with plastic deformation ahead of crack tips constrained, it has been reported that only the effect of less crack closure stress contributes to the fast growth rates of this kind of small crack (Lankford and Davidson, 1986).

Although the converging condition proposed is reasonable, and was supported by the limited data, more experiments on this aspect may be needed to prove its viability.

5.6 An Alternative Correlating Parameter: PZS Ahead of Crack Tip

According to LEFM, crack growth rates will be uniquely determined by the stress intensity factor range ΔK, provided that the following assumptions for the successful use of K are fulfiled:

(1) the material behaves as a continuum

(2) the crack tip plastic zone is merely a small perturbation in the linear elastic field and fully constrained by surrounding elastic material

(3) the stress distribution in the constraining elastic material adjacent to the plastic zone is, to a close approximation, a function of K alone

As presented and discussed before, small crack growth meets none of these requirements for the application of K. So it is not surprising to see the breakdown of LEFM for the description of small crack growth. An alternative correlating parameter, which needs to take all features of small crack growth, must be sought.

From the experimental technique of periodic fatigue testing and PZS measurement by selected area electron channelling patterns method, it was found that there is a relation between the small crack growth rates and the PZSs ahead of crack tips, that is, the growth rates are proportional to their PZSs , see Figures 5.13 and 5.14. They can be correlated at constant applied stress with exponential relationship as in equation 5.4.

Therefore, a question arises: can plastic zone size r_p be used as the characterizing parameter to describe small fatigue crack growth? Based on the following arguments, it is believed that it is reasonable to use r_p to correlate small crack growth.

(1). It is in agreement with the conventional description of long fatigue crack growth using stress intensity factor range, ΔK. Since plastic zone size $r_p \propto K^2$ for long cracks, the Paris law $da/dN = C\Delta K^m$ can also be written as $da/dN = C_1 r_p^{m_1}$ (where m, C, m_1 and C_1 are all material constants). By measuring the plastic zone sizes using SAECP at various frequencies and temperatures for long cracks in Nickel-based superalloy MA6000, Tekin and Martin (1989) have found that the fatigue crack growth rate was proportional to the square of the plastic zone size. This suggests that an unified growth law with plastic zone size ahead of crack as correlating parameter may exist for both small and long cracks. Since fast growth of small cracks corresponds to comparatively large plastic zone sizes, it is expected that the difference caused by using ΔK to describe small and long crack growth rates will diminish if plastic zone size is used as the correlator. On the other hand, plastic zone size seems to be a function of crack tip opening displacement (Lankford, Davidson and Cook, 1977; Nisitani and Goto, 1986). According to the BCS model, the crack tip opening displacement , CTOD, in equilibrium condition has been obtained in equation 2.20. By correlating CTOD with r_p, Tanaka et al (1980) have found that for an equilibrium slipband (ESB), CTOD increases in proportion to plastic slipband size r_p when the ratio r_p/c changes from 0 to 1, see the broken line in Figure 5.16. This implies that the

use of r_p in the equilibrium condition to describe small crack growth is identical to that of CTOD on the basis of the BCS model. Since CTOD has been found to possess a relation with crack growth like equation 5.4 and often successfully used to characterize small crack growth (Tanaka et al 1986, Navarro and de los Rios 1988, Eastabrook 1984), it is fairly reasonable to expect the existence of the relation like equation 5.4 between r_p and da/dN of small cracks. The advantage of using plastic zone size r_p to correlate small fatigue crack growth, instead of CTOD, is that the definition of the latter is not clear and is difficult to measure in practical circumstances.

(2). From consideration of the blocking effect of grain boundaries and subsequent discontinuous growth for small fatigue cracks, it will be advantageous to use plastic zone size to describe small crack growth. The deceleration, or retardation, of the growth rates of small fatigue cracks is widely believed to be caused by microstructural discontinuities, especially grain boundaries. Experimental evidence from the present work has indicated that the actual deceleration of small crack growth starts once its plastic zone, not its tip, encounters a grain boundary. The different crystal orientation in the next grain over the grain boundary affects the continuous propagation of plastic deformation ahead of the crack tip and subsequently causes the decrease in growth rate. This decrease, or retardation, of crack growth will continue until plastic deformation has passed the grain boundary into the next grain. When a plastic zone is blocked by a grain boundary, its actual size is the distance, λ, between the crack tip and the grain boundary. It is more straightforward and easier for the new correlating parameter, r_p, to describe the decrease, or even the arrest, of small crack growth when plastic zones are blocked by grain boundaries, causing shorter zone sizes than those under equilibrium conditions. This relation between blocked PZS and crack growth rates of small cracks can find support from Morris's work (1980) on crack tip opening displacement measurements of small cracks. By measuring tensile cracks at different locations relative to grain boundaries, Morris found that for the case of a blocked plastic zone by a grain boundary the CTOD is proportional to the distance, z_0, from

the crack tip to the grain boundary, see Figure 5.17. For a shear crack under torsional loading, it has been assumed (de los Rios, Tang and Miller, 1984) that the crack tip sliding displacement, CTSD, is proportional to the product of the shear strain $(\tau-\tau_f)/\mu$ and the size r_p of the plastic zone blocked by a grain boundary,

$$CTSD \propto \frac{(\tau-\tau_f)r_p}{\mu} = \frac{(\tau-\tau_f)(D-a)}{\mu} \qquad (5.6)$$

where μ is shear modulus, τ and τ_f are applied shear stress and friction stress, and D is the grain size of the material. During a fatigue test, the applied stress is kept constant, so CTSD is actually proportional to the distance from the crack tip to the next grain boundary. But the above equation implies that CTSD depends not only on the distance from the crack tip to the next grain boundary but also on applied stress τ. Both the experimental result from Morris (1980) and the analysis from de los Rios et al (1984) (for a constant applied load) indicate that using r_p in the case of blocked PZS situation is equivalent to using CTOD, or CTSD.

(3). The fast growth rates of small cracks correlate with their comparatively large ratio of r_p/c. As a crack grows, its length becomes longer, the ratio of r_p/c decreases, and so do their growth rates. Although the maximum crack length for the plastic zone size measurement was not over 400 μm in order to keep to small scale yielding requirements during the fatigue test, the general trend for plastic zone size development was decreasing with crack length. This was coincident with the developing trend of small crack growth rates.

(4). Actually, the assumption that fatigue crack growth rates are proportional to the plastic zone sizes ahead of cracks was proposed as early as in 1963 (Liu, 1963). Taira and Tanaka (1972) found that when the growth rates of long cracks of annealed steel was higher than $2x10^{-5}$ mm/cycle, the growth rates were not adequately described by

the stress intensity factor K. By measuring the slipband zones of several kinds of annealed steels by optical microscopy, they found that an equation equivalent to equation 5.4 existed between crack propagation rate and plastic zone size. They obtained an equation for expressing plastic zone size as,

$$\frac{r_p}{a} = C_2 \left(\sec(\frac{\pi\sigma}{2C_3\sigma_y}) - 1 \right)$$ (5.7)

where C_2, C_3, like C_1 and m_1 in equation 5.4, are material constants. By comparison, they concluded that equation 5.4 was applicable to more extensive cases than that expressed by a form of the Paris-Erdogan growth law.

Very recently, by correlating both small and long crack growth rates, Nisitani et al (1992) found that two different fatigue crack growth laws hold for both long and small cracks. Based on experimental results of the measurement of plastic zone sizes on long fatigue cracks of alloy Fe-3%Si by etching (Nisitani and Kawagoishi, 1984), which revealed that the crack growth rate of the alloy was proportional to the reversible plastic zone size Δr_p, Nisitani et al (1992) explained the difference in growth laws of long and small fatigue cracks in terms of the effect of applied stress amplitude, and an unified growth law for both long and small crack propagation could be obtained by assuming that the crack growth rates of both long and small cracks are proportional to cyclic plastic zone size Δr_p. They obtained the following equation for small crack growth from notches under high applied stress,

$$da/dN \propto \Delta r_p = C\, a\, \sigma^m$$ (5.8)

where C and m are constants. But no experiments were carried out on the measurement of PZS on small fatigue cracks to support the assumed relation between

da/dN and Δr_p, and no consideration was given to the blocking influence of grain boundaries on crack propagation in their analysis.

It should be noted that the relation between r_p and small crack growth rate was obtained at one stress ratio and constant stress amplitude. From the consideration of the characteristics of cyclic deformation, it would be more appropriate to use cyclic plastic zone size Δr_p to correlate fatigue crack growth which can reduce the influence of stress ratio. But r_p is used here as a correlator for fatigue crack growth on the basis of the following considerations: (1), only monotonic plastic zone size r_p can be measured in the present study using ECP method; (2), the exponential relationship between r_p and da/dN was obtained experimentally; (3), it is not inconsistant with using Δr_p in the description of fatigue crack growth as far as the present experimental condition concerns. According to Rice's superposition argument (1967), Δr_p is a fraction of r_p for the stress ratio of R=0.1. But the general conclusion concerning which parameter is better can be drawn by carrying out more extensive PZS measurement on growing fatigue cracks at different stress ratios in the future.

So it appears reasonable to use plastic zone size, r_p, to correlate crack growth, especially for small cracks. Plastic zone size can be regarded as a measure for the stress, or strain, field ahead of crack tips. When the local plastic deformation ahead of a crack is small, r_p can be described by equation (2.3) and it, like other EPFM parameters (e.g. J integral, CTOD) will be equivalent to stress intensity factor K which uniquely characterizes the stress field of the crack tip. When the plastic deformation is not negligible, however, a parameter reflecting the local strain field, like r_p or other EPFM parameters, should be used. It has been shown both by finite element calculation (Chiang and Miller 1982) and experimental measurement (Lankford and Davidson 1984) that the relatively large plastic zone sizes associated with small fatigue cracks correspond to large crack tip strains compared with long cracks at an equivalent ΔK.

81

Although a good correlation between da/dN and r_p of small fatigue cracks has been obtained which could be used for the prediction of fatigue life, the obvious disadvantage of using r_p as correlator is that difficult and time consuming measurements of small crack plastic zone sizes must be made for each material studied. On the other hand, an analytical model of small crack growth, on the basis of experimental findings, is necessary for the better understanding of the behaviour of small cracks. Therefore, a model, for the calculation of small crack plastic zone size and for the characterization of small fatigue crack growth is necessary and an example will be introduced in the next chapter.
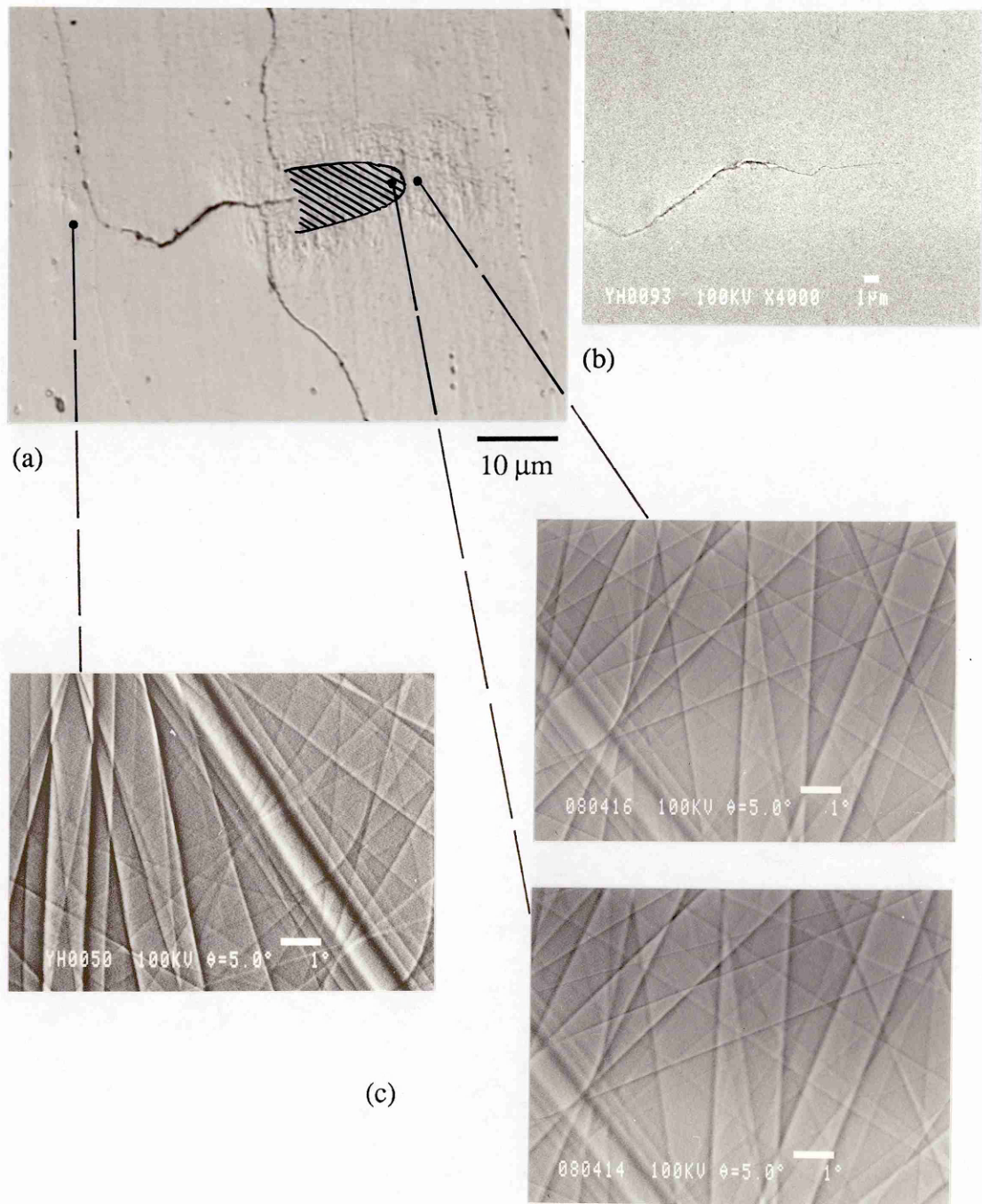
Figure 5.1   Measurement of the plastic zone size of a small crack: (a), the optical
micrograph of the crack (hatched area is plastic zone and dashed line
delineates plastic zone boundary). (b), the right crack tip image taken
from STEM. (c), electron channelling pattern taken from the positions
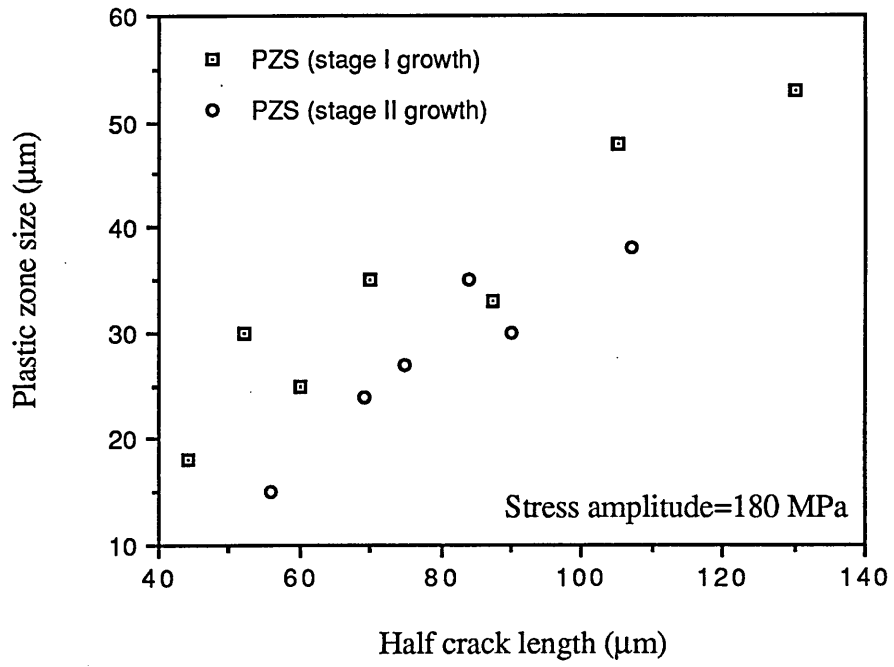shown in (a).

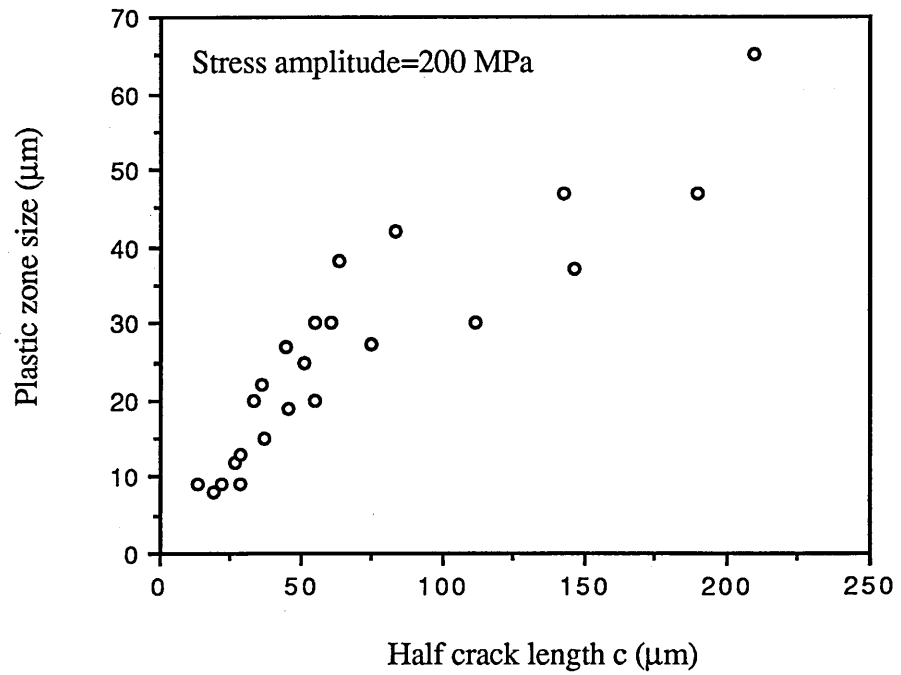Figure 5.2   Measured plastic zone size plotted against half crack length for alloy A.

Figure 5.3   Measured plastic zone size plotted against half crack length for alloy B.
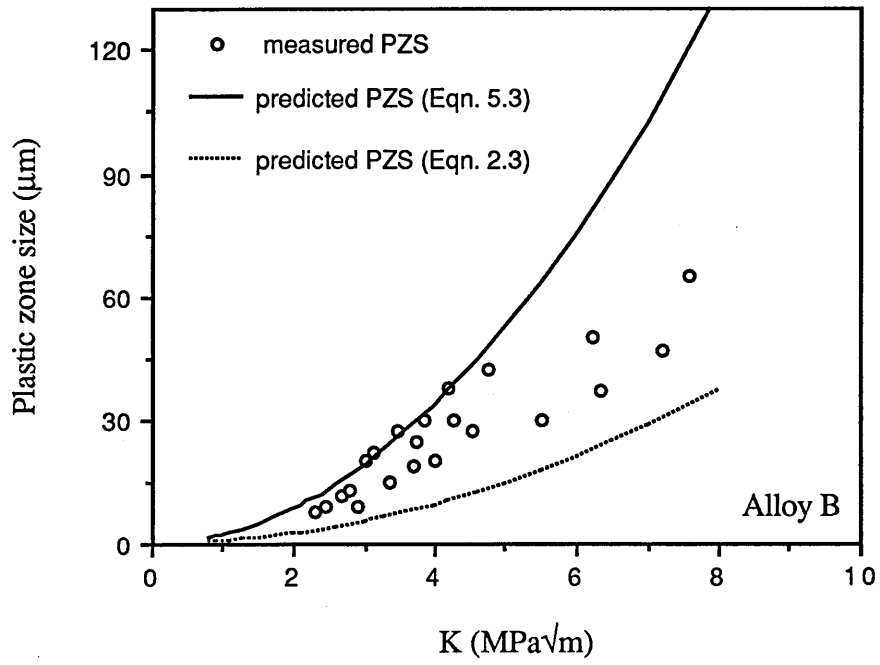
Figure 5.4   Comparison of measured plastic zone size with predictions from K
with one term (broken line) and high order terms (solid line) at
σ_{max}=444 MPa (σ_a=200 MPa, R=0.1)

(a)

100 μm
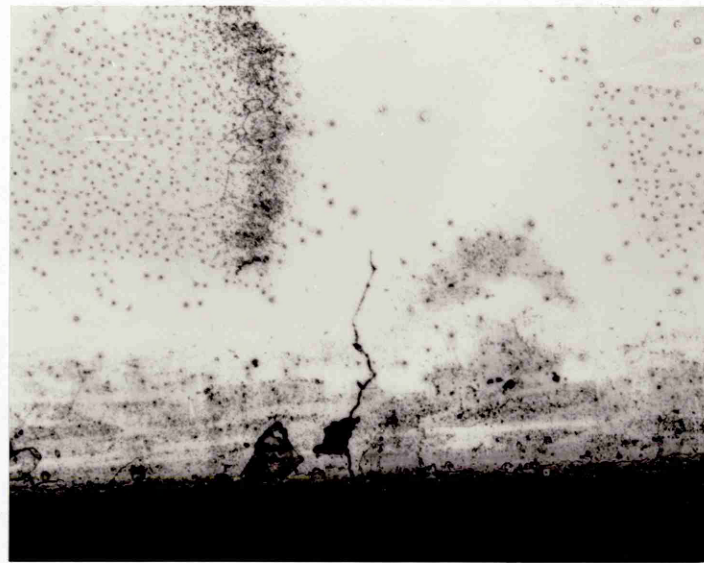
YH1001   100KV X4000   1μm
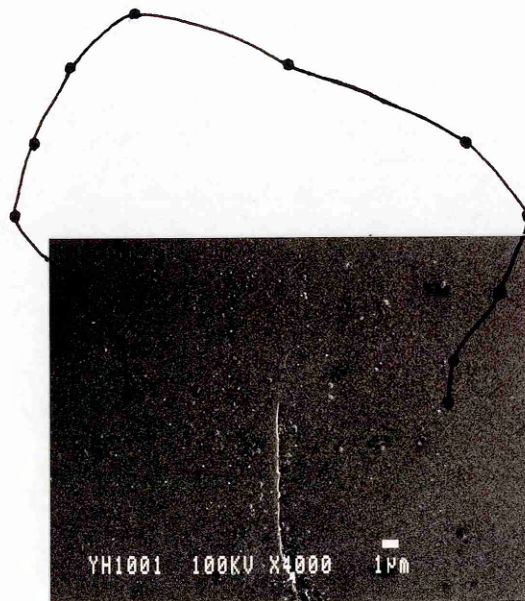
(b)

Figure 5.5   Plastic zone size measured ahead of a crack tip in depth direction. (a), optical micrograph of the crack after sectioning and electropolishing. (b), SEI image of the crack and the measured plastic zone size.
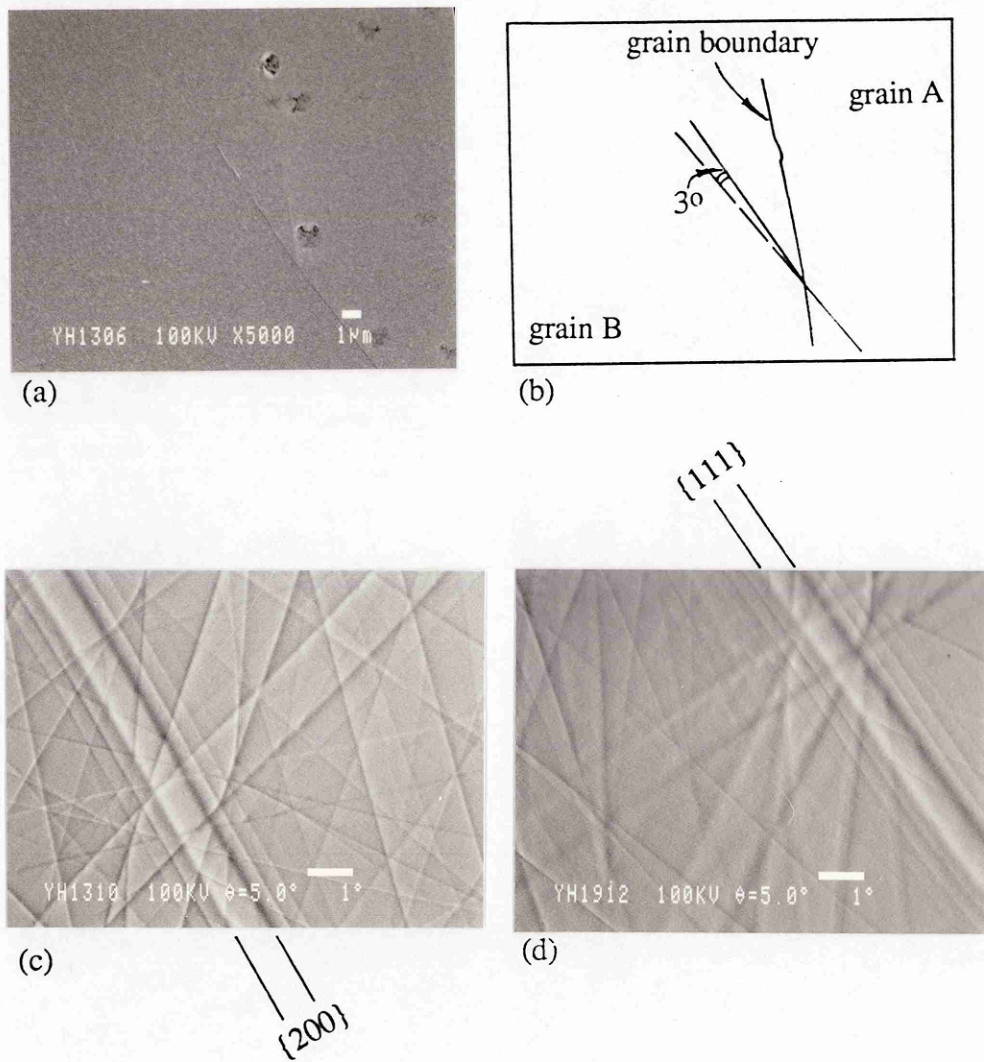
Figure 5.6   A crack tip showing no deceleration when passing a grain boundary:
(a), SEM photo of the crack tip when it just propagated through the
grain boundary. (b), schematic illustrating the relative positions of the
crack and the grain boundary. (c) and (d) channelling patterns taken
from undeformed areas within grains B and A respectively.
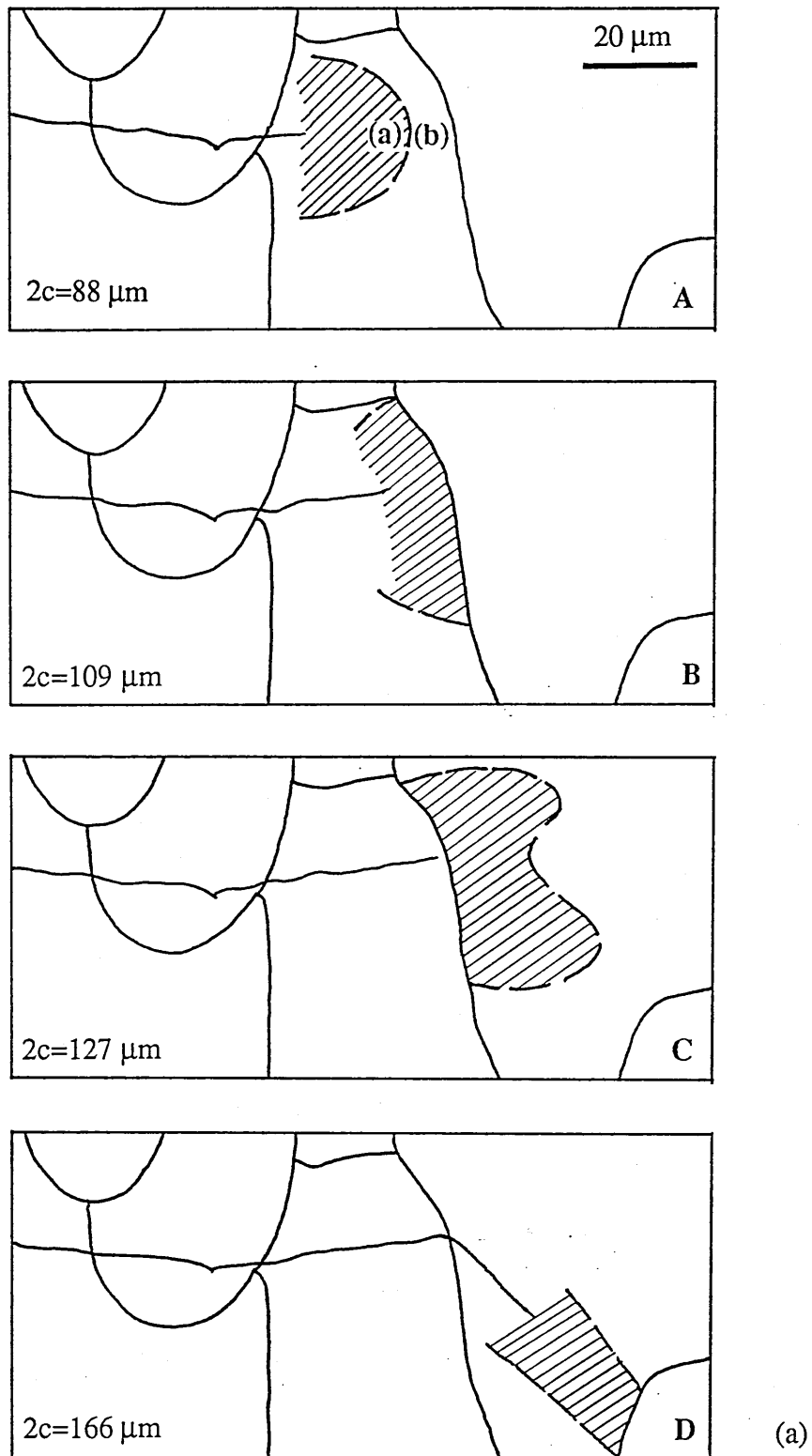
Figure 5.7   Interaction of the plastic zones of a small fatigue crack with grain
boundaries: (a), schematics showing the crack tip and its attendant
plastic zone as it propagates through the microstructure.

(b)

(c)

(d)
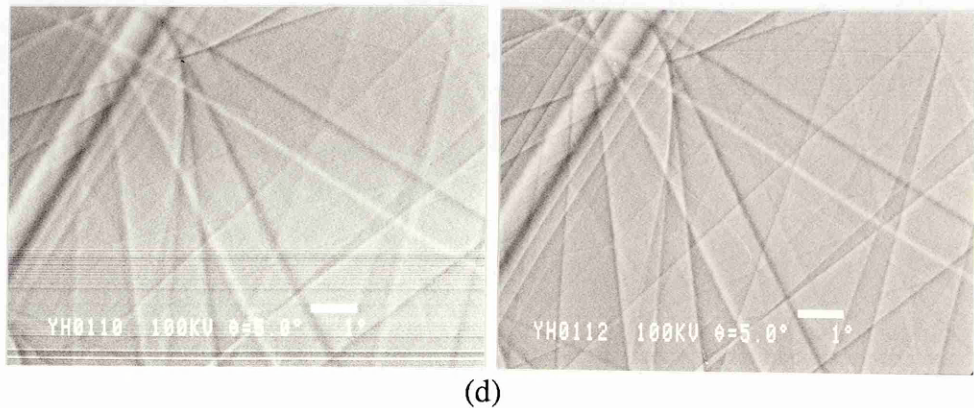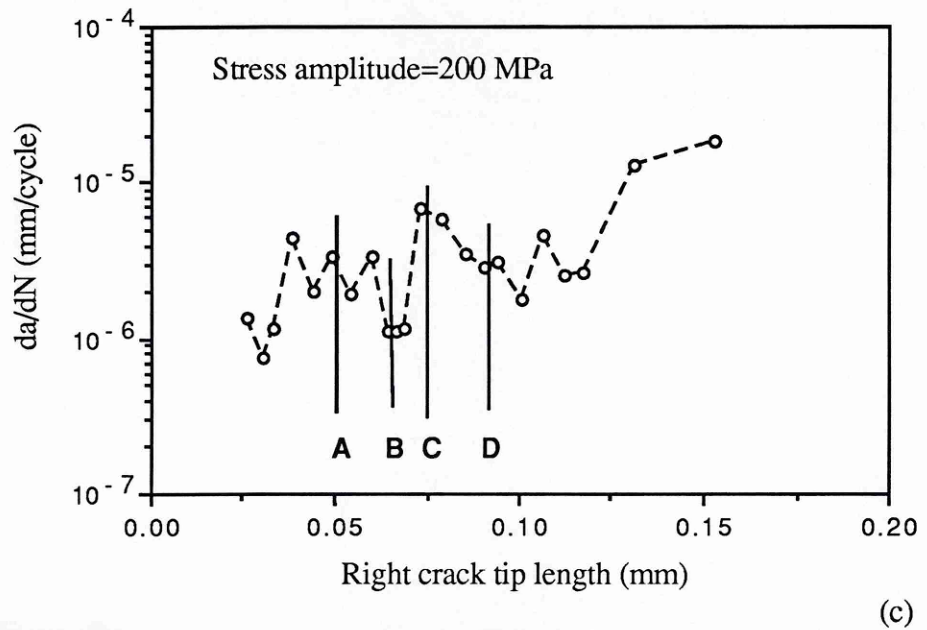
Figure 5.7 (cont.) (b), a micrograph taken when the crack tip was at position A in (a). (c), measured crack growth rates at each stage of crack length. (d), comparison of channelling patterns taken both within and outside the plastic zone from A of (a).
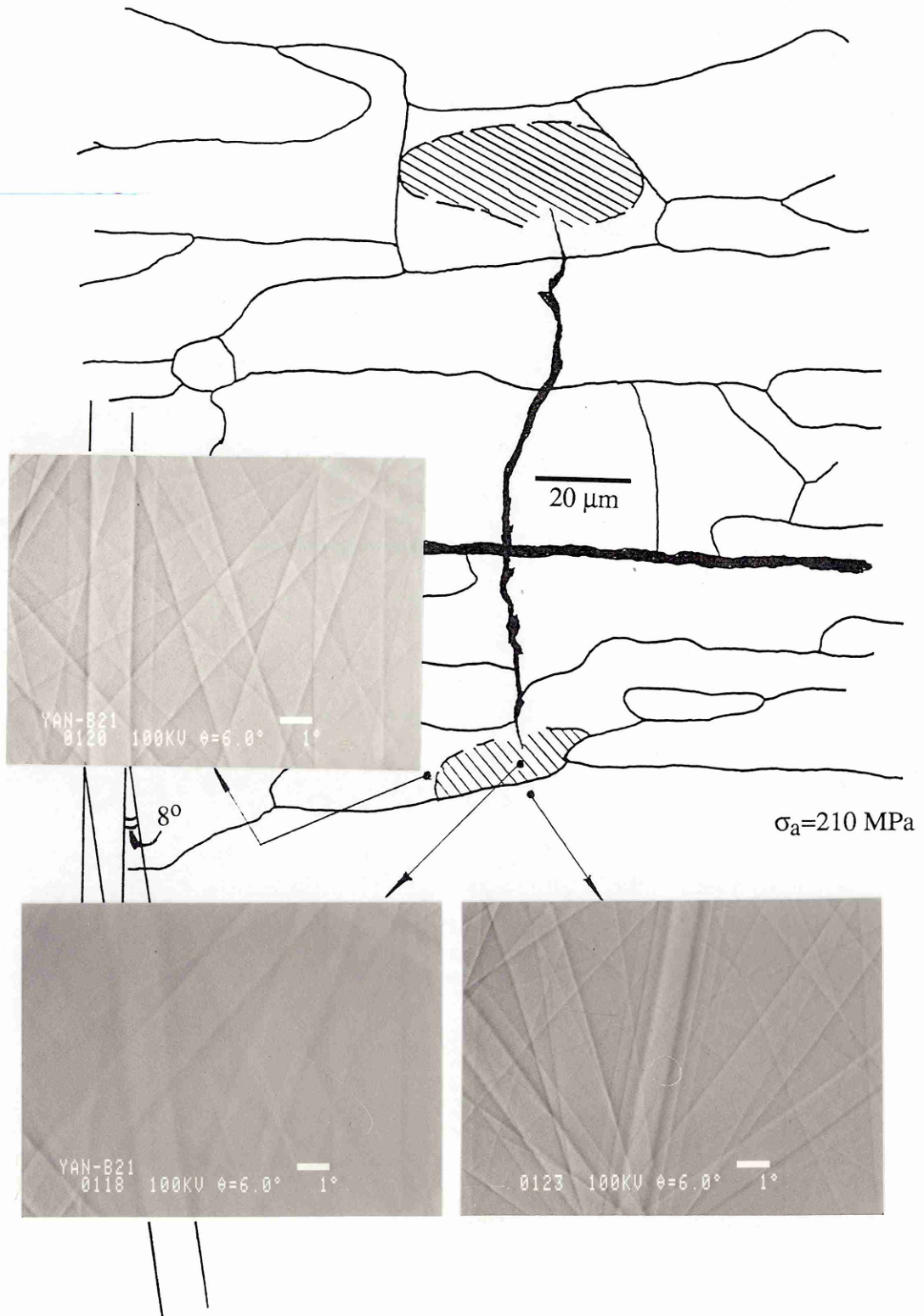
Figure 5.8   Another example of grain boundary blocking on the development of plastic zone size. Note the heavy deformation indicated by the blurring of ECPs and the rotation of one crystallographic plane in the blocked plastic zone.

(a)

(b)
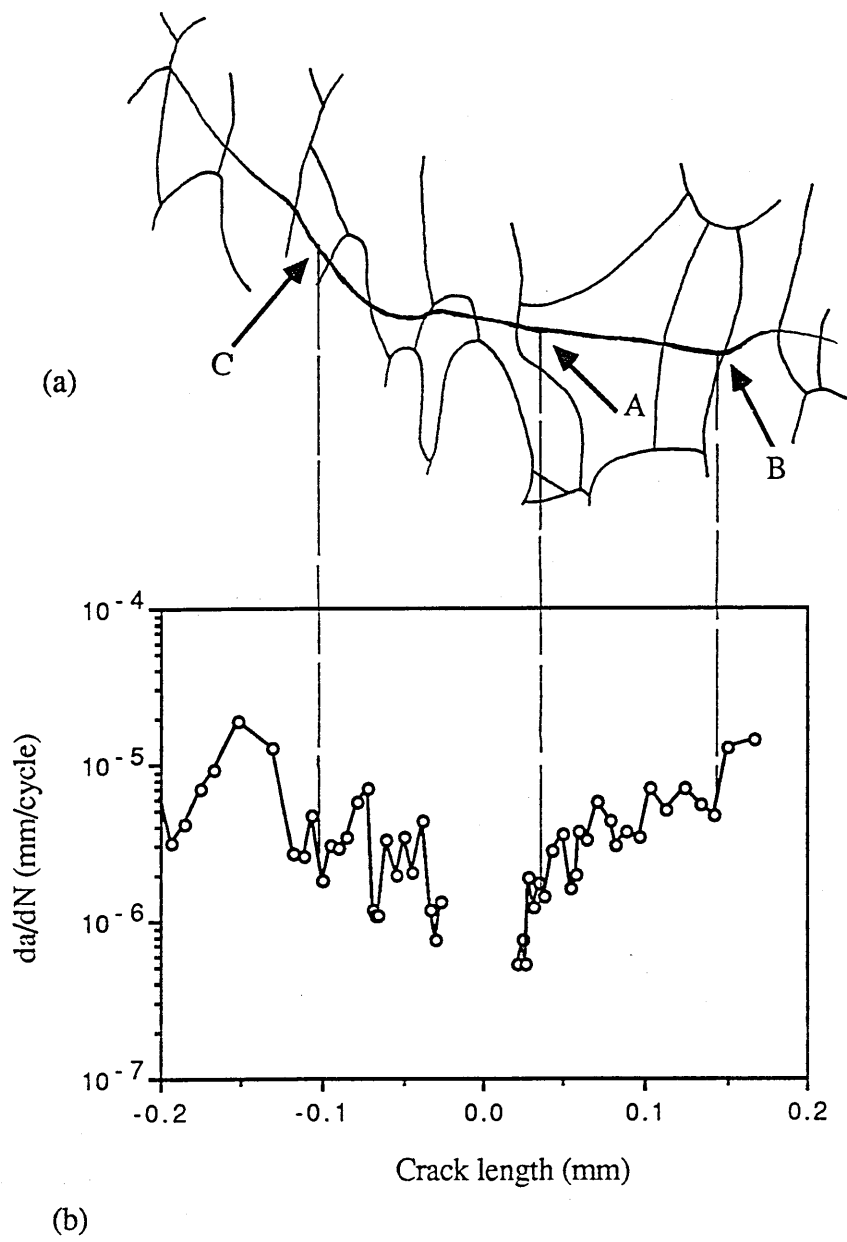
Figure 5.9   The development of plastic zone shape at a small crack: (a), sketch of
the crack and microstructure. (b), the crack growth rate.

20 μm

(c)

2c=72 μm

47 μm

2c=270 μm

(d)

grain boundary

grain boundary

28 μm

2c=166 μm

YH0141 100KV X4000 1μm

(e)
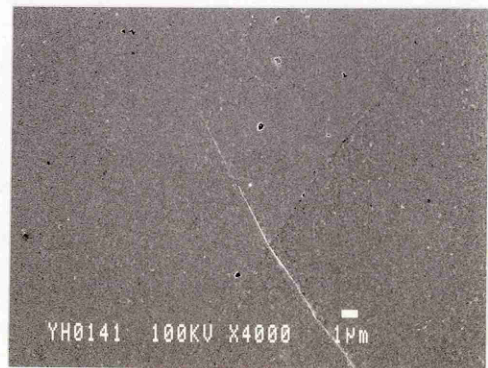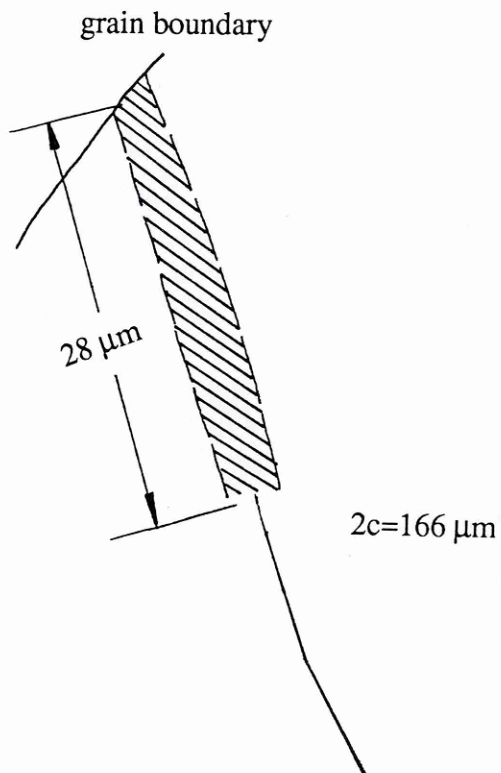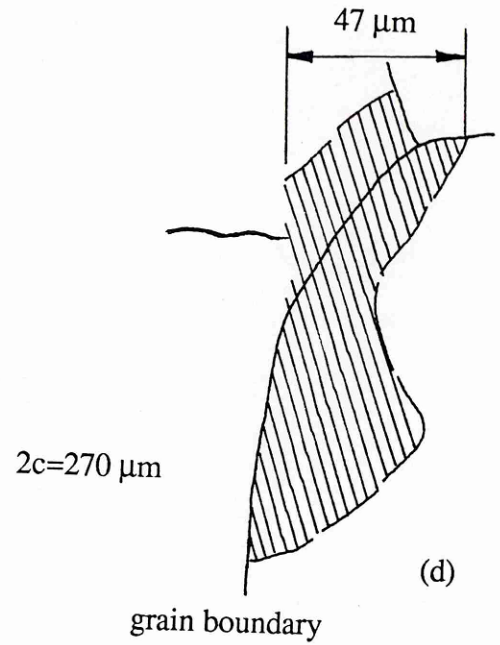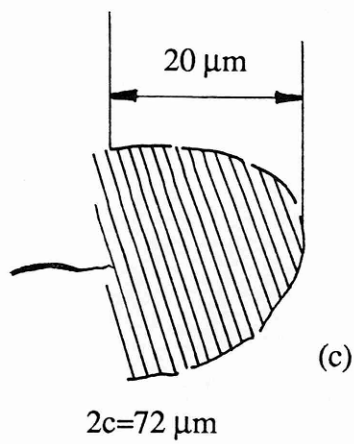
Figure 5.9 (cont.)   (c), a semi-circular plastic zone shape from point A. (d), the lobed plastic zone shape from position B. (e), a long, slender plastic zone shape from position C.
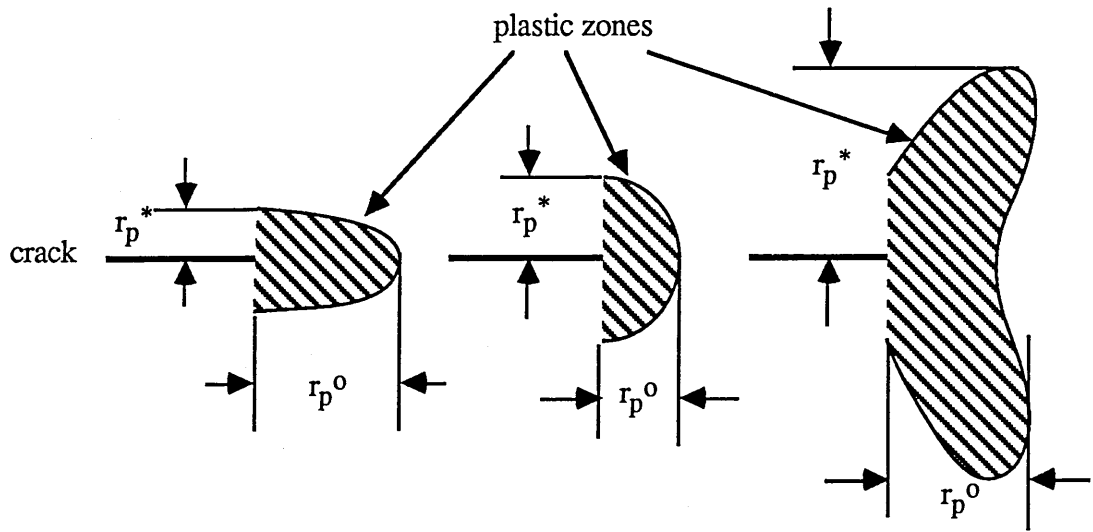
Figure 5.10   A schematic showing $r_p{}^o$ and $r_p{}^*$ for the three different plastic zone shapes.
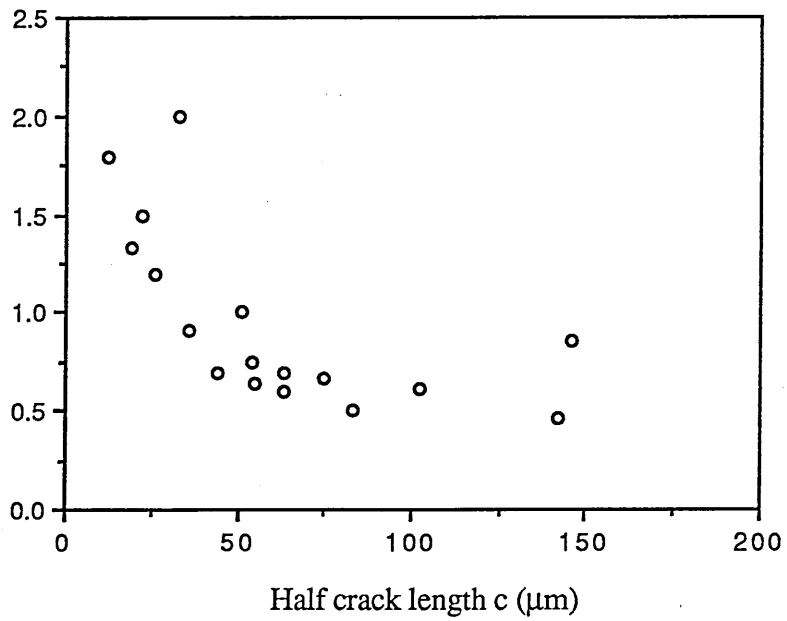
Figure 5.11   The variation of small crack plastic zone shape with crack length.
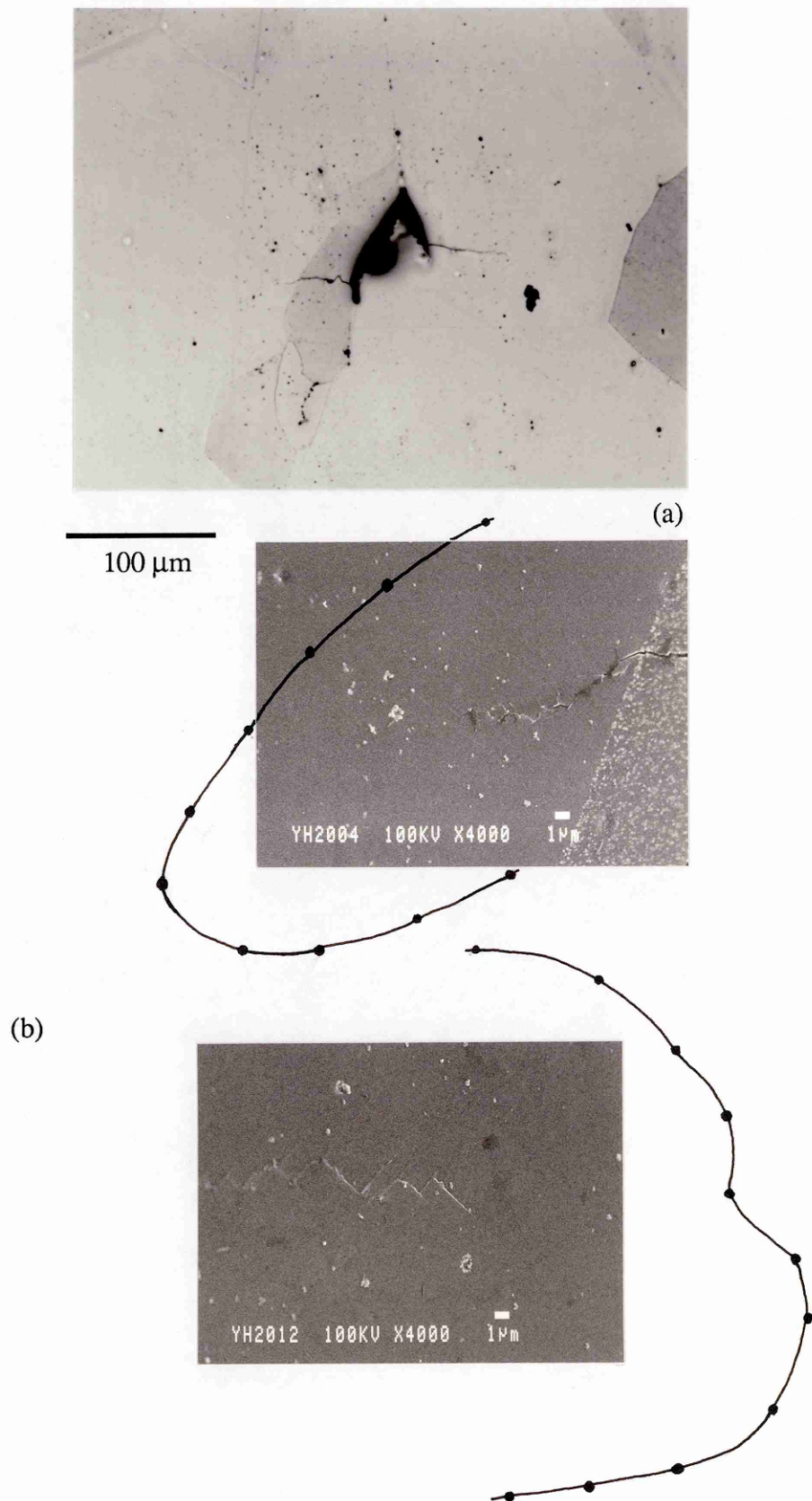
Figure 5.12   The plastic zone sizes and shapes of a small crack initiated from an inclusion in alloy A. (a), optical micrograph of the crack, (b), the measured plastic zones ahead of the two crack tips.
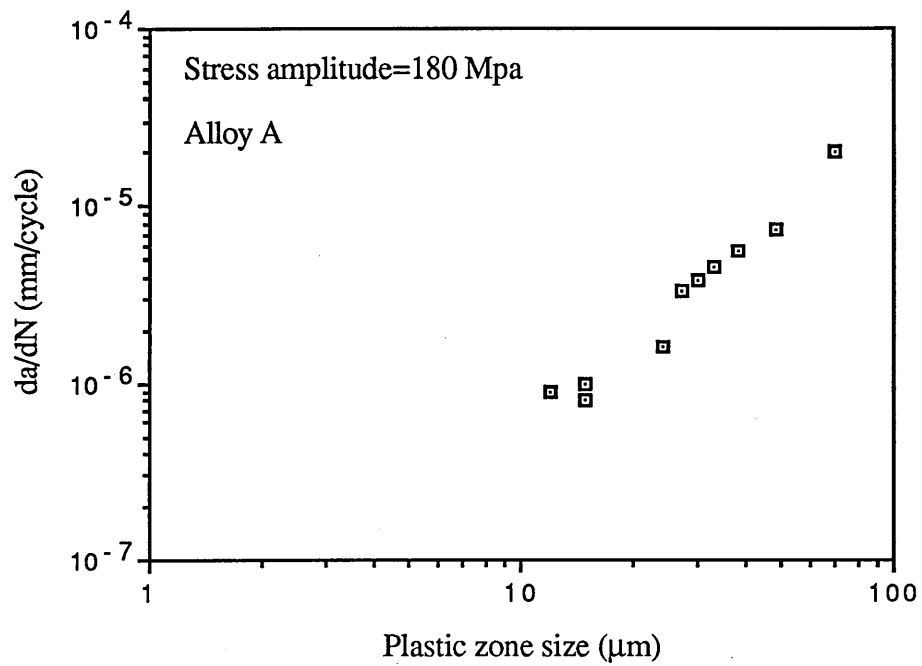
Figure 5.13   The correlation between plastic zone size and crack growth rate in alloy A.
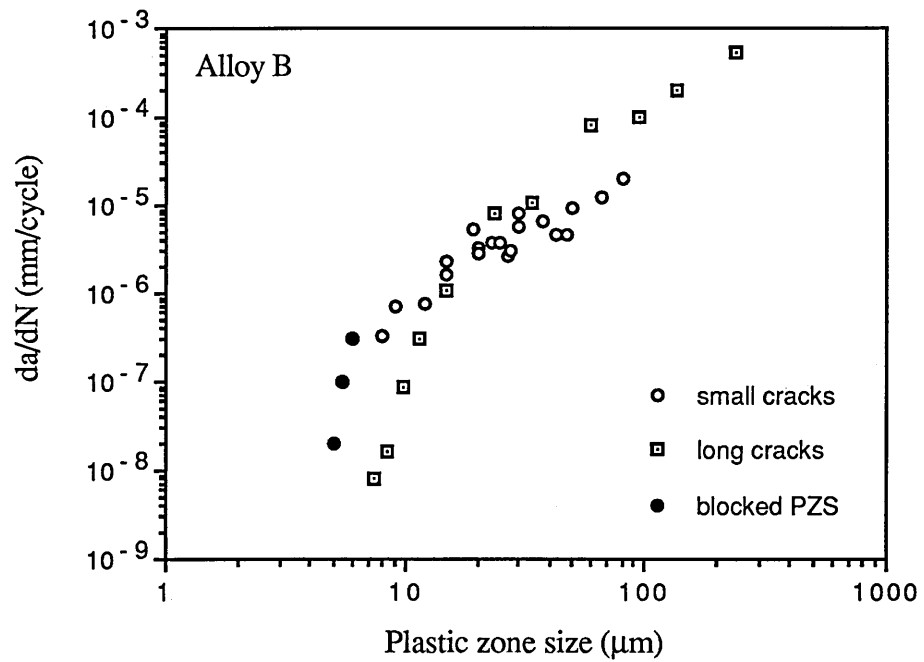
Figure 5.14   The correlation between plastic zone size and crack growth rate in alloy B.
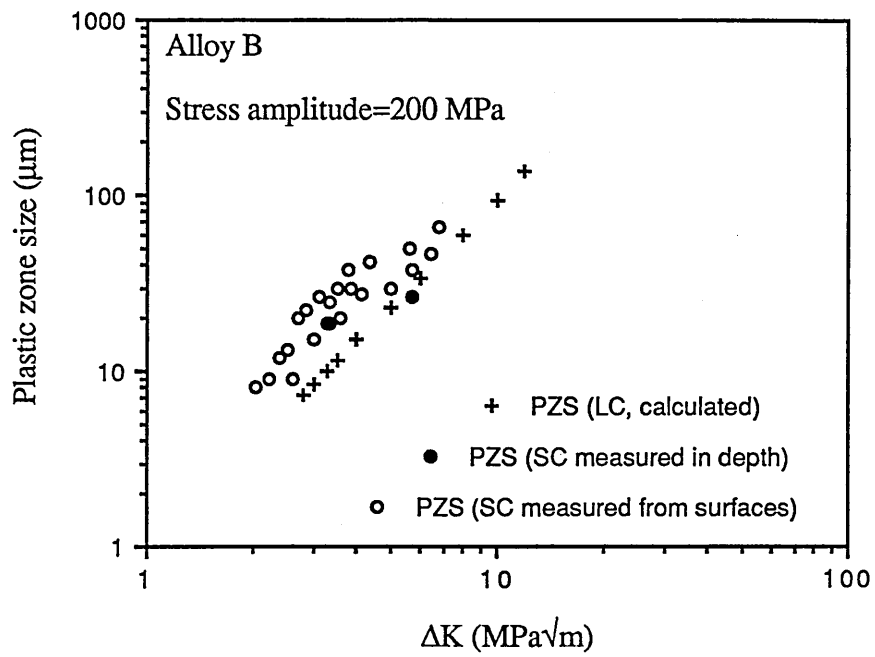
Fgure 5.15   The relation of plastic zone size with ΔK for alloy B.
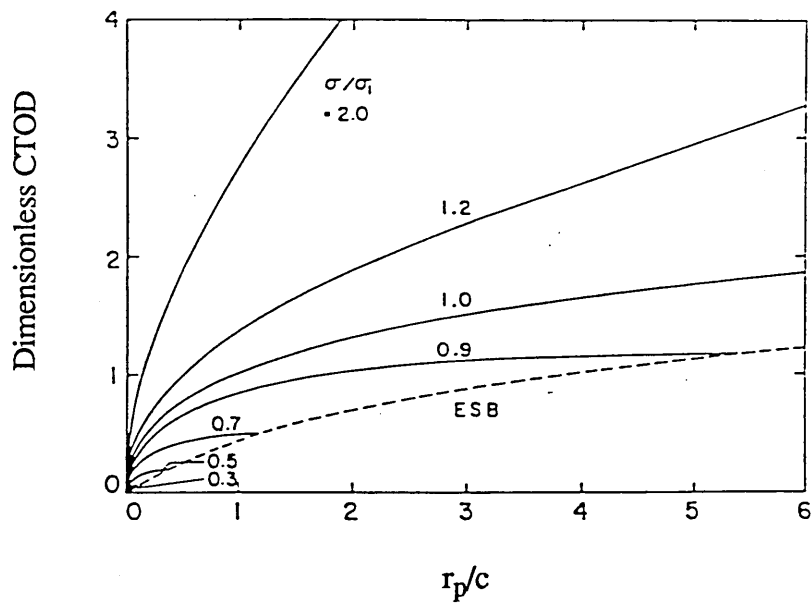
Figure 5.16   Relation between crack tip opening displacement and slip band zone size (after Tanaka et al, 1986).
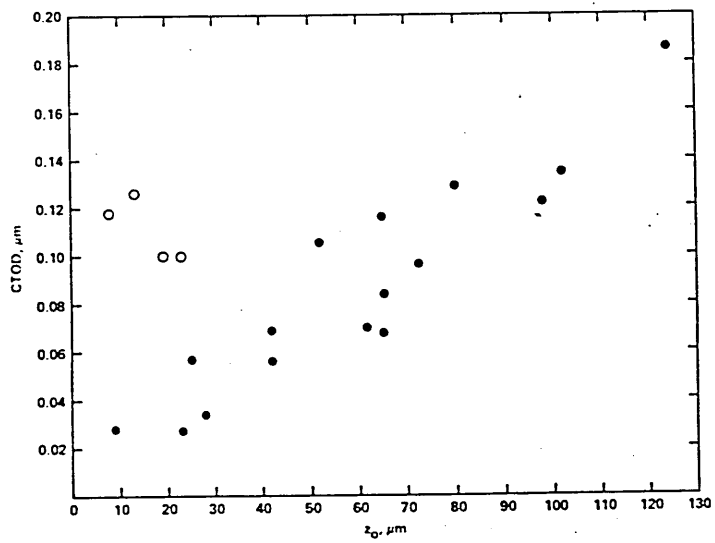
Figure 5.17   Comparison of CTOD to distance of crack tip from grain boundary, z_0. Open circles are especially long cracks with small z_0 at the tips (after Morris, 1980).

CHAPTER SIX

MODELLING SMALL FATIGUE CRACK GROWTH

6.1 Introduction

Since the fast growth rates of small fatigue cracks in comparison with long cracks at the same stress intensity factor range, ΔK, has been mainly attributed to the inability of K to describe the crack tip stresses and deformation fields associated with small cracks as the extent of local plasticity is comparable with the crack size, an alternative elastic-plastic fracture mechanics (EPFM) parameter is needed to correlate small crack growth. Several mechanics based EPFM parameters such as the J integral, crack tip opening displacement (CTOD), and strain energy density S, have been used in attempts to correlate small crack growth. But they all have their own deficiencies, as reviewed in chapter 2, and none are widely accepted for the description of small fatigue crack growth. Any modelling must be able to predict the behaviour of the frequent deceleration, or arrest, of small crack growth. Modelling this behaviour must clearly involve microstructural parameters and small crack growth has been modelled by several researchers by considering the interaction of crack tip slip bands with grain boundaries (Tanaka et al, 1986; Navarro and de los Rios, 1988; Sun et al, 1991).

From the experimental results of periodic plastic zone and fatigue crack growth measurements, as well as the analyses given in the previous chapter, it was found that the plastic zone size ahead of a small crack is an important parameter and can be used to characterize small crack growth. Nearly all the anomalous behaviour associated with small crack growth, such as fast growth rates compared with long cracks at the same nominal ΔK, deceleration and acceleration and growth below the threshold ΔK_{th} for long cracks, can be explained and solved if plastic zone size r_p is used in the description of small crack growth. Therefore, an alternative parameter to correlate

small crack growth, based on plastic zone size r_p, is proposed and a small crack growth model is set up in this chapter. It will first deal with the calculation of plastic zone size of small cracks. The strength of microstructural barriers, as judged by the misorientation between grains, is incorporated in the calculation of plastic zone sizes and a criterion predicting whether a crack will pass a barrier or not is used based on a comparison of the stress concentration ahead of the crack tip and the barrier strength. Finally, the predicted small crack growth will be compared with those experimentally obtained to check the efficacy of the model.

6.2. The Model

6.2.1. Calculation of Plastic Zone Sizes

Much of the published work on small fatigue cracks reveals that cracks prefer to initiate from large grains with the most favourable crystallographic orientation to the loading to achieve a maximum shear stress. So the local yield stress will be significantly reduced, causing greater plastic zone sizes within these large grains. When a crack is long and its plastic zone includes many grains, this yield strength will increase to the level of the material's yield stress. This implies that the resistance of a material to plastic deformation must vary with crack length. It is also known that these cracks grow preferentially along persistent slip bands. According to the continuously distributed dislocation model of cracks first proposed by Bilby, Cottrell and Swinden (BCS) (1963), the following equation can be obtained from the condition of vanishing dislocation density at the tip of a slip band (bounded condition) for an infinite isotropic elastic medium subject to a uniform applied stress τ,

$$n = \frac{c}{b} = \cos\left(\frac{\pi\tau}{2\tau_f}\right)$$
(6.1)

So
$$\frac{r_p}{c} = \frac{\left\{1 - \cos\left(\frac{\pi\tau}{2\tau_f}\right)\right\}}{\cos\left(\frac{\pi\tau}{2\tau_f}\right)}$$
(6.2)

where $b = c + r_p$ and τ_f is the friction stress opposing the movement of dislocations in the plastic zone. Originally the "slip planes" of these dislocations were not considered to be crystallographic but were analogous to the lines defined in the macroscopic theory of plasticity. According to this model, the macroscopic applied stress τ is weaker than the resistance to dislocation motion, friction stress σ_f, particularly in the case where long thin plastic zones entend across many grains. An ideal uniform medium was assumed and the effects of grain boundaries were not considered so that the friction stress σ_f in the model is the combination of the intrinsic friction stress σ_0 (encompassing the effects of crystal lattice characteristics, solute atoms, precipitates, and stress fields of other dislocations) and the strengthening due to grain boundaries and is equal to the yield stress, σ_y. This is a reasonable assumption if the grain size is much smaller than the plastic zone size. From equation 6.2, it can be seen that the ratio of plastic zone size to crack length (r_p/c) is only dependant upon the ratio of applied stress to yield stress (τ/τ_y).

This is not the case for small fatigue cracks, however, where both the crack and its accompanying plastic zone may be contained within a single grain. This situation, which is the one considered in the present model is shown in Figure 6.1. D is the grain diameter, so that $iD/2$ is the distance of each subsequent grain boundary from the crack origin and λ is the distance between the crack tip and the next grain boundary. The crack is assumed to initiate in the centre of a grain.

In the present measurement of plastic zone sizes of small cracks it was found that the ratio r_p/c reached a maximum value of about 0.8 when the crack was small (about one or two grain sizes) and gradually decreased during crack growth to a value of about

0.2 as the crack became longer. To reflect this, the concept of an equivalent friction stress is used here for the calculation of plastic zone size on the basis of the BCS model. This concept was first proposed by Sun et al (1991) in the modelling of small crack growth, and is essentially a variable friction stress which incorporates the strength of grain boundary barriers. It may be expressed in the form, (see chapter 2):

$$\tau_{ef} = \frac{1}{2}m^*\tau_0^* = \tau_y - m^*\tau_c\sqrt{\frac{r_0}{iD}} \qquad i=1, 3, 5, \dots\dots \qquad (6.3)$$

where τ_0^* is defined as an equivalent intrinsic friction stress, m^* is the orientation factor, and r_0 is the distance between the grain boundary and a dislocation source in the next grain. Equation (6.3) indicates that, since τ_y is constant for a given material, then τ_{ef} will vary as the crack grows (and i increases). When i=1, τ_{ef} has a minimum value, corresponding to the intrinsic friction stress τ_0 in a single crystal. At the other extreme, when i approaches infinity, (in the case of long crack), the equivalent friction stress τ_{ef} achieves its maximum value and equals the yield stress, τ_y. By replacing τ_f in equation (6.1) with τ_{ef}, the following equation is obtained for the calculation of plastic zone sizes of small cracks:

$$n = \frac{c}{b} = \phi \cos\left(\frac{\pi\tau_{max}}{2\tau_{ef}}\right) \qquad (6.4)$$

where ϕ is a scaling parameter which is introduced in order to correlate the predicted plastic zone size with that experimentally measured. Inspection of equations (6.3) and (6.4) shows that the ratio, c/b increases and r_p/c decreases as the crack length increases (i from 1 to ∞), as shown in Figure 6.2. This indicates that small fatigue crack plastic zones will initially be large with respect to crack length but will gradually decrease as crack length increases. This, of course, agrees with experimental observations. Furthermore, when the crack becomes long, i.e. i approaches infinity, τ_{ef} equals τ_y, and equation (6.4) achieves the same form as equation (6.1), that is, the original BCS model. Comparing equation 6.4 with equation 5.3 derived from the

86

consideration that when the applied load is high a complete solution for describing K should be used (Allen and and Sinclair 1982), both equations predict a decrease in effective friction stress, and therefore an increase of plastic zone size for the situation of small cracks, although they were derived from different considerations. But the present calculation of plastic zone size shows the variation of r_p with crack size, and predicts that the plastic zone size will gradually merge with that of long cracks, which is in agreement with the developing trend of small crack growth rates.

One assumption has to be made for the effect of plastic zone shape on crack growth rates. As observed, the plastic zone shape of small cracks varied as the crack length increased. Although it is difficult at this stage to accurately describe the influence of plastic zone shapes of small cracks on crack growth rates, it is assumed that the growth rates are only proportional to plastic zone sizes ahead of crack tips, no matter how the the plastic zone shape evolves. This assumption is reasonable, as far as the present experimental results of plastic zone size measurements on growing small fatigue cracks is concerned.

In the above, the continuously distributed dislocation theory is used to solve the problem of stage I crack. The solution for stage II cracks are obtained through the following substitution to the solutions for stage I cracks:

$$\sigma \rightarrow \tau, \qquad \sigma_f \rightarrow \tau_f \qquad \sigma_y \rightarrow \tau_y \qquad\qquad (6.5)$$

6.2.2. Retardation of Crack Growth

Observations of the plasticity associated with growing fatigue cracks, which has been described in the previous chapter, showed most grains containing the tips of small cracks were not wholly deformed, in agreement with the observations of Lankford et al (1984). When a crack and its accompanying plastic zone approached a grain

boundary, on occasion, both the crack and its preceding plastic zone were found to pass easily through into the next grain and on these occasions, there was almost no deceleration in crack growth rate. But more usually, particularly when the ratio of applied stress/yield stress was low and the crack length was small (typically less than 5 grain sizes), the plastic zone would be blocked by the grain boundary, and a decrease in crack growth rate was observed.

In particular, it was found that the growth rate of small fatigue cracks began to be retarded when their relatively large plastic zones, not their crack tips, were blocked by grain boundaries. Typically, the crack then temporarily arrested and further propagation occurred only after the development of plastic deformation in the next grain. This suggests that it is the initiation of plasticity in the next grain that is probably the controlling step and thus crack retardation or arrest will only cease when the stress concentration caused by the accumulated strain in the blocked plastic zone is of sufficient magnitude to overcome the barrier caused by the misorientation of grains and thus activate slip sources in the next grain.

This situation can be modelled in the following manner. The upper limit of the stress S acting on a dislocation source in the next grain for the case where the plastic zone is blocked by a grain boundary has been given by Navarro and de los Rios, (1988), as:

$$S(\zeta_0) = \frac{\sigma}{\sqrt{2}\sqrt{\zeta_0-1}} (1 - \frac{2\sigma_0 \cos^{-1}n}{\pi\sigma}) + \sigma_0 \qquad (6.6)$$

where $\zeta_0 = (b+r_0)/b$. The stress concentration ahead of the plastic zone increases as the parameter ζ_0 decreases, which occurs as the crack tip approaches the grain boundary.

Whether this stress operates the dislocation source depends, of course, on its strength. The critical stress to operating a dislocation source which may not lie in the plane of maximum shear stress has been given by Armstrong, (1983), as:

$$S(\zeta_0) = \frac{1}{2} m^* \sigma_c \qquad (6.7)$$

where σ_c is the critical stress required to operate a dislocation source and m^*, as defined earlier is the misorientation factor. As mentioned before, cracks usually initiate from these "soft spots" (i.e., large grains with the most favourable orientations) and grow through less-favourably oriented grains, so the orientation factor m^* will take a lower value of 2.2, as for a single crystal (Taylor 1938), in the first grain. Since the severe deceleration, or arrest, of small crack growth most often happens when the crack is within one or two grains, and from the consideration of simplicity in the modelling, an average value of the Taylor parameter (m=3.1 for f.c.c. metals) is taken in the later stage. Comparison of equations (6.5) and (6.6) are used in the model to judge whether a blocked plastic zone can pass a grain boundary.

6.3 Application of the Model

As shown previously, at least for the two high purity 7000 series aluminium alloys studied here, small fatigue crack growth rates are proportional to their experimentally measured plastic zone sizes and a relation like equation 5.4 exists between them. Since the plastic zone size ahead of small crack tips can be calculated with equations 6.4 and 6.2 and correlated with experimental results of PZS measurement well, then equation 5.4 allows the prediction of crack growth rates from calculated plastic zone sizes. When the plastic deformation ahead of crack tips is not blocked by a grain boundary r_p is calculated from equations 6.4 and 6.2. And if it is blocked by a grain boundary and the stress concentration caused is not large enough to overcome the

89

barrier, as judged by equations 6.5 and 6.6, the distance between the crack tip and the grain boundary, λ, is assumed to be the plastic zone size.

For each experimental value of da/dN obtained from the fatigue tests, a corresponding value of PZS r_p was calculated using equations 6.4 and 6.2. For each complete set of data (da/dN, r_p), a least squares fit was performed on equation 5.4 to determine the corresponding values of parameters C and m. In the calculation, the parameters r_0 and τ_c are assumed to be constants for simplicity. According to Navarro and de los Rios (1988), the value of r_0 is between 0.1-1 μm, τ/τ_0 between 5-20 and τ_c is the initial yield point (smaller than τ_y). The values of these parameters used in the modelling are: r_0=0.1; τ/τ_0=10; τ_c/τ_y=0.96. The determined constants C and m are respectively $1.0*10^{-7}$ and 1.36 for alloy A and $2.0*10^{-9}$ and 2.0 for alloy B. The predicted results are compared with experimental growth data obtained at a stress amplitude of 180 MPa for alloy A in Figure 6.3, and at a stress amplitude of 200 MPa for alloy B in Figure 6.4, (the predictions are given by the solid lines). It can be seen that the crack growth deceleration at small crack lengths is well predicted and general agreement is good. The generality of the model is illustrated in Figure 6.5 where the plastic zone size data of the present study is used to predict growth rates in a 7075 Aluminium alloy used by Lankford, (1982). It can be seen from Figures 6.3 to 6.5 that the predictions of small crack growth produced by the model correlate the available experimental data well.

6.4   Discussion

Evaluating plastic zone sizes associated with small fatigue cracks by means of experiments, such as the SAECP method, is difficult and time consuming, and data is therefore not generally available. Thus, it is important that an analytical model is developed for evaluating the local values of plastic zone sizes r_p based on global variables, such as applied load, crack length, yield stress and grain size.

The relatively large plastic zone size associated with small fatigue cracks can be attributed to the large applied stress and the surface measurements of PZS, as explained by Lankford et al (1984). This phenomenon is well described by the present model which also predicts, on the basis of experimental plastic zone measurements, that the ratio of r_p/c (for unblocked cracks) will be a function of crack length. This means that, after the plasticity has passed a grain boundary barrier, the plastic zone size is predicted to be less than the extrapolated plastic zone size value from the previous grain due to the introduction of the equivalent friction stress. This assumption and the consequently calculated ratio of r_p/c is consistent with the experimental results.

It also has some support from the literature. By calculating the local effective stress intensity factor range, ΔK_{eff}, which is determined from crack tip displacement and strain range measurements, and comparing it with the nominal ΔK, Chan (1986) found ΔK_{eff} to be larger than ΔK. The ratio of $\Delta K_{eff}/\Delta K$ depends on both crack length and the ratio of the maximum applied stress/yield stress, showing decrease with crack length and increase with the ratio of σ_{max}/σ_y. To improve the agreement between theory and experiment, Chan suggested (1986) that the effect of microstructure must be incorporated into the Barenblatt-Dugdale crack model. One possibility is to consider the yield stress to depend on crack length so that σ_y would take on a value lower than the macroscopic yield stress when the monotonic plastic zone size is within a single grain or microstructural unit. This idea, although just a suggestion and not implemented in any modelling, is in agreement with the present application of the concept of the equivalent friction stress in the model for the calculation of plastic zone size of cracks. In the explanation of the occurrence of large scale yielding ahead of crack tips for the fast growth rates of small cracks, Tanaka et al (1986) also realized that the actual yield strength in the plastic zone is variable. It will have a smaller value when a crack is small owing to the lower constraint on plastic deformation, and will increase with crack length due to the grain size effect as suggested by the Hall-Petch

relation. This increase in yield strength results in a decrease in plastic zone size as well as ΔCTOD, which leads to a lowering of growth rates and consequently the convergence of small and long crack growth data.

When using stress intensity factor K to correlate crack growth, the deceleration, or arrest, of small crack growth, which is one of the main features associated with small fatigue crack growth, cannot be predicted, since ΔK will always predict an increase of crack growth rate with crack length (at constant applied stress). Using plastic zone size as the correlator for small crack growth, however, the deceleration of small cracks can easily be predicted due to the blocking of microstructural barriers on plastic deformation. The prediction from the model shows a good agreement with the experimental data. This, in turn, indirectly supports the general viewpoint that the deceleration, or arrest, of small crack growth is related with the blocking of grain boundaries of materials.

Recently crack growth laws for both long and small cracks were obtained from experimental data by Nisitani et al (1992). An unifying explanation for these growth laws was made based on an assumption that the crack growth rate is proportional to the reversed plastic zone size. This is similar to the present assumption which is based on the maximum plastic zone size since this is the plastic zone size that can be measured experimentally by means of electron channelling patterns. It is believed that the good predictive accuracy of the present model derives from the use of measured rather than calculated plastic zone sizes. The obvious disadvantage is that difficult and time consuming measurements must be made for each material studied. Although this may limit the use of the model for engineering use it does describe the micromechanisms of crack advance reasonably well.
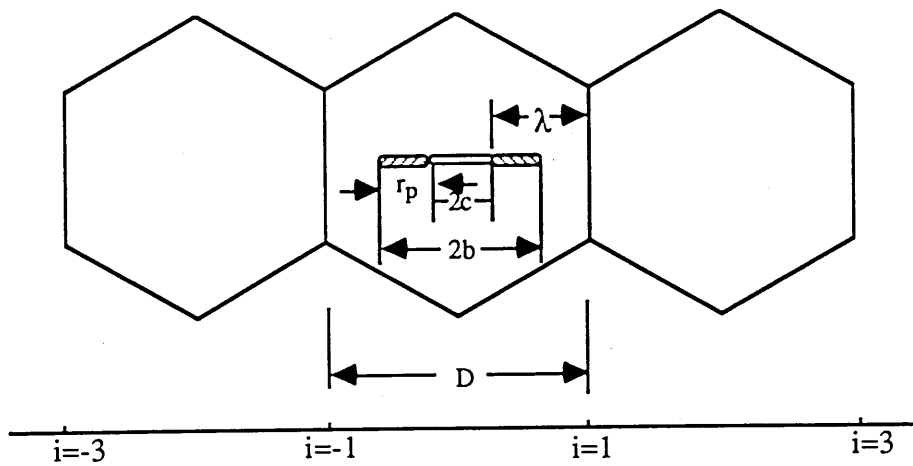
Figure 6.1   A schematic of a crack within a grain, illustrating the parameters of the model.
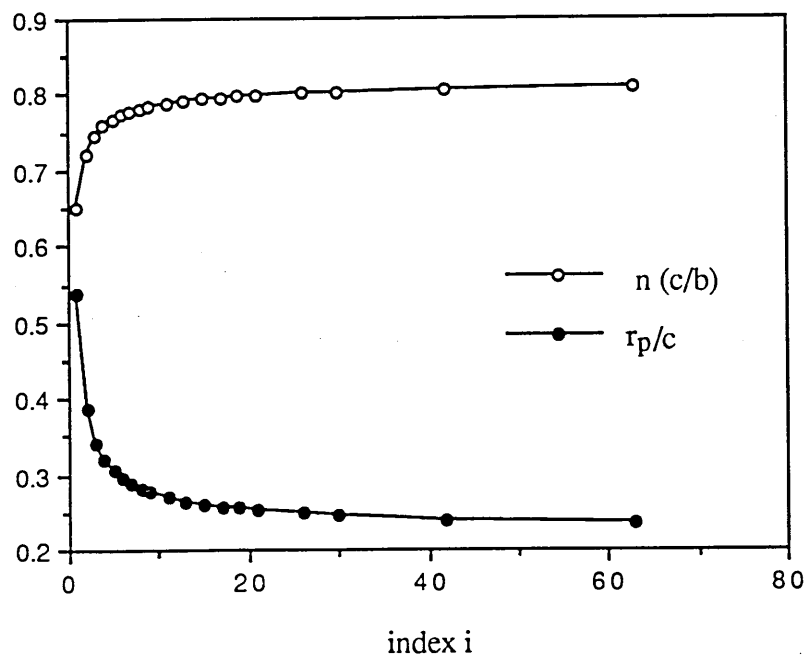
Figure 6.2   The predicted variation of ratio n (c/b) and r_p/c with index i.
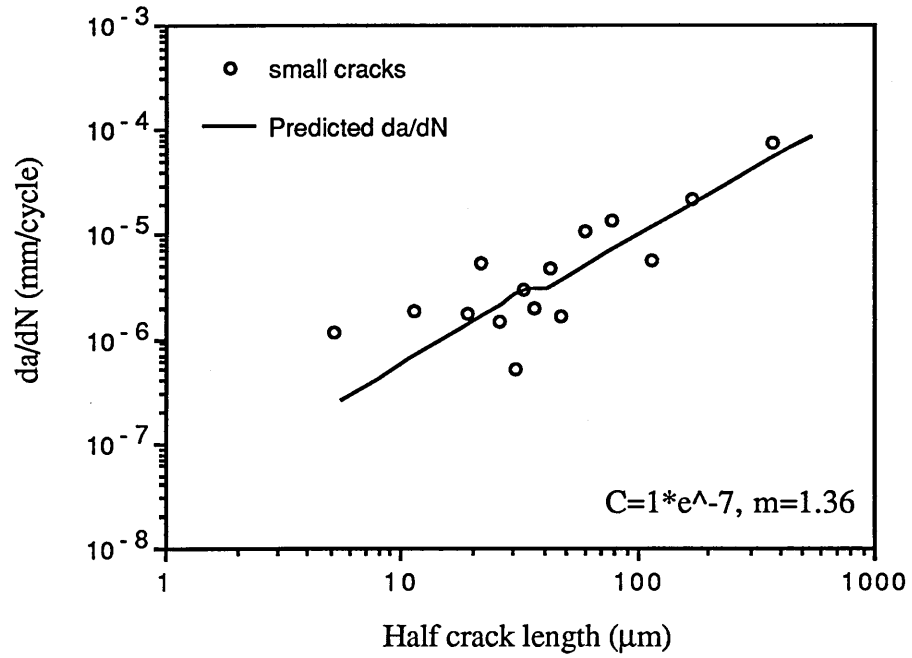
Figure 6.3   Comparison of predicted crack growth rates (solid line) with
experimental data for alloy A (σ_a=180 MPa).
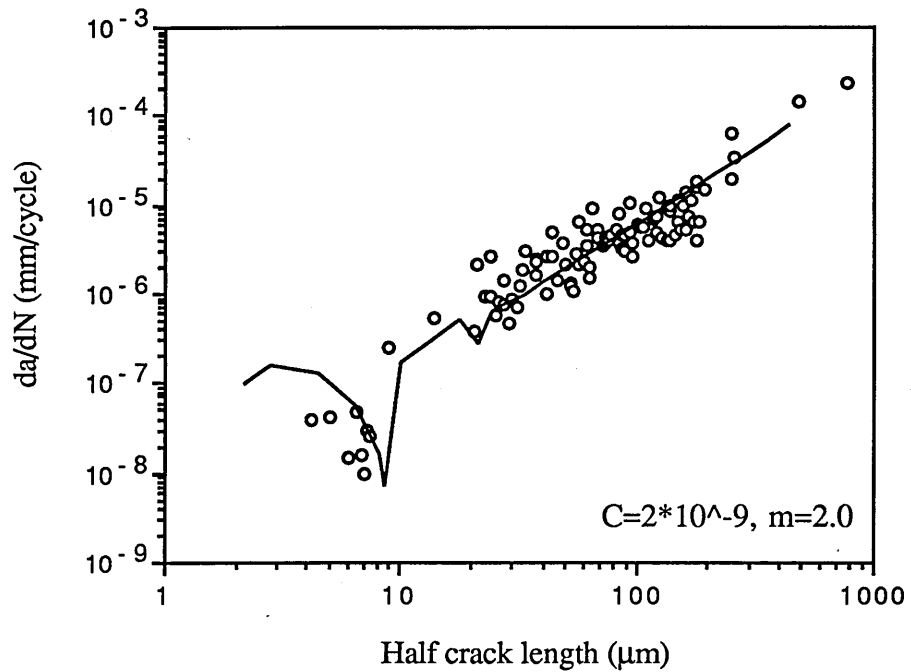
Figure 6.4   Comparison of predicted crack growth rates (solid line) with
experimental data for alloy B (σ_a=200 MPa).
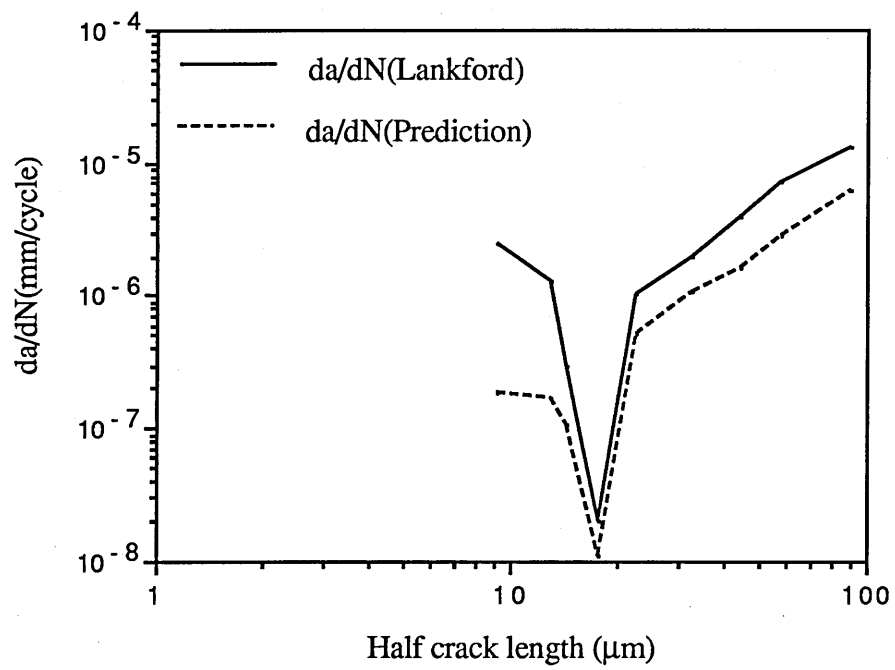
Figure 6.5   Comparison of predicted crack growth rates with experimental data from Lankford (1982).

CHAPTER SEVEN

CONCLUSIONS AND FUTURE WORK

7.1 Conclusions

Based on the investigation of the growth behaviour of small fatigue cracks on four Al-Zn-Mg-Cu alloys by fatigue testing, plastic zone size measurements and modelling, the following conclusions can be drawn:

1. Small fatigue cracks in Al-Zn-Mg-Cu alloys exhibited fast growth rates compared to long cracks at the same stress intensity factor range, ΔK, at R=0.1, and also grew at crack sizes and applied stress levels which were below those predicted from long crack threshold data.

2. Small crack growth exhibited a growth pattern of deceleration and acceleration. It was observed that the deceleration, or even temporary arrest, of small fatigue crack growth was related with blocking at grain boundaries, especially from the first grain boundary.

3. By adding different amounts of Cr to a Al-Zn-Mg-Cu alloy to change the distribution of slip, it was found that slip distribution did not have noticeable effect on the growth rates of small fatigue cracks, confirming a similar result reported in Al-Mg-Si alloys.

4. Less deflection in crack growth path and blocking by grain boundaries in the large-grained microstructure of alloy A resulted in faster growth rates than seen in alloy B which possessed a fine-grained microstructure.

5. By comparing the growth rates of small cracks at R=0.1 and long cracks at R=0.8, it was found that the difference in growth rates characterized with ΔK between them was reduced, but small cracks still showed faster growth rates than long cracks. This indicates that, apart from the effect of crack closure stress, there must be other factor(s) which contribute to the difference between long and small crack growth rates.

6. A novel experiment of plastic zone size measurement on growing small fatigue cracks was developed for the study of the characteristics of plastic deformation ahead of small fatigue cracks. It was found that the plastic zone shapes were dependent upon both crack length and crack growth path. When the crack length was small with respect to the grain size its growth was mainly crystallographic and the plastic zone adopted a slender shape extending directly ahead of the crack tip. Such plastic zones were often blocked by grain boundaries. As the crack lengthened, the plastic zone changed shape becoming first semi-circular in shape before finally adopting the typical lobed configuration normally found associated with long fatigue cracks.

7. Small crack growth was accompanied with relatively large plastic zone sizes ahead of crack tips, which violates the small scale yielding assumption for the successful application of LEFM using the stress intensity factor K as a correlating parameter.

8. Through periodic measurement of plastic zone sizes of growing small fatigue cracks, it was found that small cracks began to decelerate when their relatively large plastic zones, not crack tips, were blocked by grain boundaries. Further propagation of the crack required the development of plastic deformation in the next grain showing that it is the initiation of plasticity in the next grain that is probably the controlling step.

94

9. By plotting the growth rates of small cracks against their measured plastic zone sizes, it was found that the following relation was obeyed between them, i.e.,

$$da/dN = C\, r_p^m$$

where C and m are material constants.

10. A new parameter, i.e., the local plastic zone size ahead of crack tip, was proposed for the description of small crack growth. By comparison with the application of ΔK, the use of plastic zone size reduced the difference between long and small crack growth rates. There is a possibility to use a single parameter r_p to determine both long and small crack growth rates. The advantages of using r_p as a correlating parameter for small crack growth have been discussed.

11. The present criteria for predicting the converging condition for long and small crack growth rates failed in the case of alloy A which possessed a large grained microstructure. It appears that the growth rates of small cracks will merge with that of long cracks once the plastic zone sizes of small cracks can be predicted using ΔK on the basis of LEFM.

12. Based on the results of the novel experiment of periodic PZS measurement and fatigue test, small crack growth was characterized by the PZS ahead of it. Plastic zone sizes of small cracks were calculated by introducing the equivalent friction stress into the BCS model and correlated with the PZS experimentally measured. The features of discontinuous development of PZS ahead of small fatigue crack tips, the comparatively large ratio of r_p/c during early crack growth, and then decreasing with crack propagation, were well characterized by the model. Crack deceleration was described by blocked PZS and the recovery of growth was expressed by the necessity of a stress concentration within the

plastic zone to overcome the next grain boundary barrier to operate a dislocation source in the next grain. The prediction was compared with the experimental results and showed good agreement.

7.2 Future Work

Plastic zone size measurement using SAECP method on growing small fatigue cracks has proved to be a very useful tool for the study of small fatigue crack growth behaviour. Much information on the characteristics of small crack growth, such as the development of plastic zone sizes and shapes of small cracks during growth, the interaction between plastic zones with grain boundaries and subsequent crack growth, the relation between plastic zone size and small crack growth rates etc, could be obtained. Although some fields have been exploited and some interesting results have been obtained, a further investigation using the technique developed on small crack growth is necessary in the following aspects:

1. Since the experiment was mainly carried out at one stress amplitude and stress ratio for each alloy, it is not clear whether stress amplitude and stress ratio will affect the efficacy of equation 5.4 showing the relation between the growth rates of small cracks and their plastic zone sizes. In other words, more experiments on plastic zone size measurement are needed at different stress amplitudes and stress ratios to confirm the existence of the equation 5.4 for fatigue cracks.

2. It seems that there is a possibility to use a universal parameter of plastic zone size ahead of crack tips to characterize both long and small crack growth rates. It also seems that the growth rates of small fatigue cracks will behave like long cracks once their plastic zone size can be predicted with ΔK using LEFM analysis. This needs to be confirmed by the plastic zone measurement on both long and small growing cracks using the same material and same technique.

3. Based on the experimental results, a small crack growth model has been proposed in the present work and showed a good agreement with the experimental data in one alloy. The generality of this small crack growth model needs to be confirmed by applying the developed technique of plastic zone measurement on growing small cracks in other alloys with different microstructures, chemical compositions and crystal structures.

4. The application of the proposed model to predict the fatigue life of materials should be expoited. One obstacle for accurate fatigue life prediction is concerned with the estimation of the stress concentration. When a crack tip has reached a grain boundary, the distance between the crack tip and the grain boundary, λ is 0, and the prediction of fatigue life from the model will be infinite. To overcome this obvious problem, the stress concentration ahead of the blocked plastic zone should also be related with damage accumulation theory. Furthermore, a more accurate relation between the misorientation of two neighbouring grains and the decelerating extent of the crack growth rate should be established. This could be achieved by using SAECP and/or Electron Backscattered Patterns techniques for the crystal orientation determination in the crack region.

REFERENCES

Akiniwa, Y., Tanaka, K. and Matsui, E. (1988), Mater. Sci. Engng., A104, 105.

Allen, R. J. and Sinclair, J. C. (1982), Fatigue Engng. Mater. Struct., 5, 343.

Armstrong, R. (1983), Yield Flow and Fracture of Polycrystals (edited by Baker, T. N.), Appl. Sci. Pub., New York, 1.

Bathias, C. and Pelloux, R. M. (1973), Metall. Trans., 4, 1265.

Beevers, C. J., Cooke, R. J., Knott, J. F. and Ritchie, R. O. (1975), Metal Science, 9, 119.

Bilby, R. J., Cardew, C. E. and Howard, I. C. (1977), Fracture 1977 (edited by Taplin, D. M. R.), Pergamon, New York, 3, 197.

Bilby, B. A., Cottrell, A. H. and Swinden, K. H. (1963), Proc. Roy. Soc., A272, 304.

Blom, A. F., Hedlund, A., Zhao, W., Fathula, A., Weiss, B. and Stickler, R. (1986), The Behaviour of Short Fatigue Cracks (edited by Miller, K. J. and de los Rios, E.), MEP, London, 37.

Bolingbroke, R. K. and King, J. E. (1986), The Behaviour of Short Fatigue Cracks (edited by Miller, K. J. and de los Rios, E.), MEP, London, 101.

Breat, J. L., Mudry, F. and Pineau, A. (1983), Fatigue Engng. Mater. Struct., 6, 349.

Broek, D. (1974), Elementary Engineering Fracture Mechanics, Noordhoff Int. Pub., The Netherlands.

Broek, D. (1988), The Practical Use of Fracture Mechanics, Kluwer Academic Pub., The Netherlands.

Brown, C. W. and Hicks, M. A. (1983), Fatigue Engng. Mater. Struct., 6, 67.

Brown, C. W. and King, J. E. (1986), Small Fatigue Cracks (edited by Ritchie, R. O. and Lankford, J.), AIME, Warrandale, PA, 407.

Brown, C. W., King, J. E. and Hicks, M. A. (1984), Metal Science, 18, 374.

Brown, M. W. (1986), The Behaviour of Short Fatigue Cracks (edited by Miller, K. J. and de los Rios, E.), MEP, London, 423.

Chan, K. S. (1986), Small Fatigue Cracks (edited by Ritchie, R. O. and Lankford, J.), AIME, Warrandale, PA, 407.

Chan, K. S. and Lankford, J. (1983), Script Metall., 17, 529.

Chiang, W. T. and Miller, K. J. (1982), Fatigue Engng. Mater. Struct., 5, 249.

Coates, D. G. (1967), Phil. Mag., 16, 1179.

Cotterell, B. and Rice, J. R. (1980), Int. J. Fract., 16, 155.

Cottrell, A. H. and Hull, D. (1957), Proc. Roy. Soc. A242, 211.

Davidson, D. L. (1979), SEM 1979, SEM, Inc., AMF O'Hare, IL, 2, 79.

Davidson, D. L. (1984), Int. Metal Review, 29, 75.

Davidson, D. L. (1988), Acta Metallurgica, 36, 2275.

Davidson, D. L., Campbell, J. B. and Page, R. A. (1991), Metall. Trans., 22A, 377.

Davidson, D. L. and Lankford, J. (1976), J. Engng. Mater. and Tech., 98, 24.

Davidson, D. L. and Lankford, J. (1980), Fatigue Engng. Mater. Struct., 3, 289.

Davies, R. G. and Stoloff, N. S. (1965), Trans. AIME, 233, 714.

Dowling, N. E. (1977), ASTM STP 637, ASTM, 97.

Dugdale, D. S. (1960), J. Mech. Phys. Solids, 8, 100.

Eastabrook, J. N. (1984), Int. J. Fract., 24, R43.

Edwards, L. (1983), Proc. 4th Risφ International Symposium on Metallurgy and Materials Science, 237.

El Haddad, M. H., Topper, T. H. and Mukherjee, R. (1981), J. Testing Eval., 9, 65.

El Haddad, M. H., Topper, T. H. and Smith, K. N. (1979), Engng. Fract. Mech.,11, 573.

Elber, W. (1970), Engng. Fract. Mech., 2, 37.

Ewing, J. A. and Humphrey, J. C. (1903), Phil. Trans., A200, 241.

Fine, M. E. and Kwon, I. B. (1986), Small Fatigue Cracks, (edited by Ritchie, R. O. and Lankford, J.), AIME, Warrandale, PA, 29.

Fine, M. E. and Ritchie, R. O. (1979), Fatigue and Microstructure, American Society for Metals, Ohio, 245.

Forsyth, P. J. E. (1961), Proc. of the Crack Propag. Symp., Cranfield, England, 1.

Forsyth, P. J. E. (1963), Acta Metall., 11, 703.

Forsyth, P. J. E. (1969), The Physical Basis of Metal Fatigue, American Elsevier Pub. Co., New York.

Forsyth, P. J. E. and Stubbington, C. A. (1957), J. Inst. Met., 86, 90.

Frost, N. E., Marsh, K. J. and Pook, L. P. (1974), Metal Fatigue, Clarendon Press, Oxford.

Garrett, G. G. and Knott, J. F. (1975), Acta Metall., 23, 841.

Gerdes, C., Gysler, A. and Lütjering, G. (1984), Fatigue Crack Growth Threshold

Concepts (edited by Davidson, D. L. and Suresh, S.), AIME, Warrendale, Pa, 465.

Güngör, S. (1990), PhD Thesis, The Open University.

Güngör, S. and Edwards, L. (1989), Proc. Int. conf. on Fract. VII (edited by Solomon, K. et al), Houston, Pergammon Press, 2, 1171.

Hahn, G. T. and Rosenfield, A. R. (1965), Acta Metall., 13, 293.

Hobson, P. D. (1982), PhD thesis, University of Sheffield.

Hudak, S. J. and Chan, K. S. (1986), Small Fatigue Cracks (edited by Ritchie, R. O. and Lankford, J.), AIME, Warrendale, Pa., 379.

Irwin, G. R. (1960), Proc. 7th Sagamore Conf., IV, 63.

Irwin, G. R. and Koskinen, M. F. (1963), Trans. ASME, 85D, 593.

Kitagawa, H. and Takahashi, S. (1976), Proc. 2th Int. Conf. Mech. Behaviour Mater., ASM, Boston, 627.

Lankford, J. (1982), Fatigue Engng. Mater. Struct., 5, 233.

Lankford, J. (1983), Fatigue Engng. Mater. Struct., 6, 15.

Lankford, J. (1985), Fatigue Fract. Engng. Mater. Struct., 8, 161.

Lankford, J., Davidson, D. L. (1986), Small Fatigure Cracks (edited by Ritchie, R. O. and Lankford, J.), AIME, Warrandale, PA, 117.

Lankford, J., Davidson, D. L. (1984), Fatigue Crack Growth Threshold Concept (edited by Davidson, D. L. and Suresh, S.), AIME, Warrandale, PA, 447.

Lankford, J., Davidson, D. L. and Chan, K. (1984), Metall. Trans., 15A, 1579.

Lankford, J., Davidson, D. L. and Cook, T. S. (1977), Cyclic Stress-Strain and Plastic Deformation Aspects of Fatigue Crack Growth, ASTM STP 637, 36.

Lardner, R. W. (1968), Phil. Mag., 17, 71.

Leis, B. N., Hopper, A. T. and Ahmad, J. (1986), Engng. Fract. Mech., 23, 883.

Lindigkeit, J., Gysler, A. and Lütjering, J. (1981), Metall. Trans., 12A, 1613.

Lu, H. W. (1963), J. Basic Engng., 85, 116.

Lynch, S. P. (1979), Fatigue Mechanisms (edited by Fong, J. T.), ASTM, Philadelphia, 174.

Mahmoud, M. A. and Hosseini, A. (1986), Engng. Fract. Mech., 24, 207.

McEvily, A. J., Eifler, D. and Macherauch, E. (1991), Engng. Fract. Mech., 40, 571.

Miller, K. J. (1985), Fundamentals of Deformation and Fracture (Eshelby Memorial Symposium), Cambridge University Press, Cambridge, 477.

Moffatt, J. and Edwards, L. (1991), private communication.

Morris, W. L., (1980), Metall. Trans., 11A, 1117.

Morris, W. L. and Buck, O. (1977), Metall. Trans., 8A, 597.

Morris, W. L., James, M. R. and Buck, O. (1981), Metall. Trans., 12A, 57.

Morris, W. L., James, M. R. and Zurek, A. K. (1985), Script Metall., 19, 149.

Navarro, A. and de los Rios, E. R. (1988), Phil. Mag., 57, 15.

Newman, Jr. J. C. (1982), Proc. AGARD Specialists Meeting on Behaviour of Short Cracks in Airframe Components, Toronto, Canada.

Newman, Jr. J. C. and Raju, I. S. (1981), Engng. Fract. Mech., 15, 185.

Nicholls, D. J. and Martin, J. W. (1990), Fatigue Fract. Engng. Mater. Struct., 13, 83.

Nicholls, D. J. and Martin, J. W. (1991), Fatigue Fract. Engng. Mater. Struct., 14, 185.

Nicoletto, G. (1989), Int. J. Fatigue, 11, 107.

Nisitani, H. and Goto, M. (1986), The Behaviour of Short Fatigue Cracks (edited by Miller, K. J. and de los Rios, E. R.), EGF publication, London, 461.

Nisitani, H., Goto, M. and Kawagoishi, N. (1992), Engng. Fract. Mech., 41, 499.

Nisitani, H. and Kawagoishi, N. (1984), Trans. JSME., 50, 277.

Okazaki, M. (1991), Metall. Trans., 22A, 479.

Paris, P. C. and Erdogan, F. (1963), J. Basic Engng., (Trans. ASME D), 85, 528.

Paris, P. C. and Sih, G. C. (1965), ASTM STP 513, 106.

Pearson, S. (1975), Engng. Fract. Mech., 7, 235.

Plumtree, A. and O'Connor, B. P. D. (1991), Fatigue Fract. Engng. Mater. Struct., 14, 171.

Rice, J. R. (1967), Fatigue Crack Propagation, ASTM STP 415, 247.

Rice, J. R. (1968), J. Appl. Mech. (Trans. ASME), 35, 379.

de los Rios, E. R., Mohamed, H. J. and Miller, K. J. (1985), Fatigue Fract. Engng. Mater. Struct., 8, 49.

de los Rios, E. R., Tang, Z. and Miller, K. J. (1984), Fatigue Fract. Engng. Mater. Struct., 7, 97.

Ritchie, R. O. and Lankford, J. (1986), Small Fatigure Cracks (edited by Ritchie, R. O. and Lankford, J.), AIME, Warrandale, PA, 1.

Ritchie, R. O., Yu, W., Blom, A. F. and Holm, D. K. (1987), Fatigue Fract. Engng. Mater. Struct., 10, 343.

Ritchie, R. O. and Yu, W. (1986), Small Fatigue Cracks (edited by Ritchie, R. O. and Lankford, J.), AIME, Warrandale, PA, 167.

Rooke, D. P. and Cartwright, D. J. (1976), Compendium of Stress Intensity Factors, HM's Stationery Office, London.

Smith, R. A., (1977), Int. J. Fracture, 13, 717.

Stickler, R., Hughes, C. W. and Booker, G. R. (1971), Scanning Electron Microscope-1971, Chicago, Ill., 473.

Sun, Z. Y., de los Rios, E. R. and Miller, K. J. (1991), Fatigue Fract. Engng. Mater. Struct., 14, 277.

Suresh, S. (1983), Metall. Trans., 14A, 2375.

Suresh, S. (1991), Fatigue of Materials, Cambridge University Press, Cambridge.

Suresh, S. and Ritchie, R. O. (1984), Int. Metals Reviews, 29, 445.

Taira, S. and Tanaka, K. (1972), Proc. Int. Conf. Mechanical Behaviour, 2, 48.

Taira, S. and Tanaka, K. and Nakai, Y. (1978), Mech. Res. Commu., 5, 375.

Taira, S., Tanaka, K. and Hoshina, M. (1979), Fatigue Mechanisms (edited by Fong, J. T.), ASTM STP 675, ASTM, Philadelphia, Pa, 135.

Tanaka, K. (1975), J. of Strain Anal., 10, 32.

Tanaka, K., Akiniwa, Y., Nakai, Y. and Wei, R. P. (1986), Engng. Fract. Mech., 24, 803.

Tanaka, K., Nakai, Y. (1983), Fatigue Engng. Mater. Struct., 6. 315.

Tanaka, K., Nakai, Y. and Yamashita, M. (1981), Int. J. Fract., 17, 519.

Taylor, D., and Knott, J. F. (1981), Fatigue Engng. Mater. Struct., 4, 147.

Taylor, G. I. (1938), J. Inst. Metals, 62, 307.

Tekin, A. and Martin, J. W. (1989), Metallography, 22, 1.

Thompson, N., Wadsworth, N. J. and Luat, N. (1956), Phil. Mag., 1, 113.

Tokaji, K. and Ogawa, T., (1990), Fatigue Fract. Engng. Mater. Struct., 13, 411.

Tuba, I. S. A. (1966), J. Strain Analysis, 1, 115.

Vecchio, R. S. and Hertzberg, R. W. (1985), Engng. Fract. Mech., 22, 1049.

Verhoeven, J. D. and Baker, H. H. (1976), J. Mater. Sci., 11, 388.

Wagner, L., Gregory, J. and Lütjering, G. (1986), Small Fatigue Cracks (edited by Ritchie, R. O. and Lankford, J.), AIME, Warrandale, PA, 117.

Wagner, L. and Lütjering, G. (1987), Fatigue 87 (edited by Ritchie, R. O. and

Starke, E. A.), EMAS, 1819.

Wells, A. A. (1963), British Welding Journal, 10, 563.

Wilkins, M. A. and Smith, G. C. (1970), Acta Metall., 18, 1035.

Zhang, D and Beevers, C. J. (1992), to be published in "Short Fatigue Cracks, ESIS 13", (edited by Miller, K.J.), 1992, MEP Ltd, London.

Zurek, A. K., James, M. R. and Morris, W. L. (1983), Metall. Trans., 14A, 1697.